

ESTIMATING THE WAVE CLIMATE FOR GÜLLÜK REGION
USING AN ACOUSTIC DOPPLER CURRENT PROFILER
AND EFFECT OF ISLANDS ON SWELL

by

Gökalp Topçu

B.S., in C.E., Boğaziçi University, 2007

Submitted to the Institute for Graduate Studies in
Science and Engineering in partial fulfillment of
the requirements for the degree of
Master of Science

Graduate Program in Civil Engineering

Boğaziçi University

2009

ACKNOWLEDGEMENTS

I would like to express my sincere gratitude to my thesis supervisor, Dr. Emre Otay for his guidance, support and encouragement throughout this study. It was a great honor to work together in various projects during the last three years. I had the chance to learn lots of things in the preparation of this thesis and all other field and laboratory work we did together.

I would also like to thank Dr. Osman Breki and Prof. Ali Rıza Gnbak for their valuable advises for this study.

My very special thanks are attended to my dear friends, Rouzbeh Ghabchi, Cenk Gngr, Emin ifti and especially Cihan Bayındır for their generous help. I would also like to thank the members of BoĖazii University Scuba Diving Club for their participation in the field studies.

I am grateful to my family, without whom probably I would have never done this work, for their endless support they have given me throughout my life.

ABSTRACT

ESTIMATING THE WAVE CLIMATE FOR GÜLLÜK REGION WITH AN ACOUSTIC DOPPLER CURRENT PROFILER AND EFFECT OF ISLANDS ON SWELL

Predicting the wave climate of a region is one of the main problems in coastal engineering studies. Since every structure related to the coastal zone is open to the effect of water waves, the characteristic behavior of the waves should be known. Moreover, in such structures, the bathymetric features of the site should be known as well as the wave characteristics.

Studies on the wave climate of Aegean Sea along Turkish coasts are very limited and the Güllük Region has not been investigated separately. In this study, the area in scope is monitored in terms of long term and local meteorological statistics, real-time wave records using an Acoustic Doppler Current Profiler (ADCP) and water quality parameters. Point measurements are combined with theoretical formulations to predict the wave climate in the region.

The outcomes are utilized for statistical analyses and obtaining the best fit to a well-known probability distribution, which indicated that the standardized generalized Gamma distribution best defines the wave characteristics in the region. However, it does not satisfy the goodness-of-fit tests.

One of the most important findings of this study indicated WSW (230° - 250° N) to be the most critical direction for swell waves from the 6 km wide gap between Greek Islands Leipsoi and Leros. These islands provide a natural barrier for the region against external waves such that the effective fetches are reduced to approximately 50 km inside the ring of islands except for the gap between Leipsoi and Leros, where the fetch is extended all the way to Island Naxos in that direction.

ÖZET

GÜLLÜK KÖRFEZİ DALGA İKLİMİNİN AKUSTİK DOPPLER AKINTI ÖLÇER İLE TAHMİNİ VE ÇEVRESEL ADALARIN DALGA İKLİMİNE ETKİLERİ

Dalga iklimi tahmini, kıyı mühendisliği çalışmalarında en önemli aşamalardan biridir. Kıyısız kesimde yer alan yapılar dalga etkisine her daim maruz kalacağından, o yöredeki dalgaların karakteristik özelliklerini bilmekte fayda vardır. Ayrıca, dalga iklimine ek olarak bu tür yapılar için kıyı şeridi oluşumları ve kıyı batimetrisi hakkında da bilgi sahibi olunmalıdır.

Türkiye'nin Ege Denizi kıyılarında dalga araştırmaları sınırlıdır ve özellikle Güllük Körfezi civarındaki çalışmalar yeterli seviyede değildir. Bu çalışmada, bahsi geçen bölge uzun dönem ve kısa dönem (bölgesel) meteorolojik istatistikler, Akustik Doppler akıntı ölçer kullanılarak gerçek zamanlı dalga kayıtları ve su kalitesi ölçümleri olmak üzere incelenmiş ve arazinin topografik ve batimetrik ölçümleri tamamlanmıştır. Noktasal veriler teorik hesaplama yöntemleriyle birleştirilerek bölgesel dalga iklimi analizi yapılmıştır.

Bu yöntemle elde edilen bulgular istatistiksel olarak incelenmiş ve yörenin dalga iklimini en iyi tanımlayan dağılımı bulmaya yönelik çalışmalar yapılmıştır. Standardize edilmiş genel Gamma dağılımının en uygun dağılım olduğu sonucuna varılmıştır. Ancak, istatistiksel uyum testi sonuçlarına göre bu dağılımın yetersiz olduğu görülmüştür.

Bu çalışmadaki en önemli bulgulardan biri de şüphesiz çevresel adaların dalga iklimi üzerindeki etkisidir. WSW (230°-250° N) yönünde bulunan Yunan adaları Leipsoi ve Leros arasındaki 6 km'lik açıklığın solgan dalgalar açısından kritik olduğu görülmüştür. Normalde doğal dalgakıran vazifesi gören bu adalar feç mesafesini yaklaşık 50 km'lik bir uzunluğa düşürürken, sadece bu açıklığa denk gelen yönde bu mesafe Naxos adasına kadar uzanmaktadır.

TABLE OF CONTENTS

ACKNOWLEDGEMENTS.....	iii
ABSTRACT.....	iv
ÖZET	v
TABLE OF CONTENTS.....	vi
LIST OF FIGURES	viii
LIST OF TABLES.....	xiii
LIST OF SYMBOLS/ABBREVIATIONS.....	xiv
1. INTRODUCTION	1
1.1. Objectives	1
1.2. Site Description	2
1.3. Method of Study	3
1.3.1. Topographic and Hydrographic Survey	3
1.3.2. Meteorological Statistics	3
1.3.3. Wave Climate	4
1.3.4. Water Quality Parameters	4
2. LITERATURE REVIEW	5
2.1. Previous Studies on Statistical Wave Analysis	5
2.2. Stochastic Approach to Random Waves.....	7
2.3. Prediction Methods of Wave Characteristics	9
2.3.1. JONSWAP Spectrum	11
2.4. Significant Wave Height.....	12
2.5. Statistical Representation of Significant Wave Height	14
2.5.1. Log-normal and Weibull Distributions	14
2.5.2. Generalized Gamma Distribution.....	15
2.6. Statistical Representation of Wave Periods.....	17
2.7. Joint Probability Distribution of Wave Heights and Periods.....	19
2.8. Goodness of Fit Tests	20
3. FIELD MEASUREMENTS	21
3.1. Topographic and Hydrographic Survey.....	21
3.2. Meteorological Records.....	26

3.2.1. Long Term Wind Records.....	26
3.2.2. Local Wind Measurements.....	27
3.3. Wave Measurements.....	30
3.3.1. Distribution of Wave Parameters	30
3.3.2. Distribution of Surface Currents	36
3.4. Water Quality Measurements	39
4. DATA REDUCTION AND INTERPRETATION.....	43
4.1. Time Series Analysis	44
4.2. Probability Distributions of Wave Parameters	46
4.2.1. Histograms	46
4.2.2. Directional Probability Distributions	48
4.2.3. JPD of Significant Wave Heights and Spectral Mean Periods.....	52
4.3. Statistical Presentation of Sea Severity	53
4.4. Goodness of Fit Test.....	56
5. CONCLUSIONS	59
APPENDIX A: Local Meteorological Statistics.....	61
APPENDIX B: Goodness of Fit Tests.....	80
REFERENCES	104

LIST OF FIGURES

Figure 1.1. Satellite photo of the wind and wave measurement sites	2
Figure 2.1. Schematic illustration of the random sea surface (Ochi, 1998).....	7
Figure 2.2. Example of wave spectrum (27.03.2007 07:20 Nortek-Storm Software).....	8
Figure 2.3. Predicting stochastic properties of random waves (Ochi, 1998).....	10
Figure 2.4. Derivation of significant wave height from probability density function	13
Figure 2.5. Schematic representation of zero-up crossing wave heights and periods	18
Figure 3.1. Topographic & hydrographic survey setup	22
Figure 3.2. Survey coverage on October'06	22
Figure 3.3. Field testing of the horizontal survey accuracy in kinematic mode	23
Figure 3.4. Side and top view of the hydrographic survey setup.....	24
Figure 3.5. Boat survey trajectory (over 40,000 soundings during hydrographic survey)	24
Figure 3.6. Final bathymetry contour map.....	25
Figure 3.7. Wind direction distribution of DMIGM Bodrum data for 25 years	26
Figure 3.8. Digital weather station for local meteorological parameters.....	27
Figure 3.9. Annual histograms of meteorological parameters (Nov.07 – Nov.08).....	28

Figure 3.10. Yearly total rain fall records for Bodrum (DMIGM)	29
Figure 3.11. Annual wind climate for Güllük Region (Nov.07 – Nov.08).....	30
Figure 3.12. Acoustic wave & current meter (AWAC) and its protective frame before and after deployment	31
Figure 3.13. Gyroscopic ring system holding the device in vertical position.....	32
Figure 3.14. Underwater wave gage retrieval performed by divers from Boğaziçi Scuba-Diving Club (BUSAS).....	32
Figure 3.15. Extended fetch due to gap in WSW direction between the islands Lepsoi and Leros	34
Figure 3.16. Annual directional probability distribution of significant wave heights	35
Figure 3.17. Annual directional probability distribution of spectral mean periods	35
Figure 3.18. Depth cell positions for an AWAC with 0.5m depth cells & return pulse of the surface cell distinguished	36
Figure 3.19. AWAC profiling range broken into several regions.....	37
Figure 3.20. Directional probability distribution of current speed (going to).....	38
Figure 3.21. Cyclic change in surface current directions due to sea breeze	38
Figure 3.22. Portable multi-probe system used for water quality measurements	39
Figure 3.23. Water samples taken adjacent to the fish farms	40
Figure 3.24. Water quality measurements locations	40

Figure 3.25. Time variation of water temperature at site #1	41
Figure 3.26. Time variation of water temperature at site #2	42
Figure 3.27. Time variation of water temperature at site #3	42
Figure 4.1. Satellite photo showing the measurement sites	43
Figure 4.2. Time history of predicted and measured significant wave heights	44
Figure 4.3. Time history of predicted and measured spectral mean periods	45
Figure 4.4. Time history of predicted and measured wave directions	45
Figure 4.5. Probability distribution of predicted and measured significant wave heights.....	46
Figure 4.6. Probability distribution of predicted and measured spectral mean periods...	47
Figure 4.7. Probability distribution of predicted and measured directions.....	48
Figure 4.8. Directional distribution of predicted significant wave heights.....	49
Figure 4.9. Directional distribution of measured significant wave heights	50
Figure 4.10. Directional distribution of predicted spectral mean periods.....	51
Figure 4.11. Directional distribution of measured spectral mean periods	51
Figure 4.12. Critical direction of incoming waves WSW (230°-250° N)	52
Figure 4.13. Joint probability distribution of significant wave heights and spectral mean periods derived from real-time measurements.....	53

Figure 4.14. Comparison between H_s and well-known probability distributions	54
Figure 4.15. Comparison between cumulative H_s and well-known probability distributions	55
Figure 4.16. Comparison between cumulative H_s and well-known probability distributions shown on a semi-log chart	56
Figure A.1. Time history of local meteorological parameters (November 2007)	61
Figure A.2. Time history of local meteorological parameters (December 2007).....	62
Figure A.3. Time history of local meteorological parameters (January 2008).....	62
Figure A.4. Time history of local meteorological parameters (February 2008).....	63
Figure A.5. Time history of local meteorological parameters (March 2008).....	63
Figure A.6. Time history of local meteorological parameters (April 2008).....	64
Figure A.7. Time history of local meteorological parameters (May 2008).....	64
Figure A.8. Time history of local meteorological parameters (June 2008).....	65
Figure A.9. Time history of local meteorological parameters (July 2008).....	65
Figure A.10. Time history of local meteorological parameters (August 2008).....	66
Figure A.11. Time history of local meteorological parameters (September 2008)	66
Figure A.12. Time history of local meteorological parameters (October 2008)	67

Figure A.13. Directional Wind Speed and Histograms (November 2007).....	68
Figure A.14. Directional Wind Speed and Histograms (December 2007).....	69
Figure A.15. Directional Wind Speed and Histograms (January 2008).....	70
Figure A.16. Directional Wind Speed and Histograms (February 2008).....	71
Figure A.17. Directional Wind Speed and Histograms (March 2008).....	72
Figure A.18. Directional Wind Speed and Histograms (April 2008).....	73
Figure A.19. Directional Wind Speed and Histograms (May 2008).....	74
Figure A.20. Directional Wind Speed and Histograms (June 2008).....	75
Figure A.21. Directional Wind Speed and Histograms (July 2008).....	76
Figure A.22. Directional Wind Speed and Histograms (August 2008).....	77
Figure A.23. Directional Wind Speed and Histograms (September 2008).....	78
Figure A.24. Directional Wind Speed and Histograms (October 2008).....	79

LIST OF TABLES

Table 3.1.	Summary of field activities.....	21
Table 3.2.	Annual results from the local weather station	28
Table 3.3.	Annual statistics of wind and waves (Nov.07 – Nov.08)	33
Table 3.4.	YSI 556 Multi-probe measurement results (October 2008)	41
Table 4.1.	Summary of sample statistics	57
Table 4.2.	Goodness-of-fit test results	57
Table 4.3.	Chi-Square goodness-of-fit test details.....	58
Table 4.4.	Kolmogorov-Smirnov goodness-of-fit test details	58

LIST OF SYMBOLS/ABBREVIATIONS

a	three-parameter Weibull distribution non-zero parameter
c	generalized Gamma distribution parameter
D_n	Kolmogorov-Smirnov test derived statistics
$E[.]$	expected value
f	frequency
f_m	modal frequency
g	gravitational acceleration
H_{m0}	significant wave heights (measured)
H_{\max}	max wave heights (measured)
H_s	significant wave height
k	constant depending on the shape factor
m_0	area under the spectral density function
n	sample size
R	Rayleigh parameter
R^2	regression coefficient
$S(\omega)$	spectral density function
sup	maximum value over the entire range of the sample domain
T_{m02}	spectral mean wave period (measured)
T_p	spectral peak wave period (measured)
\bar{T}_0	mean zero-up crossing period
\bar{U}	mean wind speed
x	fetch length
\bar{x}	dimensionless fetch
x_*	lower limit of highest one-third observed wave heights

α	significance level
ϵ	critical level of exceedance for Kolmogorov-Smirnov test
γ	peak-shape parameter
$\Gamma(\cdot)$	Gamma function
$\Gamma\{\cdot\}$	incomplete Gamma function
λ	generalized Gamma distribution shape parameter
μ	mean
ω	angular frequency
ω_m	modal angular frequency
Φ	error function
σ	standard deviation
θ_m	mean wave direction (measured)
θ_p	direction of the peak period (measured)
χ^2	Chi-square test derived statistics
χ^*	critical level of exceedance for Chi-square test

ADCP	Acoustic Doppler Current Profiler
AST	Acoustic Surface Tracking
AWAC	Acoustic Wave and Current Meter
BUSAS	Boğaziçi University Scuba-Diving Club
CDF	cumulative distribution function
DMIGM	Devlet Meteoroloji İşleri Genel Müdürlüğü
DO%	Dissolved Oxygen saturation
E	East
ENE	East-North-East
ESE	East-South-East
GPS	Global positioning system
JONSWAP	Joint North Sea Wave Project
JPD	Joint probability distribution
JPDF	Joint probability density function

MB	megabyte
N	North
NE	North-East
NNE	North-North-East
NNW	North-North-West
NW	North-West
ORP	Oxygen reduction potential
pdf	probability density function
Rms	Root-mean-square
rps	rounds per second
S	South
SE	South-East
SSE	South-South-East
SSW	South-South-West
SW	South-West
TDS	Total dissolved solids
W	West
WNW	West-North-West
WSW	West-South-West

1. INTRODUCTION

1.1. Objectives

Predicting the wave climate of a region is one of the main problems in coastal engineering studies. Since every structure related to the coastal zone is open to the effect of water waves, the characteristic behavior of the waves should be known. These characteristics of the waves are used in estimating a design wave for onshore and offshore structures. Statistics and directional analyses are widely used to determine such parameters.

The aim of this study is to put forth the wave and especially the swell wave climate along the Turkish coastline of Aegean Sea with a special focus on Güllük Region where there is a sheltered zone due to the surrounding Greek Islands. The Islands provide a natural barrier against the effects of long swell waves as they behave like distant-located breakwaters. The main objective of the study is to determine the wave climate in the region with a statistical approach.

Studies on wave climate of Aegean Sea along Turkish coasts are very limited and the Güllük Region has not been investigated separately. The area in scope has a significant economical value gaining its importance mainly from tourism and fishery industry. Additionally, the special configuration of the Greek Islands has a relative significance for scientific studies.

In this study, the area in scope is monitored in terms of long term and local meteorological statistics, real-time wave records using an Acoustic Doppler Current Profiler (ADCP) and water quality parameters. Long term wind data (26 years) is obtained from the nearest station of Turkish State Meteorological Services located in Bodrum and real-time measurements are taken locally. Moreover, a Nortek wave meter has been installed to continuously monitor waves. Another dimension of this study involves water quality measurements carried on simultaneously with the wind and wave measurements.

1.2. Site Description

The measurement location lies on the Southern part of Aegean Coast of Turkey, named Güllük Bay. The mainland makes an extension in the southern part of the region to form Bodrum peninsula, which limits the effect of the sea waves coming from that direction. Additionally, considering the Greek Islands surrounding the region westerly, effective fetch length of the region is limited to approximately 50 km inside the ring of islands.

The Nortek-AWAC acoustic Doppler current profiler with acoustic surface tracking (AST) has been deployed at 13 m water depth at coordinates $N37^{\circ}18'25.9''$ and $E27^{\circ}24'22.1''$. Figure 1.1 shows the location of the wave gage and the area in scope.



Figure 1.1. Satellite photo of the wind and wave measurement sites

1.3. Method of Study

1.3.1. Topographic and Hydrographic Survey

Coastal construction projects include offshore and onshore structures such as marinas, harbors, jetties, breakwaters and nourishments. In such structures, the bathymetric features of the site should be known as well as the wave characteristics.

In this study, the area in scope is selected as a base for a future construction site. The site was surveyed to have a better understanding on the bathymetry. The 4792 m long shoreline and the nearshore up to 30 m depth contour were surveyed separately. After the field efforts were concluded, the bathymetric map of the site was obtained. Section 3.1 deals with the field efforts involving the topographic and hydrographic surveying activities.

1.3.2. Meteorological Statistics

Reliable data on the wind-wave characteristics affecting any coastal region are essential for almost all coastal and marine activities. This information may be either of statistical nature, derived from data covering a sufficiently long period, or of daily predictive type, obtained by routine wind and wave forecasting. The former type of data is needed for planning, design and management purposes, whereas the latter type is required for all daily coastal and marine operations such as shipping, sailing and coastal construction activities. Coastal and harbor engineers generally use field measurements, theoretical studies, physical modeling, and numerical simulations to identify wave climate and to estimate the highest probable wave characteristics from local winds as well as annual attributes of waves.

In this study, long-term wind records and local wind measurements are used together to predict wave statistics. Section 3.2 deals with the meteorological measurements in detail.

1.3.3. Wave Climate

Many techniques are available for making routine measurements of wave characteristics, some of them involving remote sensing, but most operational, real-time systems still involve in situ sensors relaying data back to shore via either a cable or wireless telemetry system. Cost considerations typically result in a spatially sparse network of sensors, making it difficult to validate the results from one sensor to another.

In this study, an acoustic Doppler current profiler (ADCP) with acoustic surface tracking (AST) is selected as the data collecting system. The Nortek underwater wave gage is deployed at 13 m water depth to continuously monitor wave parameters such as significant wave heights, spectral mean periods, surface currents and their relative directions for one full year of measurement period. The data obtained is used to correlate and compare with the predicted wave climate. In the sections that follow, the measurement system is described in detail.

1.3.4. Water Quality Parameters

Coastal construction activities affect marine life as well as coastal features. Therefore, it is quite important to know about the possible effects of any intended near shore activity on the marine life.

This thesis is conceptually based on describing the wave climate of the Güllük Region. However, another dimension of the study is dealing with environmental monitoring. The project site is monitored for water quality parameters such as water temperature, salinity, dissolved Oxygen rate, and pH. These parameters contribute in the feasibility of future construction projects. Further detail on the environmental monitoring efforts can be found in Section 3.4.

2. LITERATURE REVIEW

2.1. Previous Studies on Statistical Wave Analysis

Characterization of the stochastic properties of ocean waves was first presented in the early 1950s; and Longuet-Higgins (1952) demonstrated the probabilistic estimation of random wave height. Following decades have seen phenomenal advances in the probabilistic analysis and prediction methods in random seas.

The basic wave model represents the sea surface elevation as a non-stationary gaussian stochastic process, which is often studied as a series of piece-wise stationary stochastic processes with relatively short durations. Each of these stationary processes is described by some characteristic spectral parameters.

Longuet-Higgins (1952) studied these characteristic quantities that are in use for describing the state of the sea; for example, the mean height of the waves, the root-mean-square height, the significant wave height describing the intensity of the waves. He derived theoretical relations between these quantities in some special cases and especially in the case when the spectrum of the waves consists of a narrow frequency band.

Several approaches have been proposed to describe the long-term variability of these parameters, from which the significant wave height is the most important one. The first model to represent H_s data is due to Jaspers (1956). He proposed the Log-normal distribution and concluded that the model fitted the data well. Later, Battjes (1972) proposed the Weibull distribution as a more appropriate model for fitting the upper range of the data. However, both the Log-normal and Weibull models can give overestimates and underestimates, respectively, of return values (Soares, 1996).

Attempts have been made to suppress the deficiencies of the Log-normal and Weibull models. Haver (1985) fitted H_s data at the upper and lower ranges by proposing to use a combination of Log-normal and Weibull distributions to describe the full range of

H_s . Ochi (1992) used several data sets to show that the Generalized Gamma distribution provides a better fit than these models.

Golshani, Taebi and Chegini (2007) made *in situ* measurements to run a 3rd generation wind-wave model for predicting the wave climate of the Iranian Coast of Caspian Sea. They concluded that truncated Gumble distribution is the most appropriate statistical distribution for both wind and wave data in the region.

Apart from the representative values of long-term data sets, there are also various studies on the theoretical expression of the statistical distribution of individual wave measurement sets. Aziz Tayfun (1981) stated that the waves are described well by the Rayleigh law under certain conditions. Specifically, the sea surface is assumed to be linear Gaussian with a narrow-band spectrum. However, in reality, the wave field is not always consistent with these assumptions. Taking into consideration the nonlinear, non-Gaussian characteristics of the sea surface, wide-band spectrum effects and wave breaking in deep and shallow waters, he proposed a theoretical expression for the statistical distribution of the heights of sea waves.

Tayfun (1990) extended his studies on wave height distributions for large values and attempted to reexamine the original theory to see if it can be simplified to a form suitable for describing the statistics of large wave heights.

Following the studies on wave period and the joint probability distribution of heights and periods, there is invaluable information in the literature. Tayfun (1993) combined his previous studies where an accurate representation for the distribution of large wave heights was obtained and its possible extension to the joint wave height/period distribution was also discussed. The corresponding joint density is equivalent to the product of the marginal density of large wave heights, in the specific form given by Tayfun (1990), with the conditional density of associated periods, in one of the two forms implied by Longuet-Higgins' theories. This line of thought is pursued further in order to derive a quantitatively more accurate expression for the joint height-period distribution of large waves.

2.2. Stochastic Approach to Random Waves

Description and assessment of wind-generated waves provide advance information for the design and operation of marine systems. Wind-generated seas vary over a wide range of severity depending on geographical location, season, presence of islands, etc. Furthermore, the wave profile in a given sea state is extremely irregular in time and space, and therefore properties of waves cannot be readily defined on a discrete basis.

Random fluctuation of the sea surface is generally attributed to energy transfer from wind to the sea. Figure 2.1 shows an explanatory sketch indicating waves consisting of infinite number of sinusoidal waves with varying amplitudes, frequencies and incoming directions.

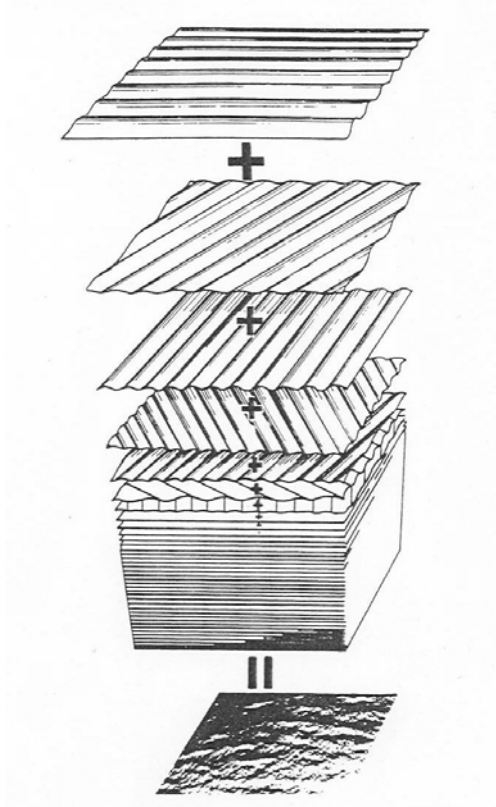


Figure 2.1. Schematic illustration of the random sea surface (Ochi, 1998)

The generation and growth mechanism of waves by wind is beyond the scope of this study, however, the concept of potential and kinematic energies of random waves should

be investigated. Wave energy mostly is represented by the spectral density function, often simply called the wave spectrum, and it plays a significant role in evaluating statistical properties of random waves.

An example of the wave spectral density function, $S(\omega)$, computed from the data obtained in the Bozbük Environmental Monitoring Program (Otay, N. E. and Topçu, G., 2008) is shown in Figure 2.2. The spectral density function illustrates the magnitude of time average of wave energy as a function of wave frequency, and the area under the density function represents the sea severity. The most commonly used definition of sea severity is the significant wave height, denoted by H_s , which is equal to four times the square-root of the area under the spectral density function.

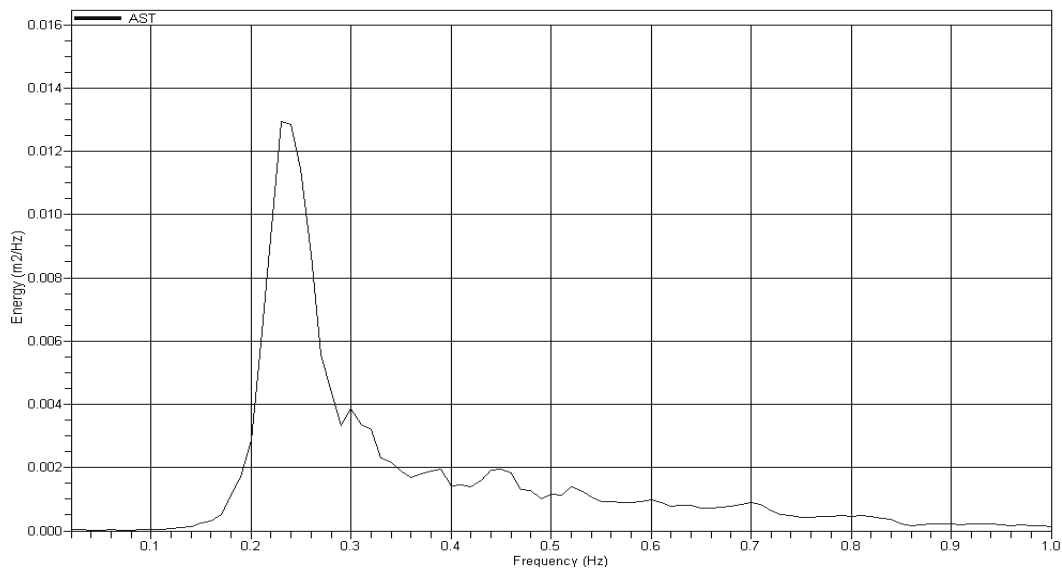


Figure 2.2. Example of wave spectrum (27.03.2007 07:20 Nortek-Storm Software)

As seen in the figure, the spectrum peaks at the frequency $\omega = 0.25\text{Hz}$ in this example. This implies that waves of 4s in period have the largest energy in this sea. It should not be interpreted from the figure that waves of 4s period are the most dominant, frequently observed in this sea. The frequency of occurrence should be evaluated from probability density function of the waves.

Characterization of the stochastic properties of ocean waves was first presented in the early 1950s; and Longuet-Higgins (1952) demonstrated the probabilistic estimation of random wave height. Following decades have seen phenomenal advances in the probabilistic analysis and prediction methods in random seas.

2.3. Prediction Methods of Wave Characteristics

There are two different approaches to acquire input information for the probabilistic analysis and prediction of random waves; one in the time domain, the other through the frequency domain. If one is interested in the statistical properties of wave height, the necessary input for the probability function can be evaluated by reading all individual wave heights from measured data, and estimating the parameters of the probability function based on statistical theories. This type of random observation method is simple and the reliability of the results is high if the number of observations is sufficiently large.

On the other hand, the spectral analysis in the frequency domain is much more mathematically rigorous than the random observation method.

The stochastic analysis and prediction of random waves span three domains; time, frequency and probability, as shown in Figure 2.3. Consider the time history of a wave measured at a certain location. The measured record represents the time history of all waves passing that location irrespective of the direction the waves are coming from. This type of wave measurement is referred as *point measurement*. As it is in our case, the most significant wave properties are evaluated by this method taking also directional measurements into consideration.

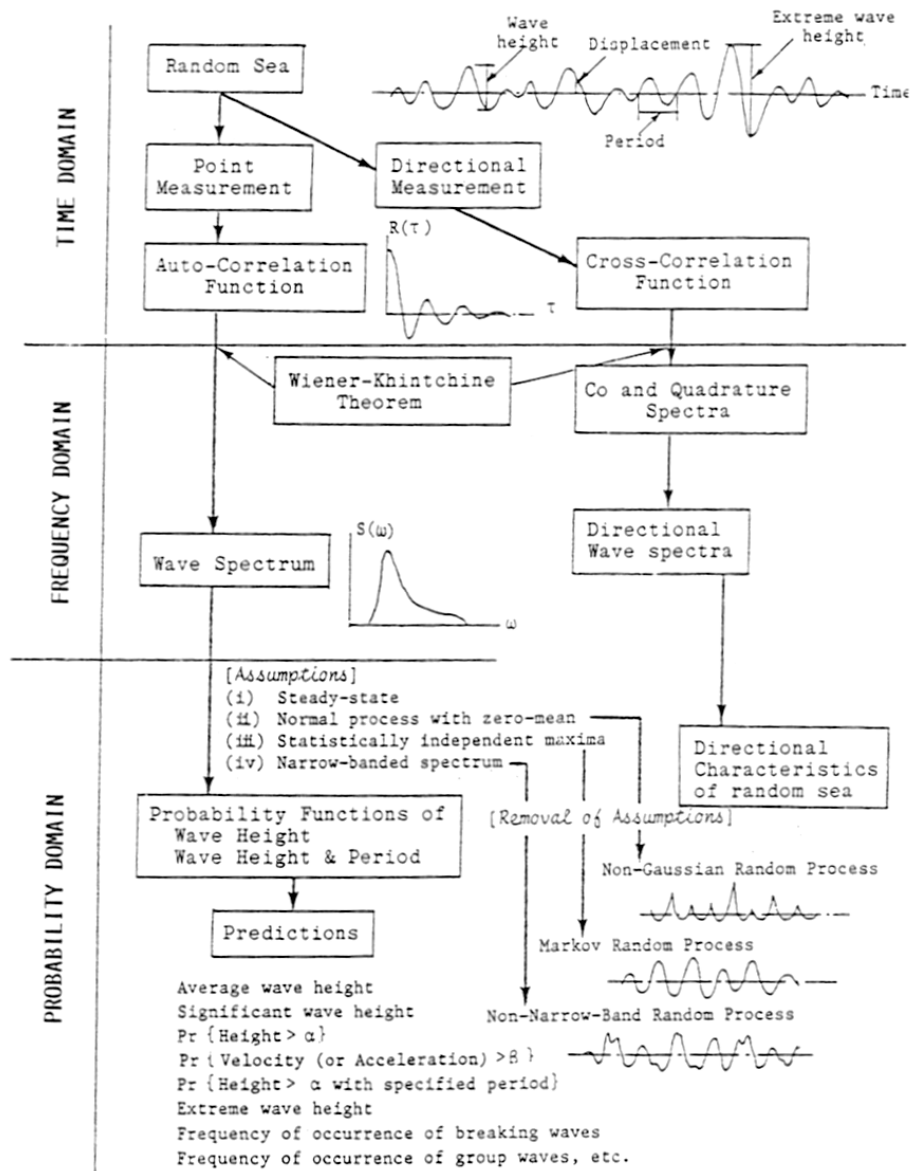


Figure 2.3. Predicting stochastic properties of random waves (Ochi, 1998)

The wave spectrum is a source of information from which the probabilistic prediction of various wave properties can be achieved in the probability domain. Many spectral formulations have been proposed since early 1950. Formulations were developed based on theoretical analysis together with the wave data primarily visually observed. Among others, the JONSWAP wave spectral formulation was a noteworthy contribution.

2.3.1. JONSWAP Spectrum

The JONSWAP formulation is based on an extensive wave measurement program known as the Joint North Sea Wave Project carried out in 1968 and 1969 along a line extending over 160 km into the North Sea from Sylt Island (Hasselmann *et al.* 1973). The spectrum represents wind-generated seas with fetch limitation, and wind speed and fetch length are inputs to this formulation. The original formulation is given as follows:

$$S(f) = \alpha \frac{g^2}{(2\pi)^4} \frac{1}{f^5} \exp\left\{-1.25(f_m/f)^4\right\} \gamma^{\exp\left\{-(f-f_m)^2/2(\sigma f_m)^2\right\}} \quad (2.1)$$

where γ = parameter, 3.30 as an average

$$\alpha = 0.076\bar{x}^{-0.22}$$

$$\sigma = 0.07 \text{ for } f \leq f_m \text{ and } 0.09 \text{ for } f > f_m$$

$$f_m = 3.5(g/\bar{U})\bar{x}^{-0.33}$$

$$\bar{x} = \text{dimensionless fetch} = g x/\bar{U}^2$$

$$x = \text{fetch length}$$

$$\bar{U} = \text{mean wind speed}$$

$$g = \text{gravity constant.}$$

The formula may be expressed in terms of the frequency ω in rps as

$$S(\omega) = \alpha \frac{g^2}{\omega^5} \exp\left\{-1.25(\omega_m/\omega)^4\right\} \gamma^{\exp\left\{-(\omega-\omega_m)^2/2(\sigma\omega_m)^2\right\}} \quad (2.2)$$

where $\omega_m = 2\pi f_m$.

The parameter γ is called the *peak-shape parameter*, and it represents the ratio of the maximum spectral energy density to the maximum of the corresponding Pierson-Moskowitz spectrum. The terms associated with the exponential power of γ is called the

peak enhancement factor, and the JONSWAP spectrum is the product of the Pierson-Moskowitz spectrum and the peak enhancement factor.

The value of peak-shape parameter is usually chosen as 3.30, and the spectrum is called the *JONSWAP spectral formulation*. The JONSWAP spectral formulation is given as a function of the wind speed. It is very convenient for the spectrum to be presented in terms of sea severity. For this, a series of computations is carried out for various combinations of fetch length and wind speed, and the following relationship is derived by Ochi (1979):

$$\bar{U} = kx^{-0.615} H_s^{1.08} \quad (2.3)$$

where k is a constant depending on the peak-shape parameter γ . \bar{U} is in m/s , x in km and H_s in m. From Eq.(2.3), the JONSWAP spectrum can be presented for a specified sea severity, H_s , and fetch length, x .

2.4. Significant Wave Height

Significant wave height, H_s , is the measure most commonly used for representing the severity of sea conditions. It is defined as the average of the one-third highest measured wave heights. However, it is rarely evaluated following the definition; instead, it is commonly evaluated by using the variance computed from a spectrum. The principle underlying the evaluation of significant wave height is based on the Rayleigh probability density function.

Wave heights follow the Rayleigh probability distribution assuming a narrow-band wave spectrum. Rayleigh distribution can be written in the form:

$$f(x) = \frac{2x}{R} \exp\{-x^2/R\} \quad 0 \leq x < \infty \quad (2.4)$$

where $R = 8m_0$ if x represents wave height and m_0 is the area under the spectral density function (or the zeroth moment of area).

If the lower limit of the highest one-third of the probability density function is written as x_* , the probability of exceeding x_* is $1/3$ as shown in Figure 2.4.

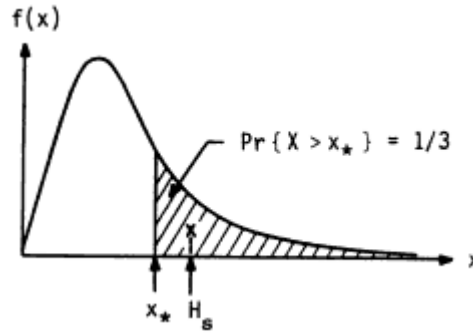


Figure 2.4. Derivation of significant wave height from probability density function

$$\Pr\{X \geq x_*\} = \int_{x_*}^{\infty} \frac{2x}{R} \exp\{-x^2/R\} dx = \frac{1}{3} \quad (2.5)$$

which yields

$$x_* = \sqrt{R}(\ln 3) = 1.048\sqrt{R} \quad (2.6)$$

By evaluating the moment about the origin, we have

$$\int_{x_*}^{\infty} xf(x)dx = x_* \exp\{-x_*^2/R\} + \sqrt{\pi R} \left\{ 1 - \Phi\left(\sqrt{\frac{2}{R}}x_*\right) \right\} = \frac{1}{3}H_s \quad (2.7)$$

where H_s is significant wave height. Then, from Eqs.(2.6) and (2.7), the significant wave height can be obtained as

$$H_s = 1.42\sqrt{R} = 1.42\sqrt{8m_0} = 4.01\sqrt{m_0} \quad (2.8)$$

Therefore, the significant wave height is commonly accepted to be equal to four times the square-root of the zeroth moment of area under the spectral density function with narrow-band wave spectrum assumption.

2.5. Statistical Representation of Significant Wave Height

For the design of marine systems, information is necessary not only on the severest sea condition expected to occur during the system's lifetime (50 years for example), but also on the frequency of occurrence of all sea conditions. The most commonly available information on sea severity is the statistical tabulation of significant wave height constructed from data accumulated over several years. Of course, the greater the number of accumulations, the more reliable the data.

In order to estimate the significant wave height expected to occur in 50 years at a location, for example, it is first required to find a well-known probability distribution which accurately represents the data. Because of this, various probability distribution functions have been proposed which appear to best fit particular sets of observed data. These include: (a) Log-normal distribution; (b) three-parameter Weibull distribution; and (c) Generalized Gamma distribution.

2.5.1. Log-normal and Weibull Distributions

It is a general trend that the greater part of significant wave height data is well represented by the Log-normal probability distribution given as:

$$f(x) = \frac{1}{\sqrt{2\pi}\sigma x} \exp\left\{-\frac{1}{2}\left(\frac{\ln x - \mu}{\sigma}\right)^2\right\} \quad 0 \leq x < \infty \quad (2.9)$$

However, the data diverge from the log-normal distribution for large significant wave heights, which is critical for estimating extreme values.

Another general trend observed on the statistical distribution of significant wave height is that the cumulative distribution function of large significant wave heights can be well represented by the Weibull distribution, but approximately 30 percent of the lower portion of data fails to follow. Weibull distribution is given by

$$f(x) = c\lambda^c x^{c-1} \exp\{-(\lambda x)^c\} \quad 0 \leq x < \infty \quad (2.10)$$

In order to improve this situation, the following three-parameter Weibull distribution is often considered:

$$f(x) = c\lambda^c (x-a)^{c-1} \exp\{-(\lambda(x-a))^c\} \quad a \leq x < \infty \quad (2.11)$$

Note that the three-parameter Weibull distribution carries a minimum non-zero value “ a ” as one of its parameters, and it is difficult to explain the physical meaning of this minimum significant wave height in the distribution. The sample space of the significant wave height has to be chosen between zero and ∞ , where zero wave height stands for calm water, which is an important portion of the distribution.

As far as is known, Log-normal distribution represents significant wave heights well except for large values, and large significant wave height data are well represented by the Weibull distribution. Some empirical model might be proposed by combining these two distributions at a certain value. However, the specification of the transition point is arbitrary in that case.

2.5.2. Generalized Gamma Distribution

In order to find an appropriate probability distribution which satisfies the condition, various probability distribution functions are standardized so that a comparison can be

made under zero mean and unit variance. It is found from the results of analysis that the cumulative distribution function of the standardized Generalized Gamma distribution is nearly equal to that of the Log-normal distribution up to 0.90, but the former converges to unity much faster above 0.90 (Ochi 1992). This feature of the Generalized Gamma distribution is considered to make use in the statistical analysis of significant wave heights.

The probability density function, $f(x)$, and the cumulative distribution function, $F(x)$, of the Generalized Gamma distribution are as follows:

$$f(x) = \frac{c}{\Gamma(m)} \lambda^m x^{cm-1} \exp\{-(\lambda x)^c\} \quad 0 \leq x < \infty \quad (2.12)$$

$$F(x) = \Gamma\{m, (\lambda x)^c\} / \Gamma(m) \quad (2.13)$$

where $\Gamma(m)$ is a Gamma function, and the numerator of $F(x)$ is an incomplete Gamma function.

The values of the three shape parameters, m , c and λ involved in the Generalized Gamma distribution may be simply estimated by equating the sample moments to the theoretical moments, since the sample size of significant wave height data is usually very large, on the order of several thousand or greater (8500 in our case). The sample moments are shown as:

$$\begin{aligned} m_1 &= E[x] = \text{mean} = \mu_1 \\ m_2 &= E[x^2] = \mu_2 + \mu_1^2 \\ m_3 &= E[x^3] = \mu_3 + 3\mu_1\mu_2 + \mu_1^3 \\ m_4 &= E[x^4] = \mu_4 + 4\mu_1\mu_3 + 6\mu_1^2\mu_2 + \mu_1^4 \end{aligned} \quad (2.14)$$

The theoretical j^{th} moment of the Generalized Gamma distribution is given by

$$E[x^j] = \frac{1}{\lambda^j} \frac{\Gamma\left(m + \frac{j}{c}\right)}{\Gamma(m)} \quad (2.15)$$

From a set of three equations for $j = 2, 3$ and 4 in Eq.(2.15), we can derive the following two equations by eliminating parameter λ :

$$\frac{\{\Gamma(m)\}^{1/2} \Gamma\left(m + \frac{3}{c}\right)}{\left\{\Gamma\left(m + \frac{2}{c}\right)\right\}^{3/2}} = \frac{E[x^3]}{\{E[x^2]\}^{3/2}} \quad (2.16)$$

$$\frac{\Gamma(m)\Gamma\left(m + \frac{4}{c}\right)}{\left\{\Gamma\left(m + \frac{2}{c}\right)\right\}^2} = \frac{E[x^4]}{\{E[x^2]\}^2} \quad (2.17)$$

The parameters m and c can be derived from the equations above, and λ can be obtained from Eq.(2.15) by letting $j = 2$ or 3 .

2.6. Statistical Representation of Wave Periods

For a complete description of wind-generated random waves, particular attention must be given to analyze wave periods as well as the wave heights. Moreover, the combined effect of wave heights and associated periods should be considered since height and period of incident waves are not statistically independent.

A widely accepted method to extract representative statistics from the wave data is the zero-up crossing analysis. For this method, a 'wave' is defined as the portion of a record between two successive zero-up crossings. Figure 2.5 shows a representative sketch of zero-up crossing wave heights and associated periods taken from the bulk wave data.

From the recorded bursts of wave data the waves are sorted according to their height (with their corresponding periods), and as mentioned before, the mean of the highest one-third is referred as significant wave height, H_s ; and the mean of the zero-up crossing periods is referred as \bar{T}_0 .

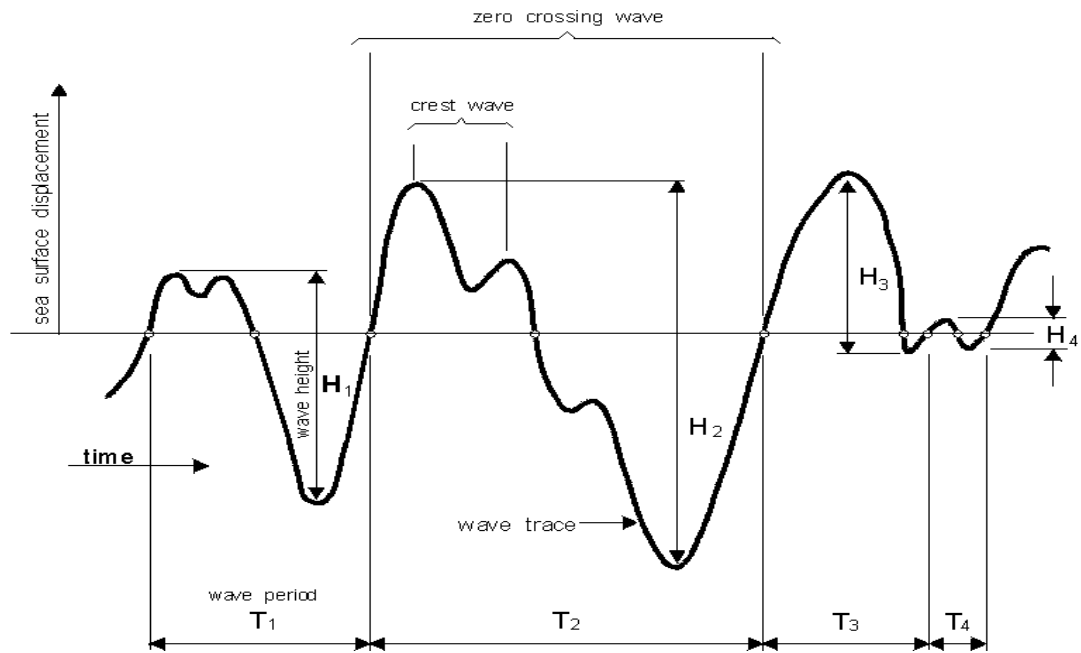


Figure 2.5. Schematic representation of zero-up crossing wave heights and periods

The spectral mean period, T_{m02} is the observed mean of the bulk wave record. Actually, the spectral mean wave period and the mean of the zero-up crossing wave periods represent the same thing. Therefore, it will be useful to note that the spectral mean wave period can be shown as follows;

$$\bar{T}_0 = T_{m02} = \sqrt{m_0/m_2} \quad (2.18)$$

where the average zero-up crossing periods are evaluated in terms of the moments of the spectral density function.

2.7. Joint Probability Distribution of Wave Heights and Periods

Information on long-term wave characteristics is best represented by making use of the joint probability densities of the significant wave heights and spectral mean wave periods. Since wave heights and associated periods are not statistically independent, their joint probability distribution plays a significant role in predicting statistical properties of waves such as the frequency of occurrence of resonant motion which may occur when spectral mean wave periods are close to the natural motion period of a structural system.

If the spectral mean wave period is sufficiently long or sufficiently short in comparison with the natural period of a system's motion, the system may be in no danger even though significant wave height is large. On the other hand, the magnitude of motion will reach a critical level if these periods are close to the system's natural period. In designing a floating marine system, it is therefore extremely important to know the combined effect of significant wave heights and spectral mean periods.

The combined significant wave height and spectral mean wave period can be presented in tabular form, often called the *contingency table* or the *scatter diagram*. The statistical information comprising the contingency table may be obtained through finding the appropriate joint probability distribution which best represents the data. However, it is difficult to derive the JPD directly from the observed data. Therefore, a method commonly considered for the derivation of $f(H_s, \bar{T}_0)$ is to find the marginal pdf $f(H_s)$, and the conditional pdf $f(\bar{T}_0|H_s)$. The JPDP can be derived from the product of $f(H_s)$ and $f(\bar{T}_0|H_s)$.

Burrows and Salih (1986) present the results of two combinations for the marginal Weibull distribution; one a conditional Weibull, the other a conditional Log-normal distribution. Mathiesen and Bitner-Gregersen (1990) demonstrate that the combination of the three-parameter Weibull distribution for $f(H_s)$ and the Log-normal distribution for $f(\bar{T}_0|H_s)$ best represents observed data. The JPDP of their model is as follows:

$$\begin{aligned}
f(H_s, \bar{T}_0) &= f(H_s) f(\bar{T}_0 | H_s) \\
&= \frac{\beta (H_s - \gamma)^{\beta-1}}{\alpha^\beta} \exp \left\{ - \left(\frac{H_s - \gamma}{\alpha} \right)^\beta \right\} \times \frac{1}{\sqrt{2\pi} \sigma H_s \bar{T}_0} \exp \left\{ - \frac{(\ln \bar{T}_0 - \mu H_s)^2}{2(\sigma H_s)^2} \right\} \quad (2.19)
\end{aligned}$$

The parameters of the conditional Log-normal distribution are given as a function of significant wave height H_s as follows:

$$\begin{aligned}
\mu H_s &= a_1 + a_2 H_s^{a_3} \\
\sigma H_s &= b_1 + b_2 \exp \{ b_3 H_s \} \quad (2.20)
\end{aligned}$$

Where a_1 , a_2 , a_3 , b_1 , b_2 and b_3 are constants determined from data.

2.8. Goodness of Fit Tests

In analyzing wave data measured in the field or obtained by experimental procedure, it is necessary to examine whether or not the data can be considered as a sample from a population having a presumed probability distribution. For example, waves in finite water depths are assumed to be a non-Gaussian random process in general, but they may quite likely be a Gaussian random process if the sea severity is mild. Therefore, it is necessary to examine the data sample with a statistically based assurance. This can be done by carrying out so called *goodness-of-fit tests* in statistical inference theory.

Although several goodness of fit tests are available in the literature, only typical tests suitable for analysis of wave data are discussed. One is the χ^2 test, which has been used extensively in various fields of applied statistics, the other is the Kolmogorov-Smirnov's test, which has the advantage of being applicable even for a sample consisting of a small number of observations.

Further detail on these tests can be found in the Appendices.

3. FIELD MEASUREMENTS

There have been 14 field trips for different purposes. Typical activities during a field trip include retrieval and deployment of underwater wave gage, replacement of batteries, water quality measurements and weather station updates. On special field trips, site survey and sea bottom investigations were carried out. Table 3.1 shows a brief summary of the dates of some important field activities.

Table 3.1. Summary of field activities

Date	Description of Study
21.06.2006	Site survey part 1
18.10.2006	Site survey part 2
	Installation of local weather station
09.02.2007	Nortek-AWAC wave gage deployment
	Sea bottom investigation dive
27.09.2007	Seawater quality measurements
17.12.2007	Special Field Trip: Storm parameters

3.1. Topographic and Hydrographic Survey

Traditionally, bathymetric data has been gathered with a single beam echo sounder, gathering one profile line at a time. These provide poor spatial resolution and may fail to identify large and potentially important seabed features, even when the line spacing is fairly close (30m). As an alternative to single line bathymetric surveys, a new system has been developed which could be used to provide high-resolution surveys across a wide area. For this purpose, a differential GPS system is used together with an echo sounder recording simultaneous depth readings (Figure 3.1).

The 4792 m long shoreline and the nearshore up to 30 m depth contour were surveyed separately. The shoreline was measured with the same differential GPS system consisting of BASE and ROVER receivers. While the base unit was set to static mode, the rover unit collected 160 points on a 4792 m long section of the shoreline in stop & go

mode. The horizontal accuracy for this survey mode is given by the manufacturer as less than 2 cm.



Figure 3.1. Topographic & hydrographic survey setup

The water level elevation and also two bench mark points were surveyed in static mode for maximum accuracy (estimated accuracy 1mm horizontal and 5mm vertical) and in order to connect the survey results to the topography maps of the state. Figure 3.2 shows the covered survey zone on October'06.



Figure 3.2. Survey coverage on October'06

During the post processing period, the collected data was adjusted for differential correction. In a field experiment where the same circle was measured for 10 consecutive times, the horizontal survey accuracy in the kinematic mode was found to be less than 5 cm (Figure 3.3).

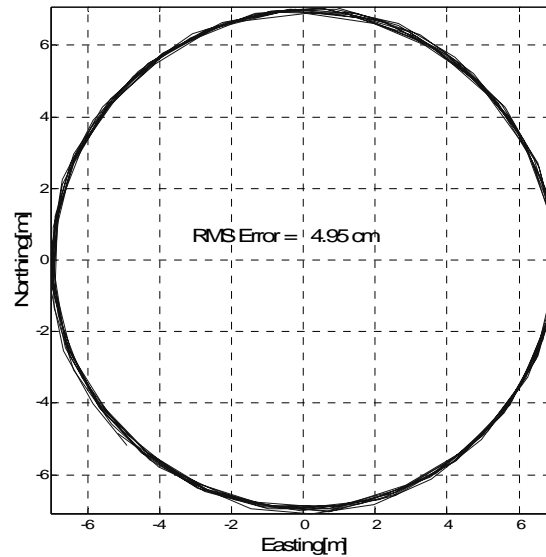


Figure 3.3. Field testing of the horizontal survey accuracy in kinematic mode

The vertical accuracy was measured by calibration of the echo-sounder using a survey rod. The regression coefficient R^2 was measured between 0.998-0.999 indicating an excellent match between the digital record and the actual depth.

The hydrographic survey was conducted with the same equipment. The echo sounder was used together with the Ashtech Promark 2 differential GPS system. The base unit was set to static mode on a fixed point on land, while the rover unit was attached to a survey rod so that the echo sounder and the rover unit are in the same vertical position as shown in Figure 3.4.

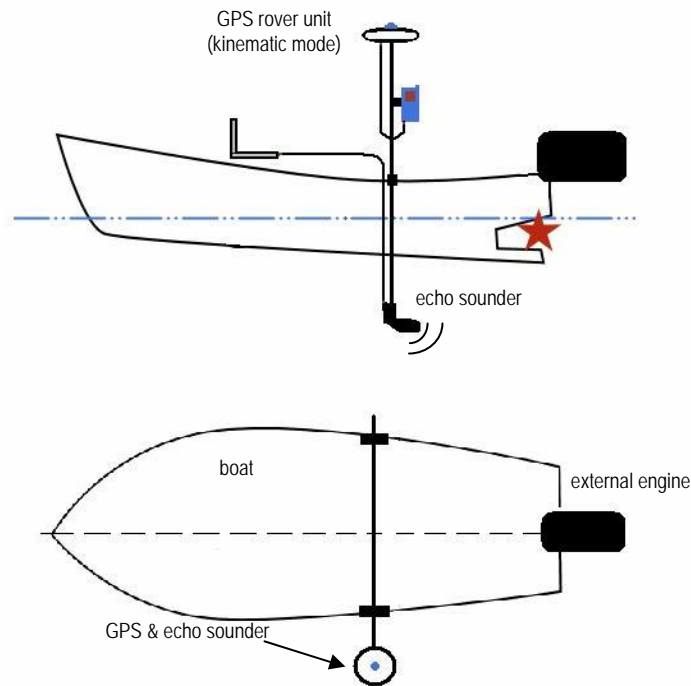


Figure 3.4. Side and top view of the hydrographic survey setup

During the hydrographic survey, 41303 soundings are recorded on a boat track of 93 km. After a triangulation analysis; the resulting bathymetry was drawn using a contour map. Figure 3.5 and Figure 3.6 show the boat trajectory during the survey and the resultant bathymetry map, respectively.

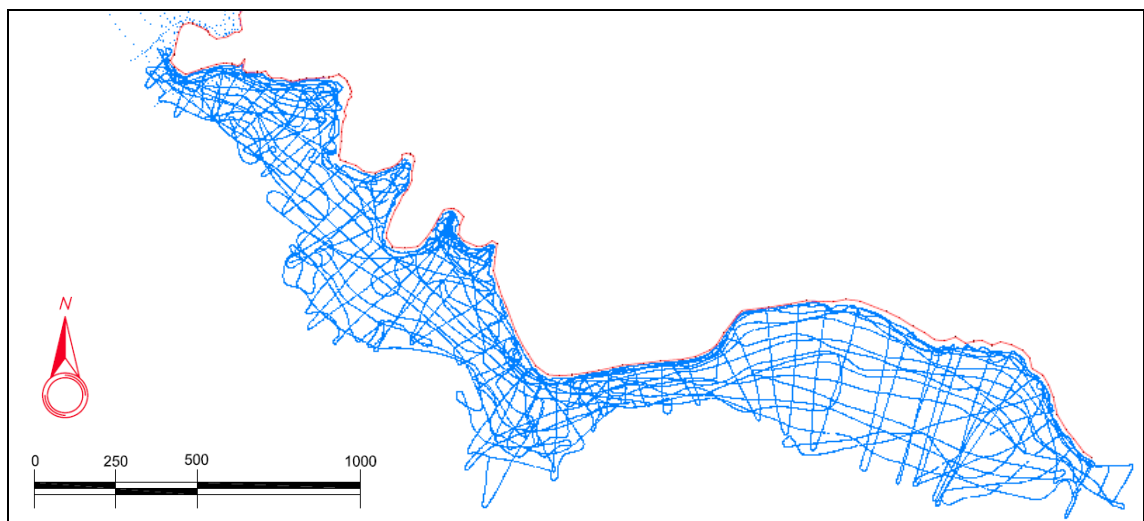


Figure 3.5. Boat survey trajectory (over 40,000 soundings during hydrographic survey)

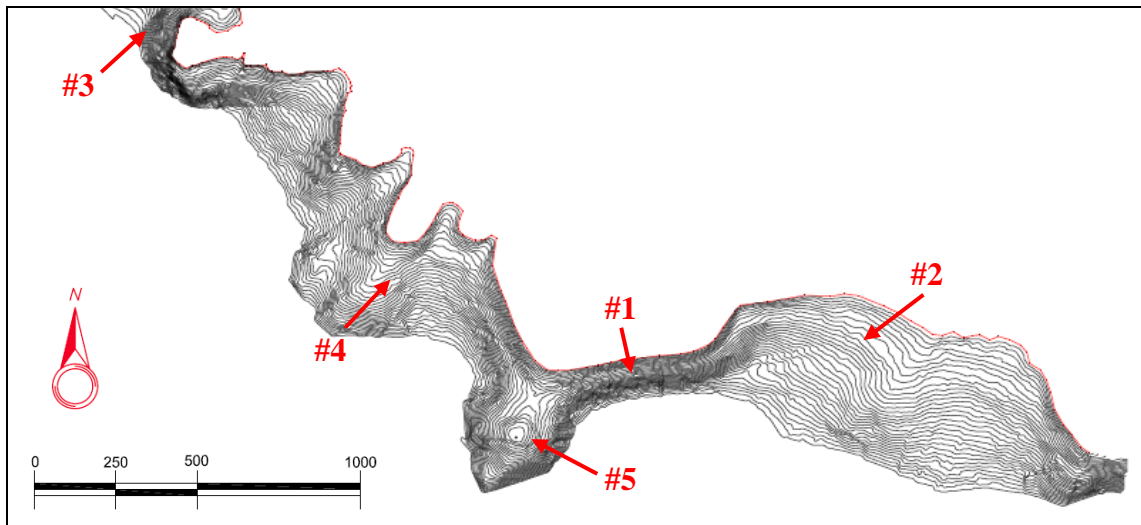


Figure 3.6. Final bathymetry contour map

The bathymetry shows a wide variety of morphologic features along the coast. The steepest slopes are located on the rocky peninsula marked as site #1 in the figure. Here, the profile slopes are as steep as 1:4. The large bay to the East of this peninsula containing South Beach (site #2) has one of the mildest slopes in the region with 1:17. Similarly, the small bays further west also have milder slopes with nearshore slopes (between waterline and -10m contour) ranging from 1:15 to 1:20. However, even these milder slopes can be regarded as being quite steep in terms of feasibility for beach nourishment.

The northern part of the region is suitable for a small harbor due to its bathymetric properties and the natural shelter against the wave impact. Although it looks quite suitable for the entrance of the marina (site #3), directional wave monitoring is required to determine the possible configuration of the pontoons and floating breakwaters. Therefore, an underwater wave gage is placed at site #4.

Another consequence of the hydrographic measurements indicates a reef formation (site #5) suitable for scuba diving activities.

3.2. Meteorological Records

3.2.1. Long Term Wind Records

Long-term wind data are taken from the stations of the Turkish State Meteorological Services (DMIGM) for Bodrum, Didim, Milas and Turgutreis to be used for the generation of wave spectra by the theoretical wind-wave formulations. Figure 3.7 shows the long-term directional wind statistics for the Bodrum Station records.

Inspection has revealed the Bodrum data set to be the only one reliable in terms of length, consistency and resolution. The Bodrum set consists of hourly data spanning the years 1980-2005 with very few instances of missing records. The hourly mean wind directions for Bodrum are analyzed to compute the directional histogram of wind occurrences.

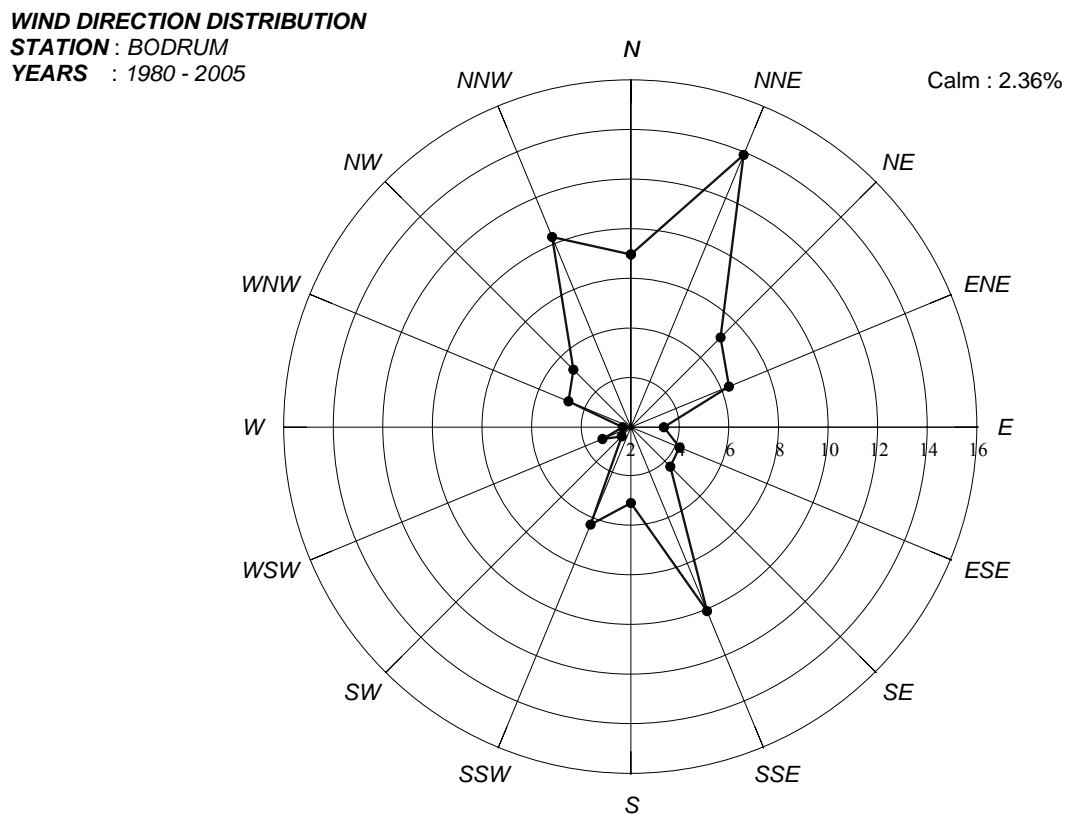


Figure 3.7. Wind direction distribution of DMIGM Bodrum data for 25 years

3.2.2. Local Wind Measurements

It is noted that the Bodrum data set gives less than 1% for winds coming from West. This can be a consequence of the orientation of the Bodrum Station or an unwanted barrier which blocks westerly winds. However, the area in scope shows a variety in the geographic conditions with a long fetch for westerly directions. Therefore, a new digital weather station is installed in the project area on October '06 to have a better insight on the local meteorological parameters (Figure 3.8).

The local station records the hourly wind speed, wind direction and other meteorological parameters such as air temperature, atmospheric pressure and rainfall. It is 10 m above the sea level in a self-contained sensor with solar power which records hourly mean and maximum values and sends them through wireless connection to a base unit connected to a PC.



Figure 3.8. Digital weather station for local meteorological parameters

Table 3.2 shows important statistical values of one-year weather data. The annual histograms of this data since November'07 are presented in Figure 3.9. Monthly time history charts of the whole record and significant meteorological statistics can be found in the Appendix section.

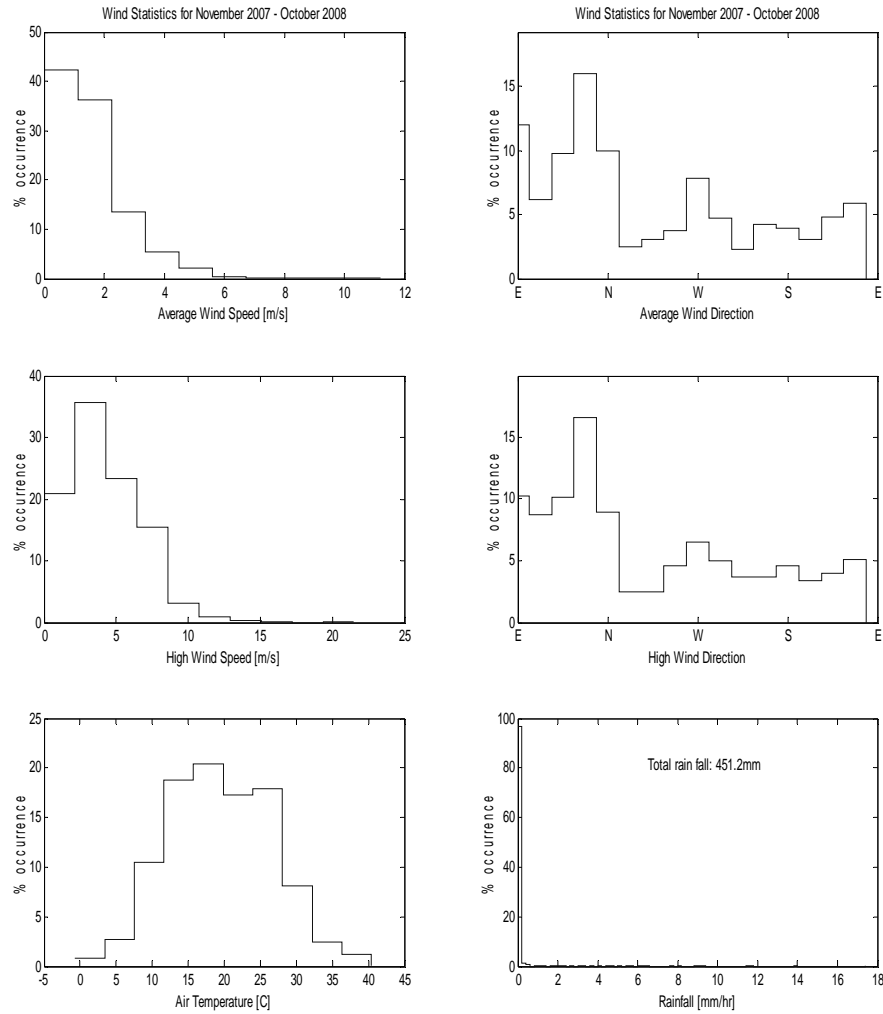


Figure 3.9. Annual histograms of meteorological parameters (Nov.07 – Nov.08)

Table 3.2. Annual results from the local weather station

ANNUAL RESULTS		Min	Max	Mean	Peak	Rms	Predominant Direction	Direction Of Maximum Wind
(Nov.07-Nov.08)	Average Wind Speed (m/s)		11.2	1.56	0.56	1.95	NNE	SW
	Wind Gust (m/s)		21.5	4.20	3.22	4.90	NNE	SW
	Rain(mm/hr)		17.4	0.05	0.10	0.52		
	Rainy Day: 60	Total: 451 mm						
	Temperature(C)	-0.7	40.4	19.5	17.8	20.8		

Average wind speed is the mean of hourly recorded wind speed data with its minimum, maximum and mean of the entire record. *Peak* value represents the most frequent wind speed, whereas *Rms*-values represent the root-mean-square of the data set. NNE is the most frequent direction for the hourly averages and the highest wind of the hourly averages come from SW.

Wind gust is the peak momentary wind speed for 1s with its minimum, maximum and mean value of the entire hourly record. These parameters are most often used for extreme case studies. Similarly the most frequent direction of highest hourly wind record is NNE and highest of hourly maximum winds come from SW.

Total rain fall in the region is 451 mm/year for the above measured period. The records from Turkish State Meteorological Services for yearly total rain fall in Bodrum are given in Figure 3.10.

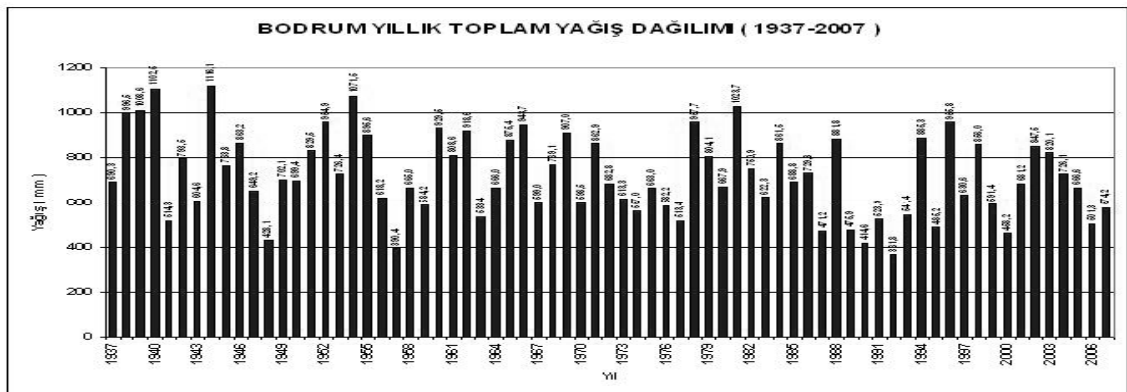


Figure 3.10. Yearly total rain fall records for Bodrum (DMIGM)

Winds during one full year (November 1st, 2007 - October 31st, 2008) are analyzed separately. The joint probability distribution of hourly mean wind velocity and mean wind direction for one full year is given in Figure 3.11.

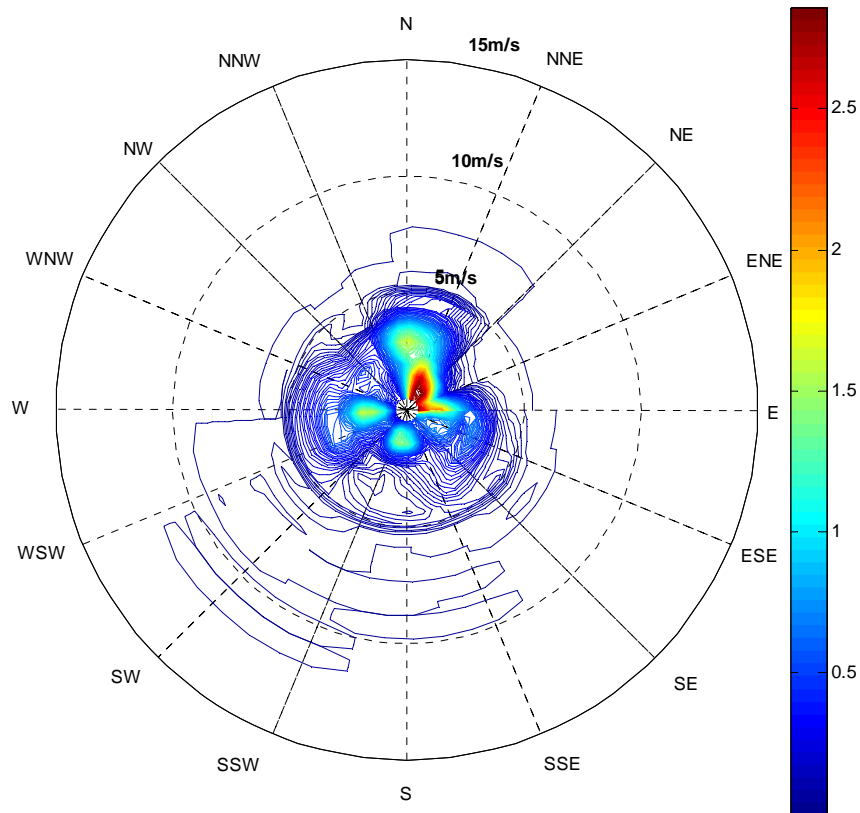


Figure 3.11. Annual wind climate for Güllük Region (Nov.07 – Nov.08)

This figure is a graphical summary of the local wind climate. It indicates that most of the time, wind blows from the northeastern quadrant, which are the directions between North and East. Although the predominant wind direction is NNE, stronger winds come from Southwest where Güllük Bay is located. Wind blows less frequently from the sea than it blows from the land.

3.3. Wave Measurements

3.3.1. Distribution of Wave Parameters

The most important part of the field efforts is the wave measurements since all other activities are related to the wave climate in reality. The local wind records are used only to

predict the wave characteristics in the region. However, actual wave data gives an advantage for comparing and correlating wind and wave data.

A Nortek-AWAC underwater wave gage with a memory capacity of 152 MB was purchased to conduct the wave measurements (Figure 3.12) with a 4 Hz sampling rate. The device supplies power from an external battery pack which provides approximately 2-3 months of measurement period in average. The main sensor head contains a tilt sensor, a temperature sensor and a pressure sensor. Additionally, the gage has its own compass measuring the earth's magnetic field. Combined with the tilt sensor, the compass enables the AWAC to convert velocity measurements to Earth coordinates.



Figure 3.12. Acoustic wave & current meter (AWAC) and its protective frame before and after deployment

The tilt sensor is set in accordance with the system orientation during operation. However, the standard AWAC is designed for vertical orientation. For making sure that the main head remains in vertical position during data collection, a gyroscopic ring system is designed which enables the instrument head to adjust its position with the help of its own weight as shown in Figure 3.13.



Figure 3.13. Gyroscopic ring system holding the device in vertical position

On February 9th, 2007, the wave gage with acoustic surface tracking (AST) has been deployed at 13 m water depth at coordinates N37°18'25.9'' and E27° 24'22.1''. Waves and currents have been measured until October 29th, 2008. The dive trips were repeated every 2-3 months to retrieve the data and to replace the batteries. During the dive trips, the gage location is found with a handheld GPS and divers from the Boğaziçi University Scuba Club (BUSAS) retrieved the instrument with the help of a lift bag (Figure 3.14).

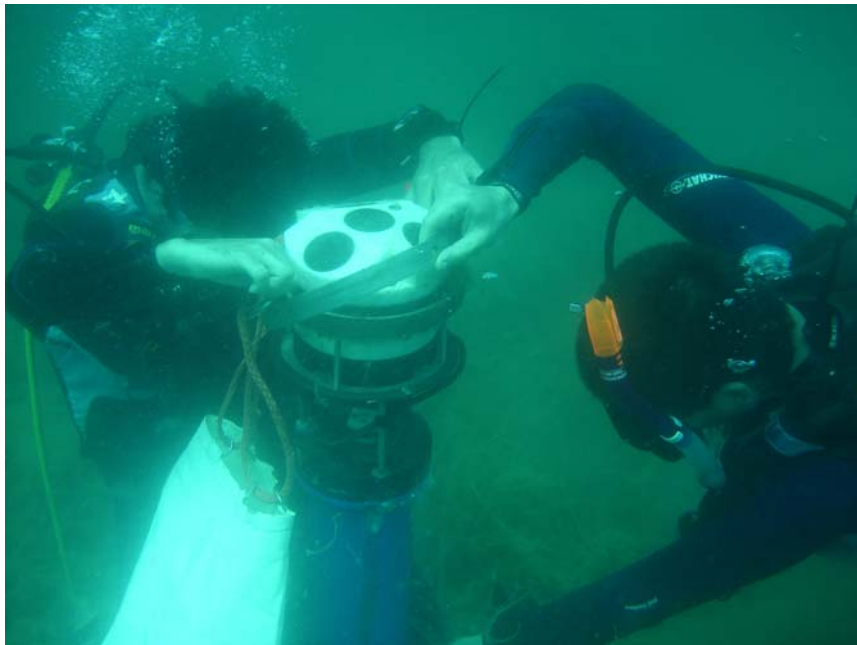


Figure 3.14. Underwater wave gage retrieval performed by divers from Boğaziçi Scuba-Diving Club (BUSAS)

The one-full-year wave record (November 1st, 2007 - October 29th, 2008) has been analyzed statistically. Important outcomes of the analysis are given in Table 3.3 along with the resultant wind statistics.

Table 3.3. Annual statistics of wind and waves (Nov.07 – Nov.08)

	<i>Yearly Average</i>	<i>Predominant (most frequent)</i>	<i>Yearly Maximum</i>	
WAVE	<i>Significant wave height (Hm0)</i>	0.26 m	0.21 m	2.59 m
	<i>Maximum wave height (Hmax)</i>	0.41 m	0.39 m	4.17 m
	<i>Spectral mean wave period (Tm02)</i>	2.2 s	2.3 s	5.3 s
	<i>Spectral peak wave period (Tp)</i>	3.7 s	4.1 s	9.4 s
	<i>Mean wave direction (θ_m)</i>	-	WSW	-
	<i>Direction of the peak period (θ_p)</i>	-	WSW	-
WIND	<i>Hourly average wind speed</i>	1.56 m/s	0.56 m/s	11.2 m/s
	<i>Direction of hourly average wind</i>	-	NNE	-
	<i>Hourly maximum wind speed</i>	4.2 m/s	3.22 m/s	21.5 m/s
	<i>Direction of hourly maximum wind</i>	-	NNE	-

The directional analysis results indicate that waves come predominantly from WSW (235⁰-250⁰ N) which coincides interestingly with the gap between Greek Islands Leipsoi and Leros (Figure 3.15). An earlier study on the gap diffraction of the islands surrounding Güllük Bay claimed that; “... islands provide a natural barrier against the swell to penetrate into the Güllük Bay ... The only exception is the 6 km wide gap between the islands of Lepsoi and Leros located WSW of the project site. This direction is expected to generate the largest sea.”

The real-time wave measurements provided the exact realization of the design storm where the waves came exactly from that critical direction in WSW. Due to the wide gap between the two islands, the normally 50 km long fetch of Güllük Bay is extended all the way to Island Naxos, 160 km WSW of the measurement location. Coincidentally, WSW is also the direction of the biggest storm waves recorded on November 10th, 2007.

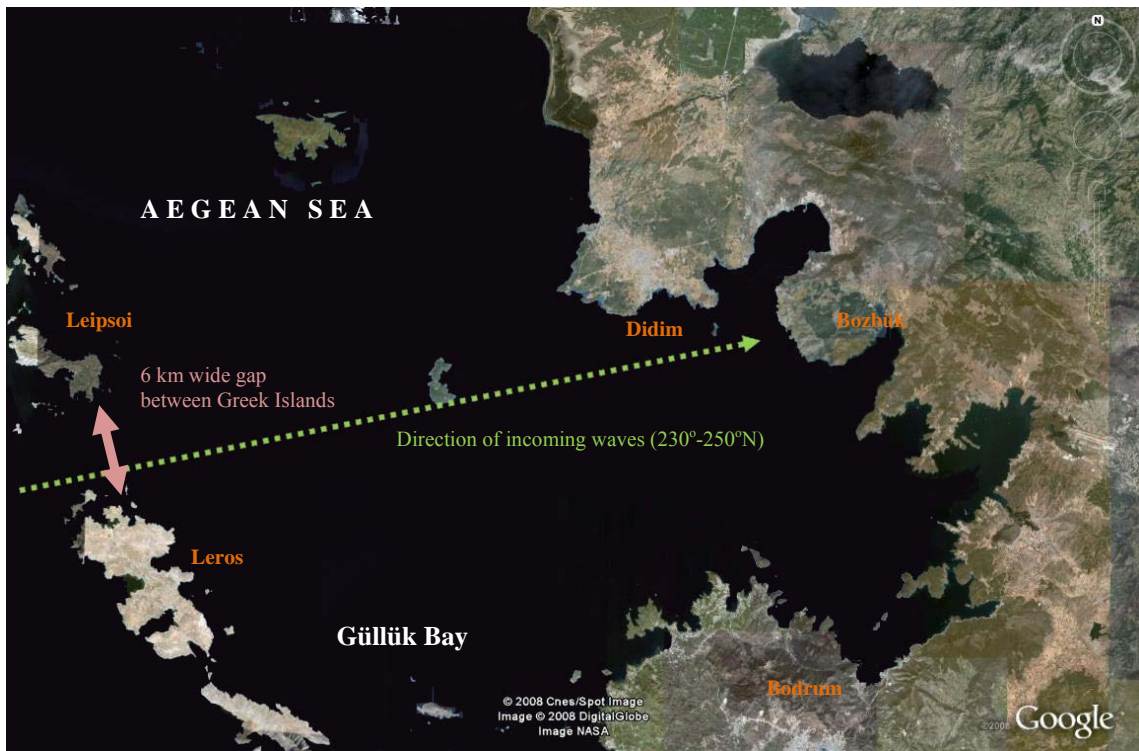


Figure 3.15. Extended fetch due to gap in WSW direction between the islands Lepsoi and Leros

Figure 3.16 and Figure 3.17 summarize the wave climate inside the Güllük Bay. It indicates no waves from landward directions (North to East). However, as expected, the reflected wave periods are quite visible in Figure 3.17 where there is a peak in the directions N-NNE and ENE-E which are landward directions (Figure 3.15) with very short fetch and therefore cannot produce wind waves at these periods. Therefore, it is clear that these are the reflected waves which are visible as wave periods but not as wave heights. This justifies a well-known wave theory stating that reflected waves lose their energy by a decrease in wave height but the wave period remains unaffected.

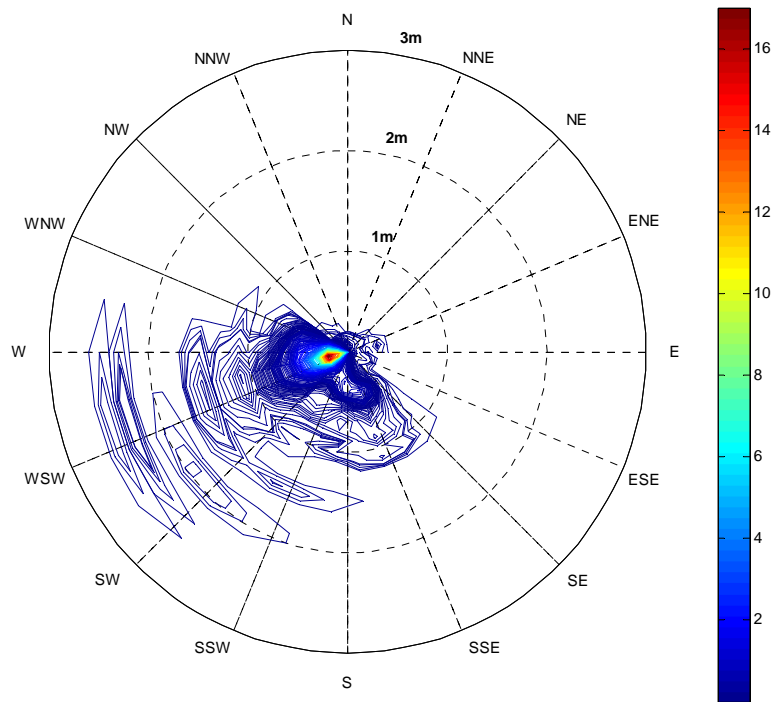


Figure 3.16. Annual directional probability distribution of significant wave heights

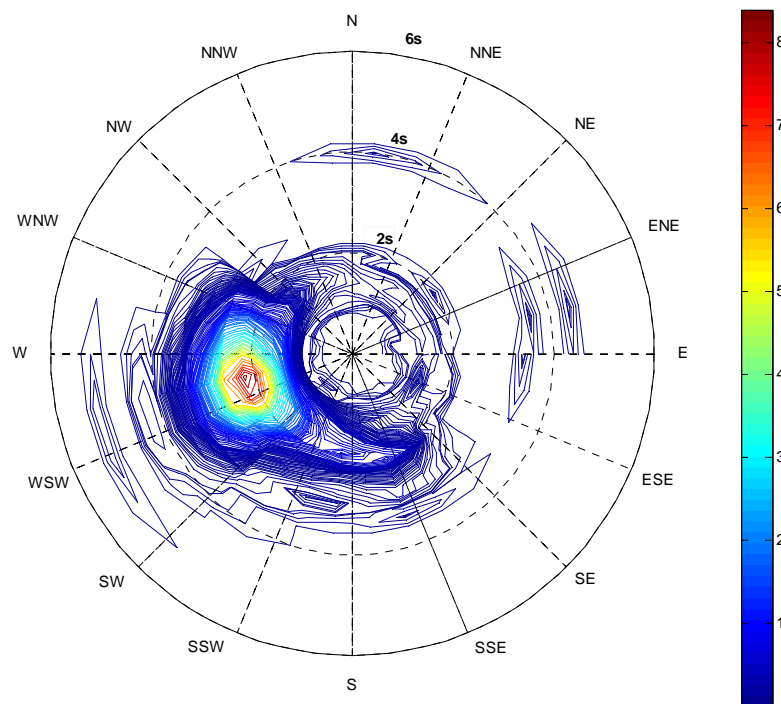


Figure 3.17. Annual directional probability distribution of spectral mean periods

3.3.2. Distribution of Surface Currents

The acoustic wave and current meter has an optional Acoustic Surface Tracking (AST) feature which enables to locate the water surface easily. It operates much like a standard acoustic range detector. The center beam is used to transmit a very short pulse. The travel time from the device to the surface and back allows us to estimate the distance to the surface for each ping. Fortunately, the strong impedance mismatch at the water-air interface provides near perfect reflection, and thus provides a strong return. An example of the return pulse is presented in Figure 3.18 to show that it is not difficult to locate the surface cell.

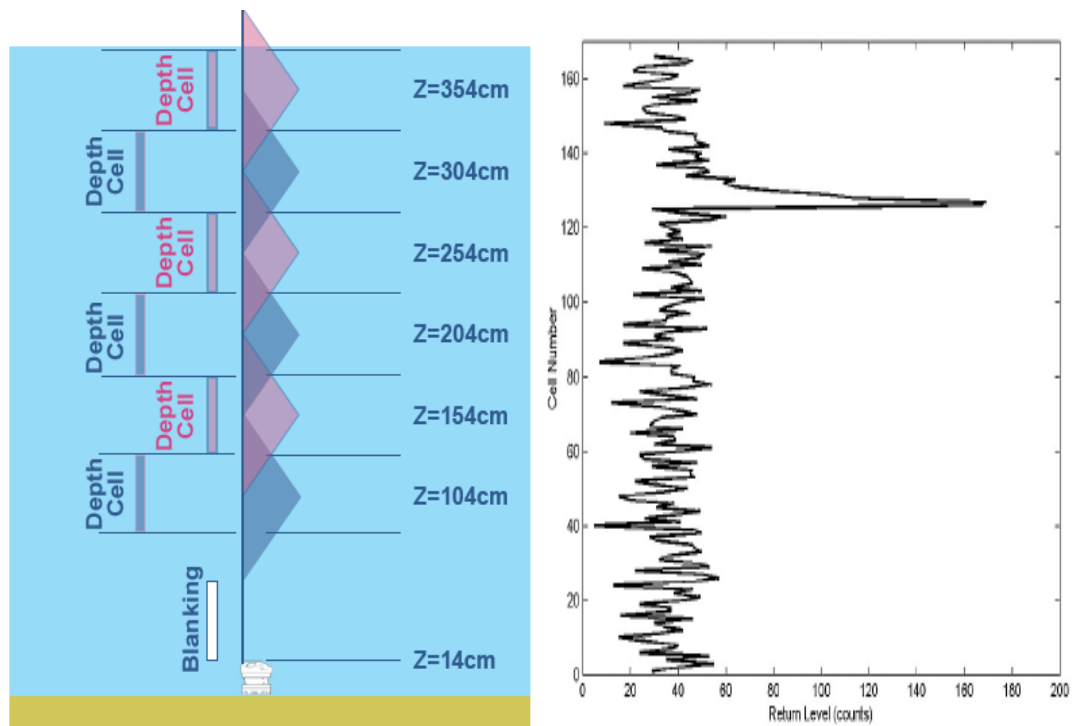


Figure 3.18. Depth cell positions for an AWAC with 0.5m depth cells & return pulse of the surface cell distinguished

The surface current data set was found to be less reliable than the wave record. Therefore, the analysis is performed on a larger window (May 07-Nov. 08) than the one-year wave analysis period. This might be a consequence of the profiling range selections. When operating near a boundary (surface or bottom), special consideration must be taken

during the data acquisition. Figure 3.19 shows the AWAC profiling range broken down into several regions. The first portion of the profile is lost while the system recovers from acoustic transmission. This region is referred to as the blanking distance, and its size depends on the acoustic frequency. No data is collected for a period following the end of the transmit pulse to eliminate any possible interference.

After the blanking distance, the instrument will make velocity measurements in multiple cells determined by the user. As mentioned before, the surface cell is easy to distinguish, thus surface currents can be studied by analyzing surface cell data.

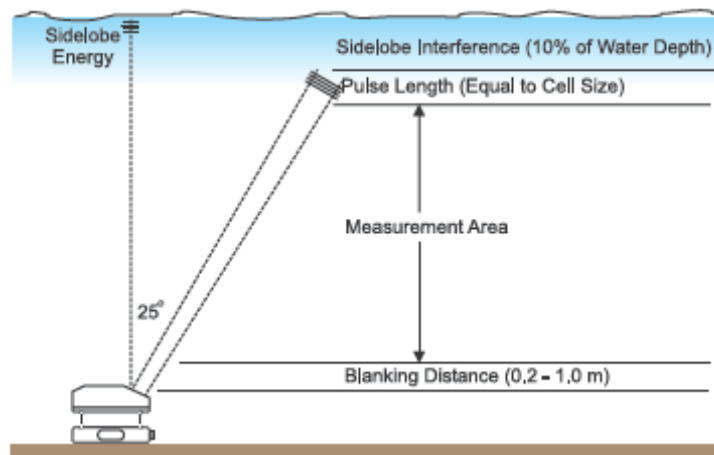


Figure 3.19. AWAC profiling range broken into several regions

For the present study, the hourly mean values of surface current speed and direction (“going to” in this case) are analyzed. Figure 3.20 summarizes the characteristics of the surface currents in the region.

The peaks marked with arrows in Figure 3.21 indicate the surface current directions with almost opposite directions. Consequently, the surface water circulation is dominated by winds that alternate directions during day and night due to the thermal difference between the land and the sea. This daily change in the wind directions quite frequently observed in Aegean Sea is called the sea breeze.

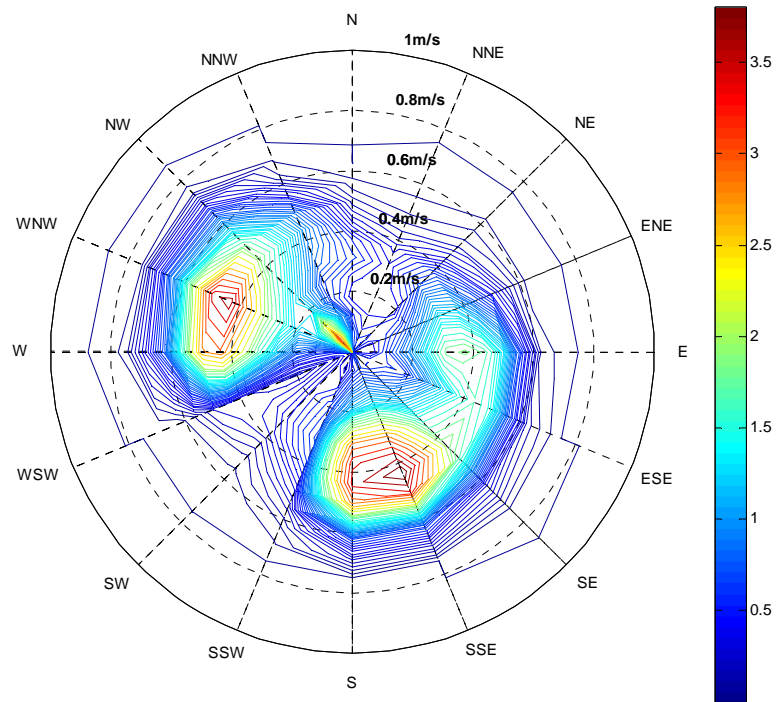


Figure 3.20. Directional probability distribution of current speed (going to)

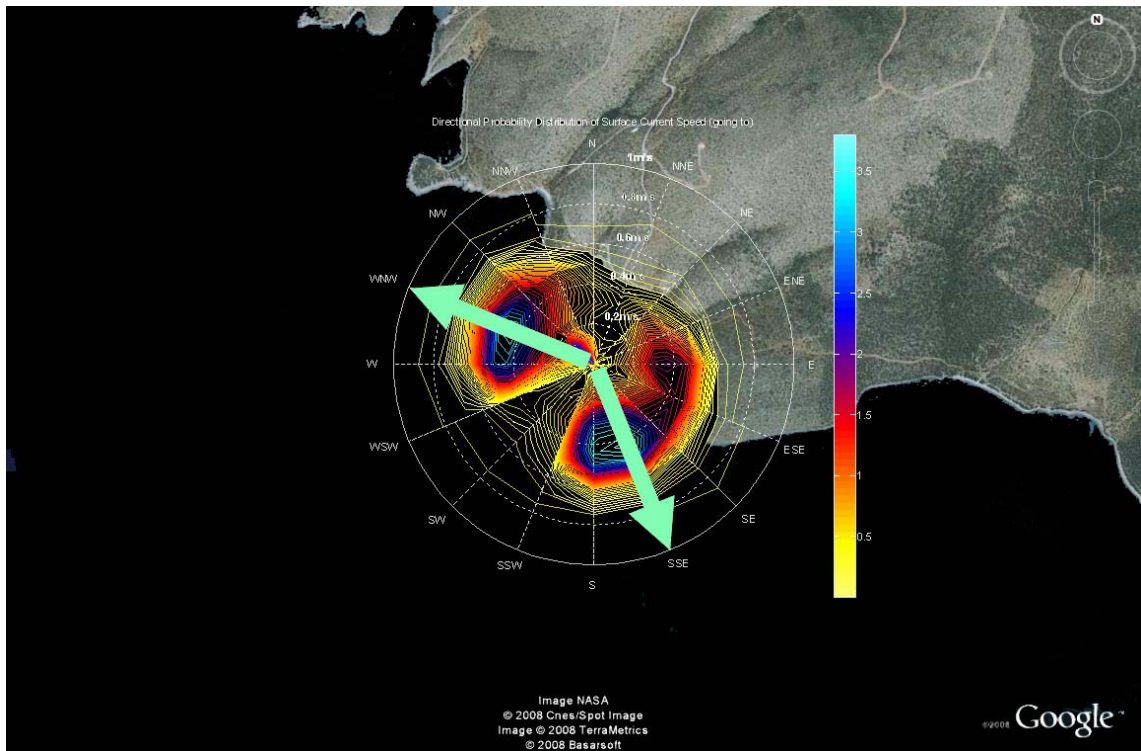


Figure 3.21. Cyclic change in surface current directions due to sea breeze

3.4. Water Quality Measurements

Water quality parameters have been measured using a portable YSI 556 multi-probe device (Figure 3.22). The multi-probe measures the following parameters:

- Water Temperature
- pH
- ORP (Oxygen Reduction Potential)
- DO % (Dissolved Oxygen Saturation)
- Conductivity
- Salinity
- TDS (Total Dissolved Solids)

In each data log the water temperature, specific conductivity, TDS, salinity, DO saturation and pH values have been recorded.



Figure 3.22. Portable multi-probe system used for water quality measurements

In addition to the real-time water quality measurements, water samples have been taken during the field trips at the specified locations (Figure 3.23). The samples were examined at the Environmental Laboratory of Boğaziçi University.

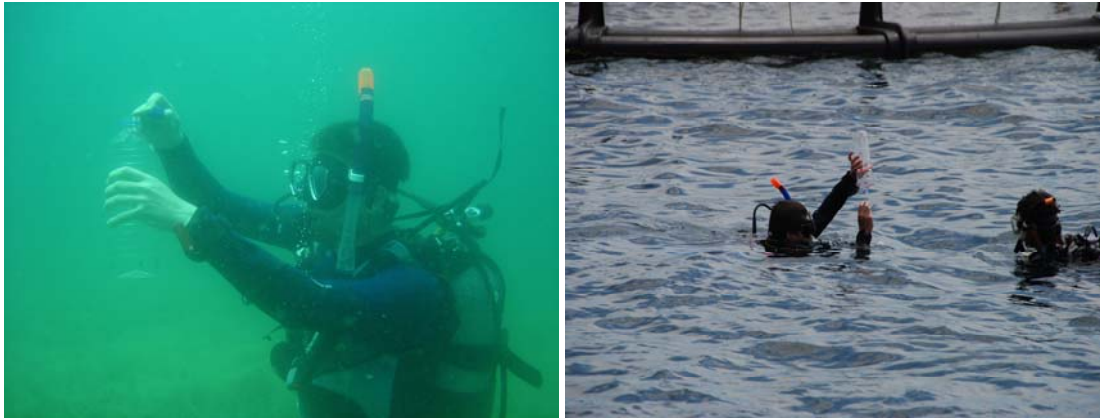


Figure 3.23. Water samples taken adjacent to the fish farms

The water quality parameters have been measured at certain sites suitable for structural and coastal activity. Additionally, the effects of fish farms on water quality have been investigated (Figure 3.24).

According to the declaration of the Ministry of Environment on the protection of small bays from fish farms, water samples were collected in May and August around the fisheries. All of the in-situ multi-probe measurements were repeated at three sites during the field trips.



Figure 3.24. Water quality measurements locations

The in-situ measurements are taken at three different depths on a water column. Table 3.4 shows the results of the measurements performed on October 2008. The variations of the parameters with time are plotted. As an example, the results for water temperature variation are presented in the following figures.

Table 3.4. YSI 556 Multi-probe measurement results (October 2008)

Location	Depth [m]	Test Results					
		Temp [°C]	Sp.Conductivity [mS/cm]	TDS [g/L]	Sal [ppt]	DO [mg/L]	PH
Site#1	-0.5	21.39	56.16	36.50	37.37	6.52	7.83
	-6	21.26	56.16	36.51	37.37	6.53	7.84
	-12	21.25	56.18	36.52	37.38	6.48	7.84
Site#2	-0.5	21.42	56.20	36.53	37.40	6.43	7.86
	-5	21.31	56.19	36.52	37.39	6.50	7.85
	-10	21.27	56.20	36.53	37.40	6.58	7.86
Site#3	-0.5	21.40	56.20	36.53	37.40	6.50	7.88
	-6	21.33	56.18	36.52	37.39	6.54	7.88
	-12	21.30	56.19	36.53	37.39	6.58	7.89

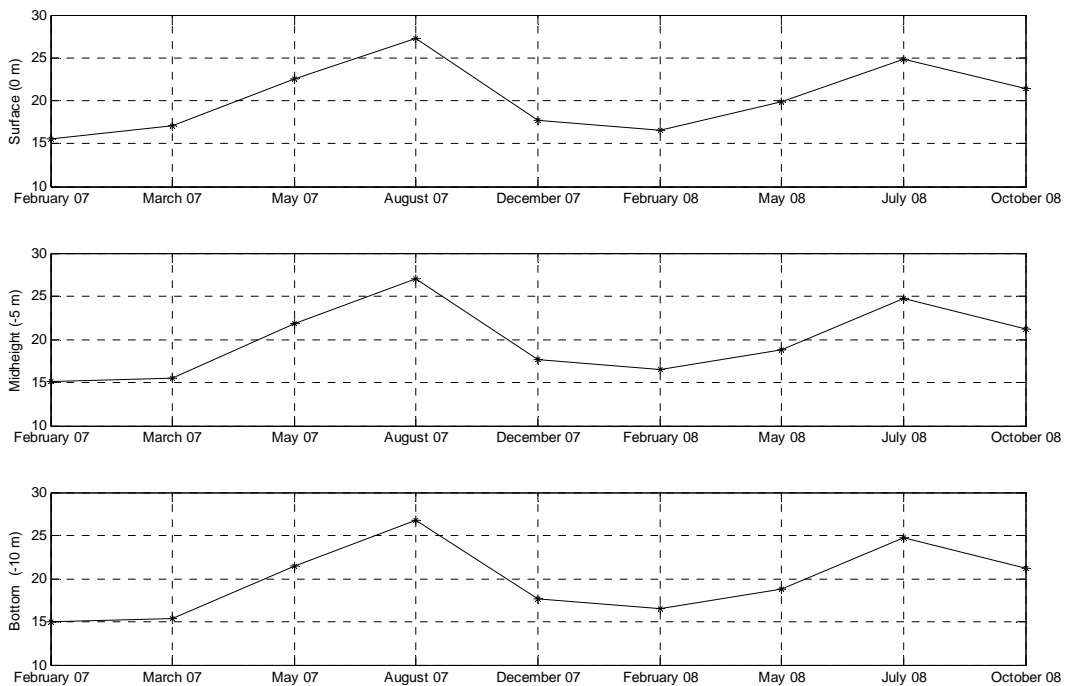


Figure 3.25. Time variation of water temperature at site #1

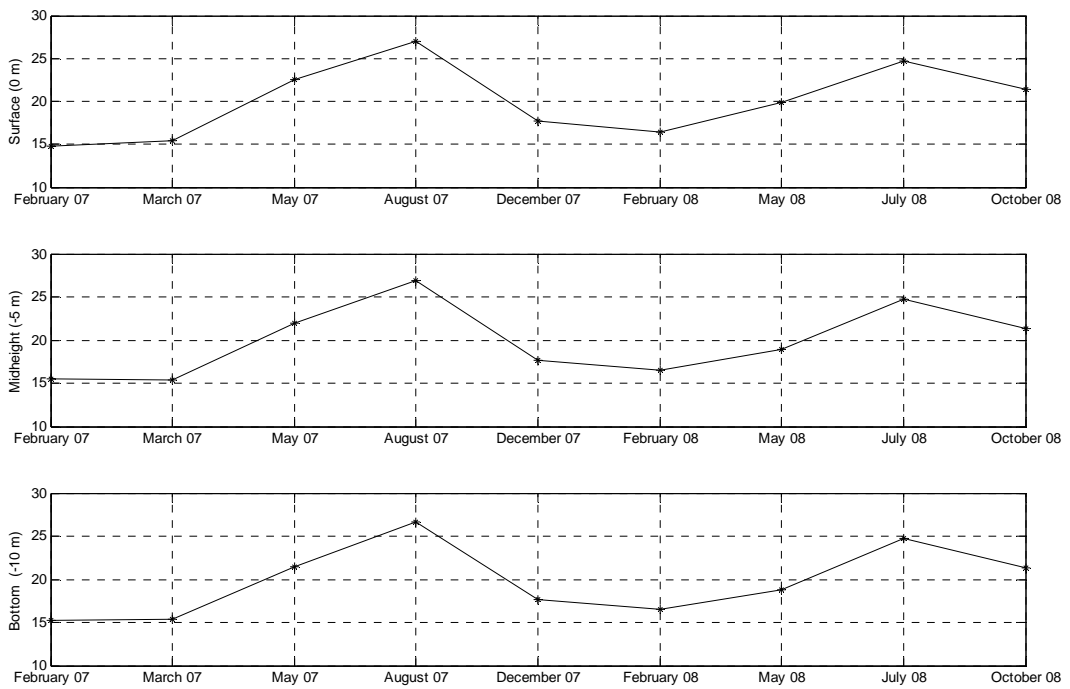


Figure 3.26. Time variation of water temperature at site #2

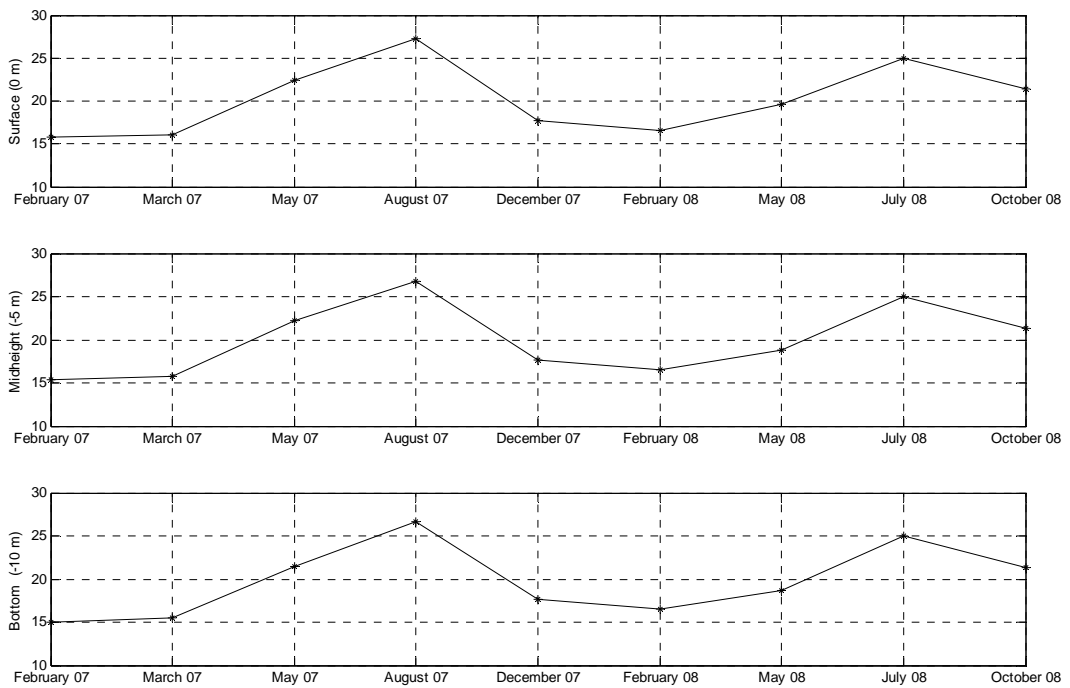


Figure 3.27. Time variation of water temperature at site #3

4. DATA REDUCTION AND INTERPRETATION

Real-time wave measurements have been conducted simultaneously with the wind records between February 9th, 2007 and October 31st, 2008. To make a full year correlation analysis, wind and wave data between November 1st, 2007 and October 31st, 2008 are used. Figure 4.1 shows the wind and wave measurement locations.



Figure 4.1. Satellite photo showing the measurement sites

The geographic conditions will play a significant role in predicting the wave characteristics out of wind measurements. For example, landward directions (North to East) will generate no waves since each direction band is assigned a fetch length according to the linear distance between the wave gage and the nearest shore in that direction. The JONSWAP formulation uses this fetch limitation and the wind speed as an input to produce waves in these direction. Therefore, their proportions should be too small to recognize in a distribution.

4.1. Time Series Analysis

First, the selected measurement period is given in time series. Figure 4.2 - 4.4 show the time histories of the predicted and measured significant wave heights, mean periods and their directions respectively. The first and second records in all three figures indicate wave parameters predicted from winds measured in Bodrum and the local weather station. The third (red colored) data shows the real-time wave measurements performed using the ADCP underwater wave gage.

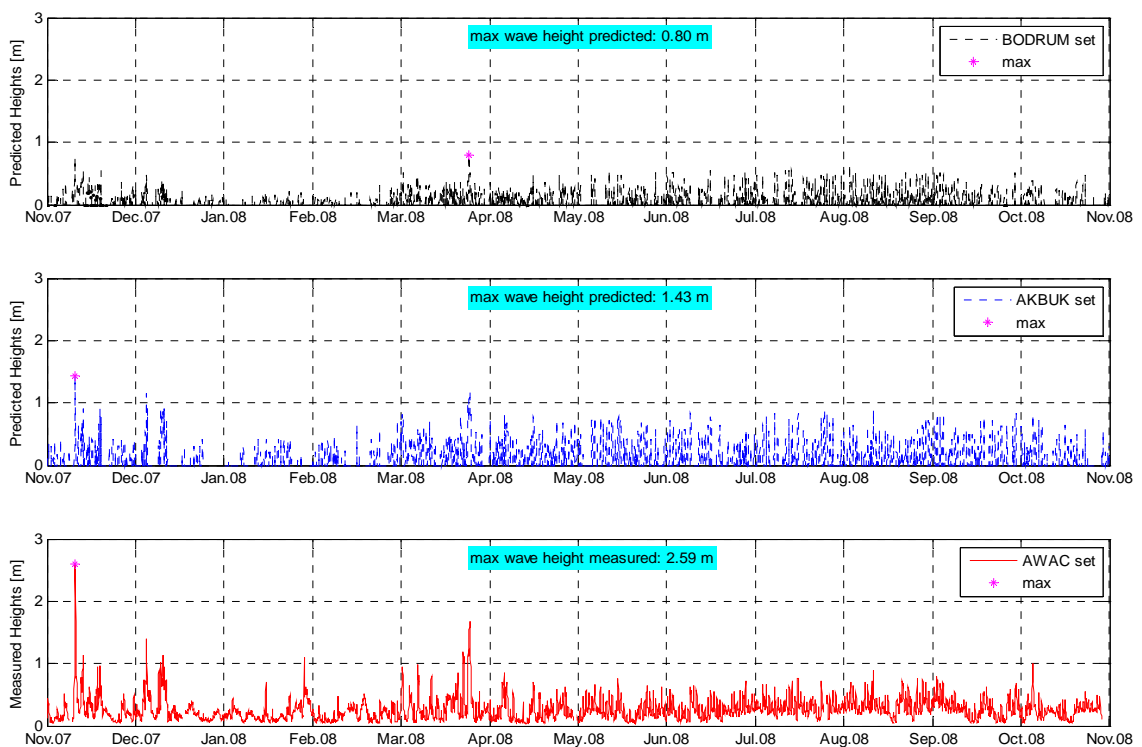


Figure 4.2. Time history of predicted and measured significant wave heights

Time series analysis of significant wave heights indicate that the measured maximum of significant wave heights is 2.59 m. Predicted results underestimate this value. Another disadvantage is that, conclusive remarks can not be made about the mean values. Moreover, abrupt changes in the wind directions produce a complicated time history of predicted wave directions, which is hard to visualize in the figure.

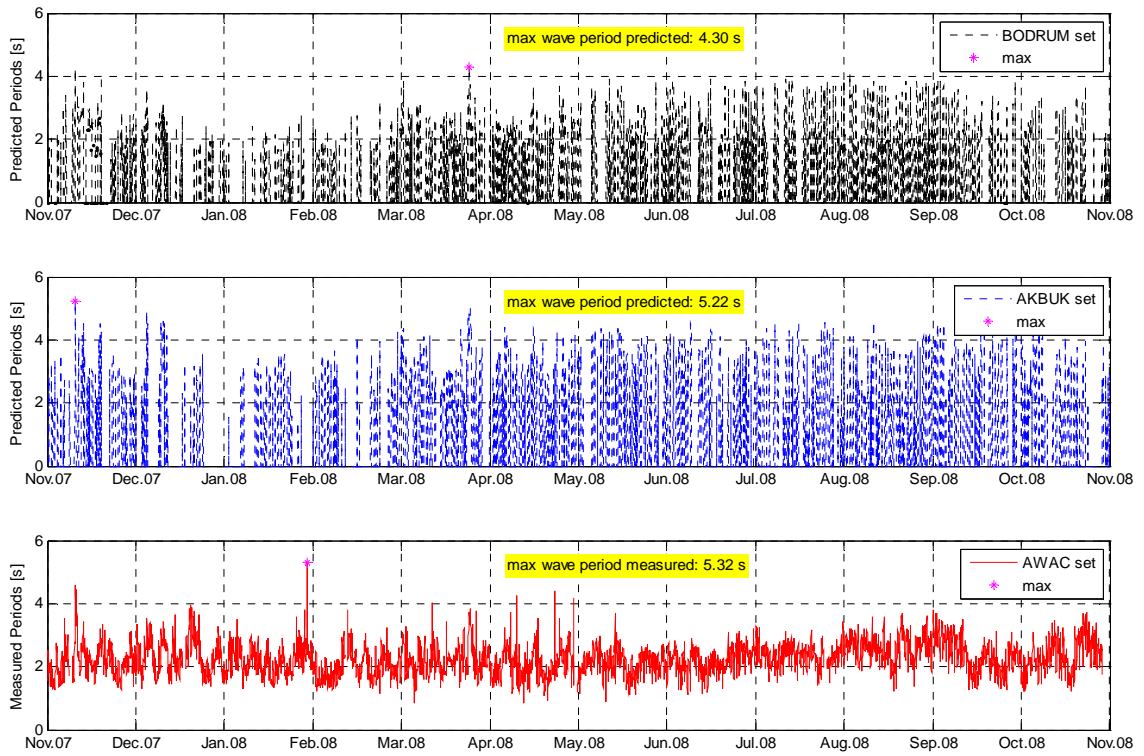


Figure 4.3. Time history of predicted and measured spectral mean periods

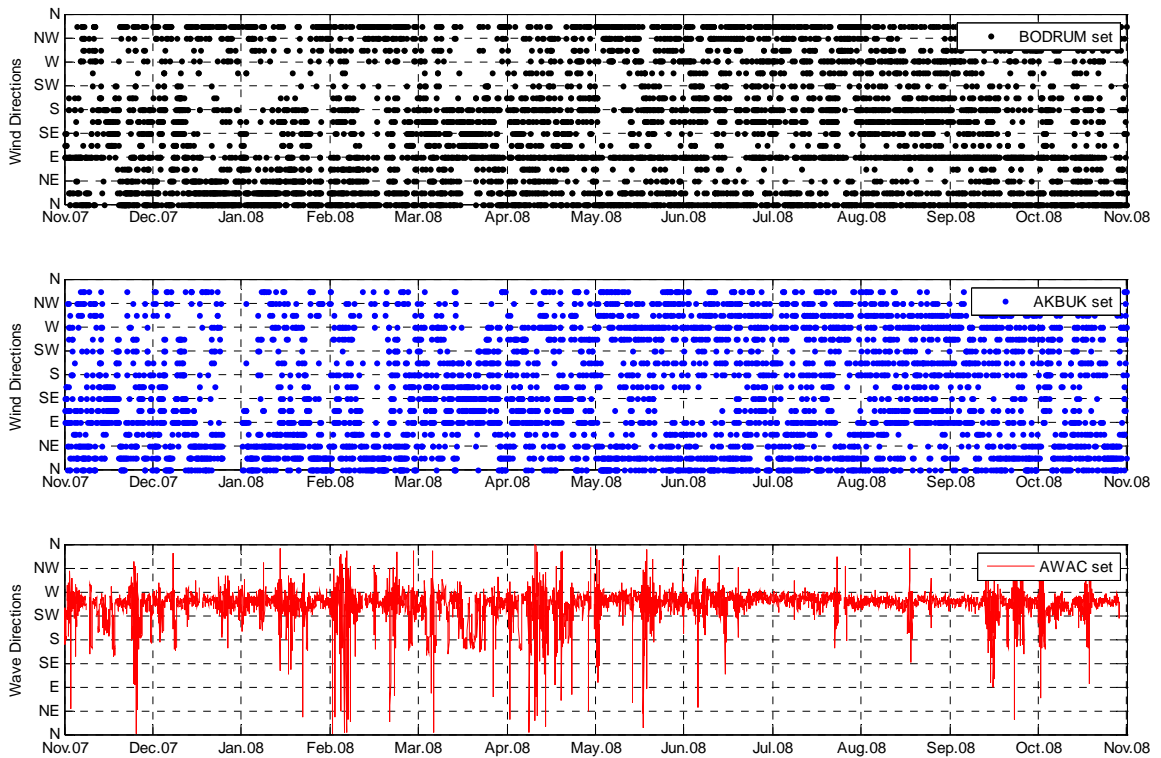


Figure 4.4. Time history of predicted and measured wave directions

Although there are some imperfections in the time series analysis, it gives an advance information about the wave parameters briefly, but it is not sufficient to understand the general wave characteristics. Therefore, the probability distribution of the wave parameters are required to make better conclusions.

4.2. Probability Distributions of Wave Parameters

4.2.1. Histograms

The significant wave height distribution of the predicted and measured sets is a useful tool to compare the theoretical expectations with the exact results. In Figure 4.5, the mean of the measured significant wave heights is larger than the predicted mean. This shows that the real wave climate may differ from the predictions which would have cause severe failures in the design steps.

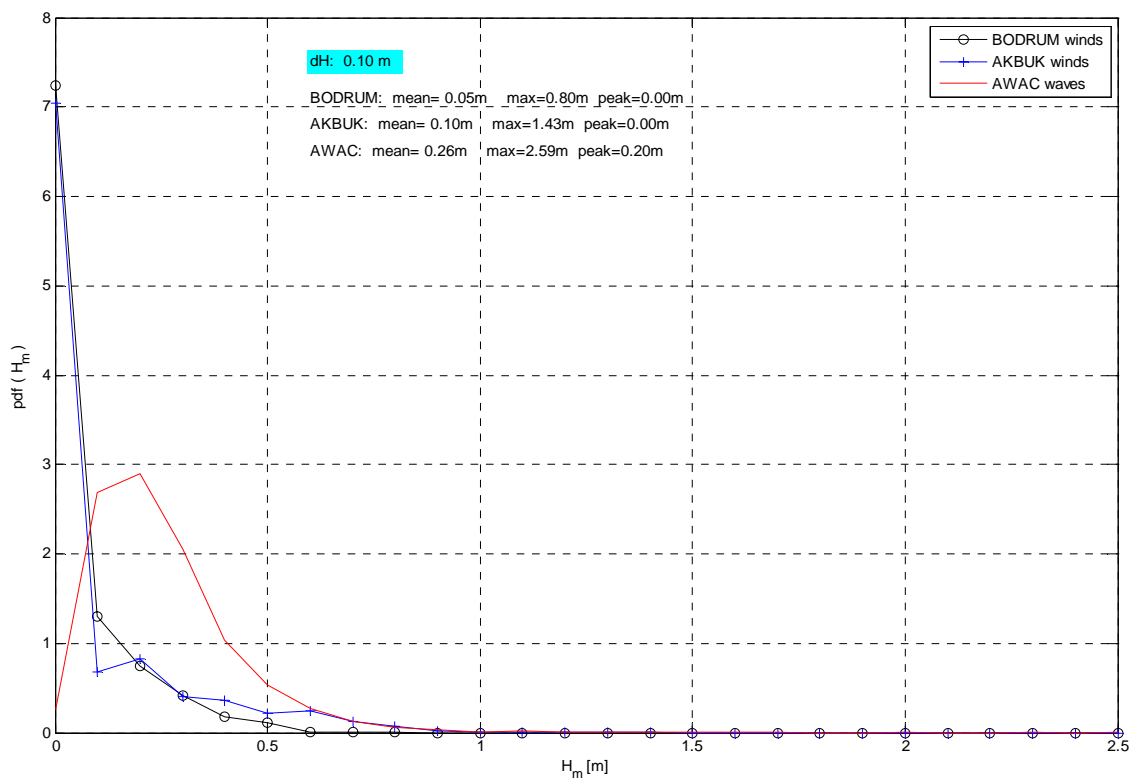


Figure 4.5. Probability distribution of predicted and measured significant wave heights

It should be noted that, the difference in the distribution of predicted and measured data might be a consequence of the swell phenomenon. On-site wind measurements take into account the local meteorological parameters which is seriously affected by the geographic conditions of the station. However, winds generated outside the circle of measurement location will also produce waves that affect the zone. These waves are called *swell waves* which originate at open sea and are not caused by local winds.

The distribution of spectral mean periods also gives invaluable information about the wave climate. By comparing the estimated level of periods with the exact wave periods, unrealistic predictions can be filtered out. Figure 4.6 shows the distribution of the predicted and measured spectral mean periods. The measured periods are less than 4 seconds. However, the predicted periods from the local winds (blue line) overestimate the 4 s level.

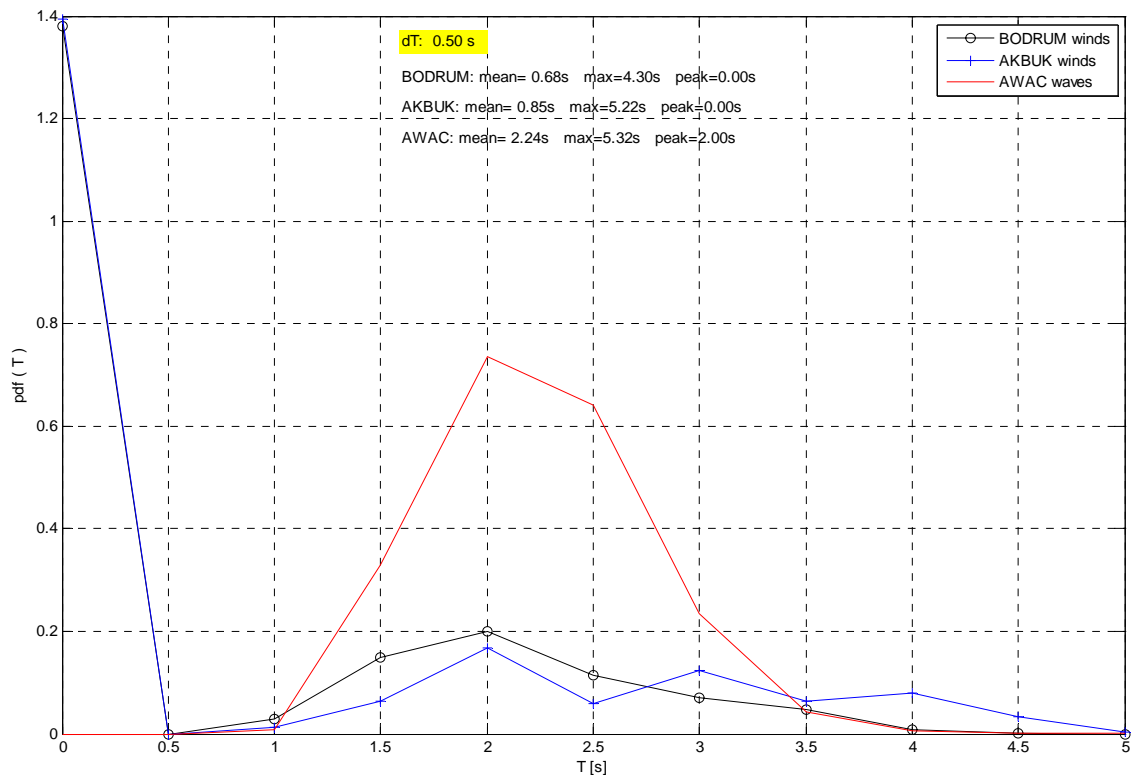


Figure 4.6. Probability distribution of predicted and measured spectral mean periods

The peak at 0 shows the calm periods (no wind or winds from the land). The project site is oriented such that northerly winds do not generate waves. Therefore, wind-to-wave formulations require a fetch filter for those directions. These fetches having a significant

proportion of the probable incoming direction of the predicted waves are supposed to be zero, which makes a sudden increase for waves with zero periods.

The similar results can be obtained through Figure 4.7. Directional probability distribution of waves is mostly related to the geographic conditions of the measurement location. Since the wave measurement area is closed to the effects of northerly directions, the distribution of waves is limited in a band of directions from SE to NW. All other directions produce zero waves and are not distinguished in the figure. However, winds from Bodrum and the local weather station estimate the peak direction as N and NNE respectively, which is not the actual case.

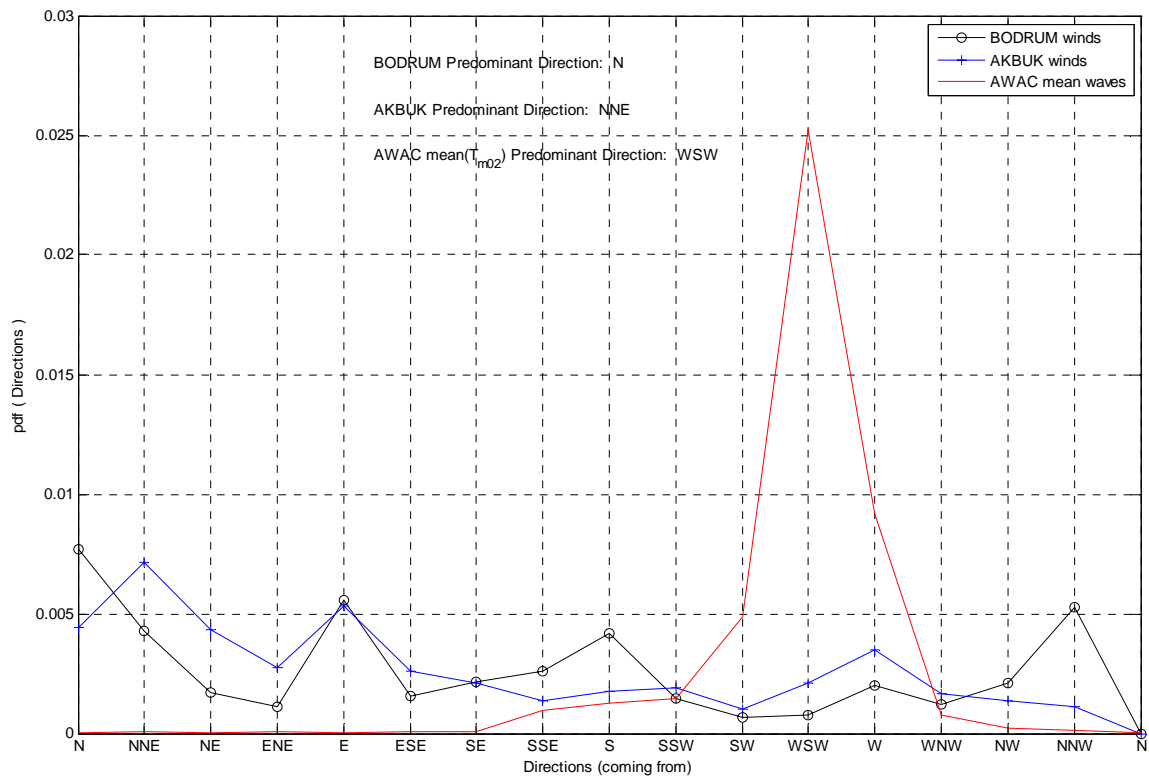


Figure 4.7. Probability distribution of predicted and measured directions

4.2.2. Directional Probability Distributions

As mentioned in Section 4.2.1, to understand the regional wave climate, one of the most crucial questions that has to be answered is the direction of incoming waves. The

joint probability distribution of significant wave heights and their directions are commonly used since they distinguish the predominant directions clearly.

The significant wave heights and spectral mean periods are redistributed after taking into account the incoming wave directions. The resultant joint probability distributions are given in polar graphs below. Figure 4.8 show that the landward directions can be filtered out by considering an imaginary line parallel to the shoreline (WNW-ESE). Theoretical significant wave heights calculated from Bodrum winds predict S as the predominant direction, whereas the local measurements predict W.

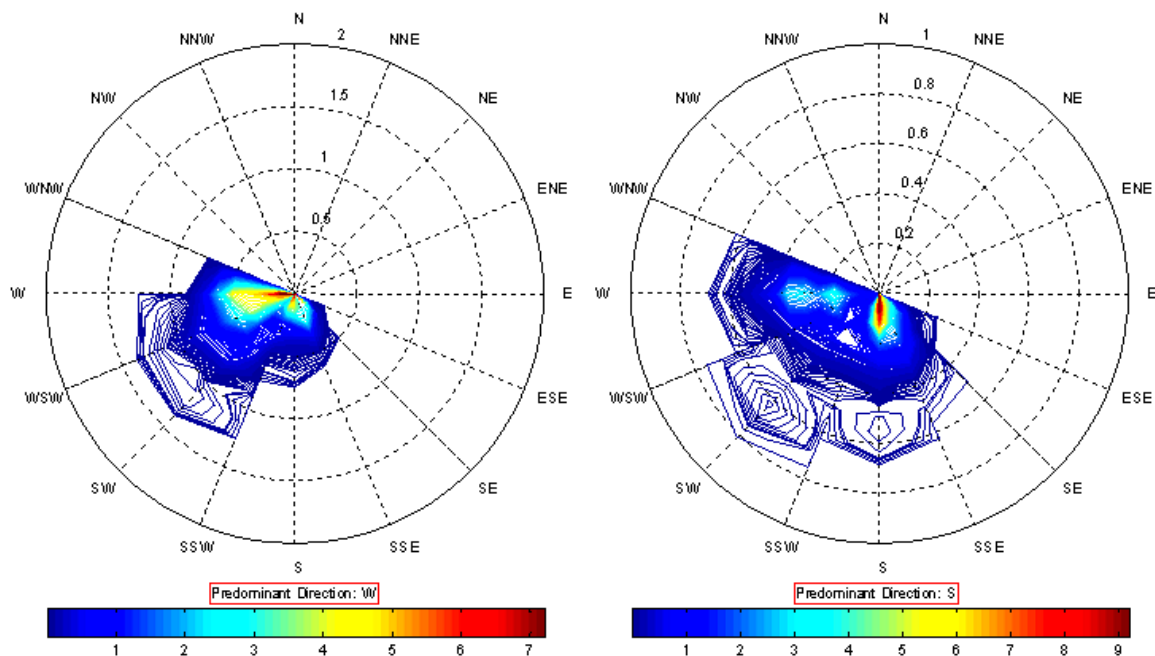


Figure 4.8. Directional distribution of predicted significant wave heights

Figure 4.9 gives the actual tendency of the significant wave heights. The directional analysis results indicate that most frequently the waves come from WSW (235° - 250° N) which coincides interestingly with the 6 km wide gap between Greek Islands Leipsoi and Leros. Due to the wide gap between these islands, the normally 50 km fetch inside Güllük Bay is extended all the way to Island Naxos, 160 km WSW of the gage. Coincidentally, this critical gap is also in the direction of the biggest storm waves recorded in November 10th, 2007.

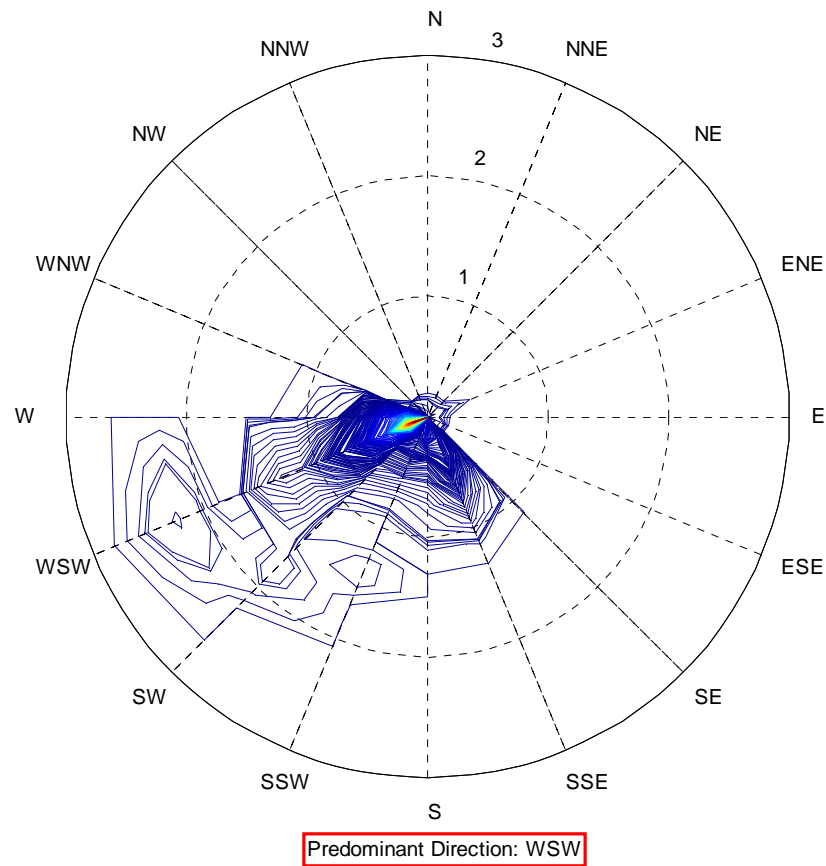


Figure 4.9. Directional distribution of measured significant wave heights

The spectral mean wave periods can be analyzed in a similar way. Figure 4.10 shows the predicted spectral mean periods, whereas Figure 4.11 shows the actual distribution of spectral mean wave periods.

An interesting finding of the directional period analysis is that there is a peak in the landward directions (Figure 4.11), where the fetch is very short and therefore can not produce wind waves at those periods. These peaks are not visible in Figure 4.9 in terms of wave heights. It is remarkable that these peaks occur just at the opposite direction of the real peaks. The imaginary peaks are obviously the reflection of the actual waves from the rocky shore. This justifies a well-known wave theory stating that reflected waves lose their energy by a decrease in wave height but the wave period remains unaffected.

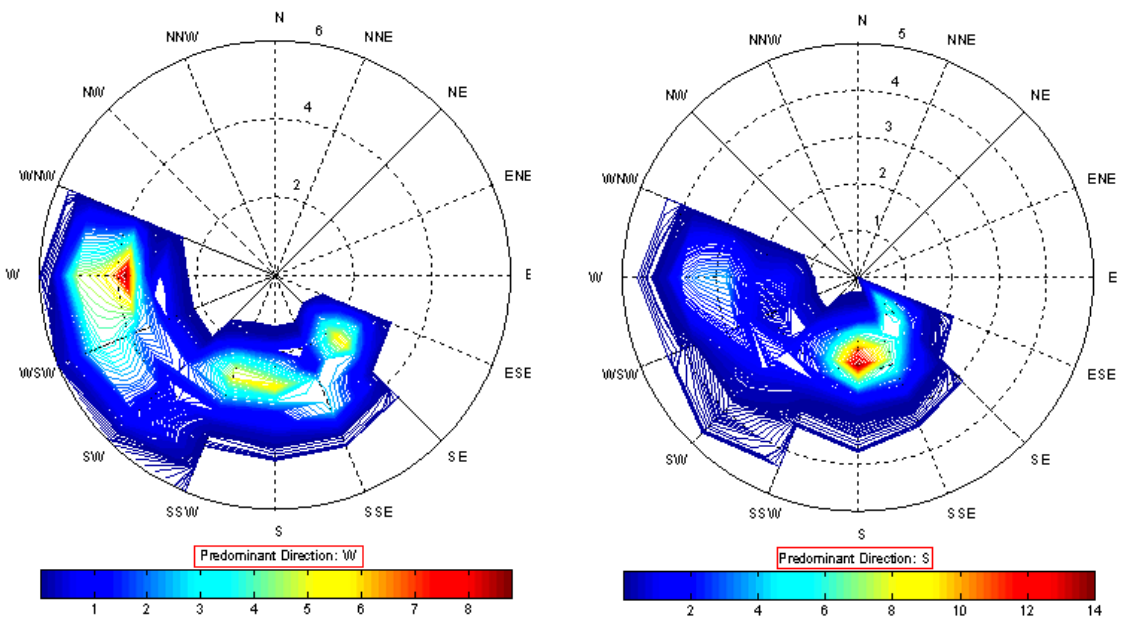


Figure 4.10. Directional distribution of predicted spectral mean periods

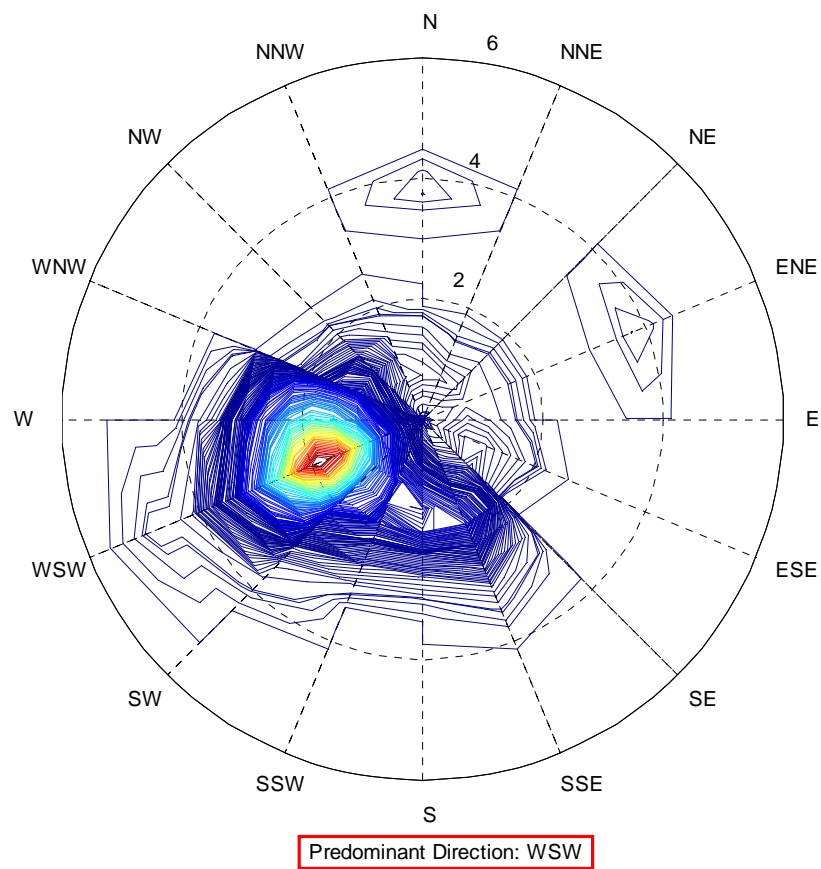


Figure 4.11. Directional distribution of measured spectral mean periods

The predicted results overestimate the range of periods. Due to fetch limitations and calm winds, predicted spectral mean periods are filtered. The results are compared with the actual spectral mean wave periods measured with the ADCP underwater wave gage. Similar with the wave heights analysis, observations indicate WSW to be the critical wave direction (Figure 4.12).

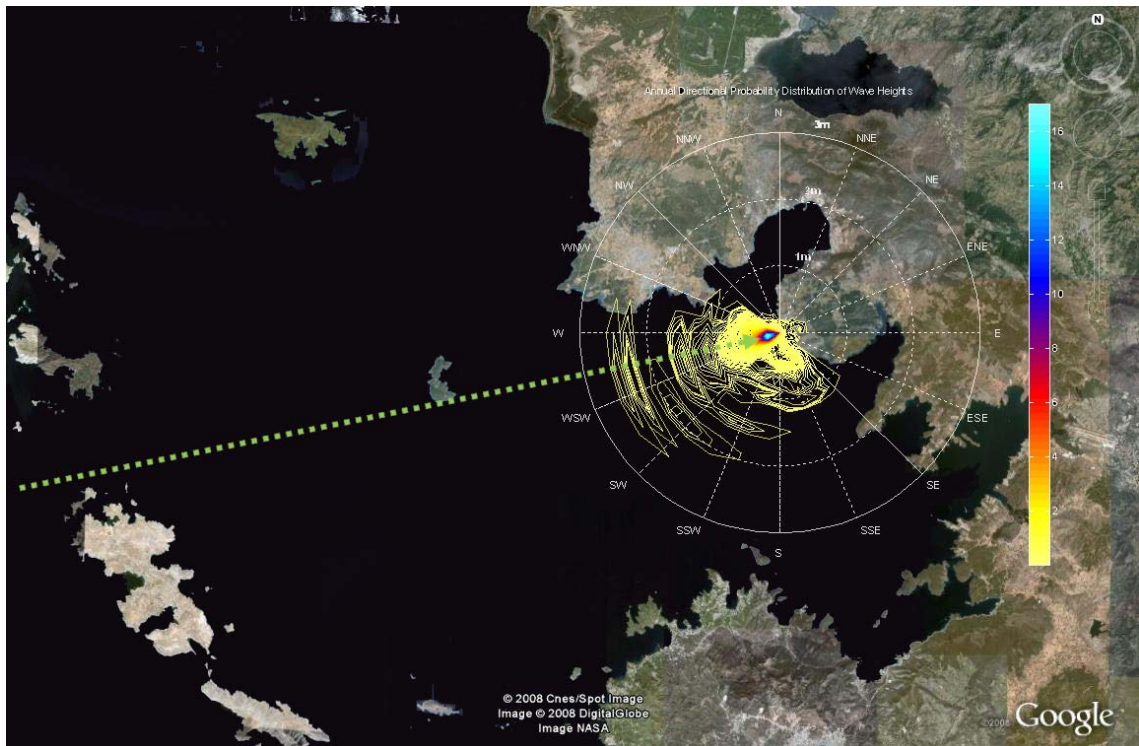


Figure 4.12. Critical direction of incoming waves WSW (230° - 250° N)

4.2.3. JPD of Significant Wave Heights and Spectral Mean Periods

Information on long-term wave characteristics is best represented by making use of the joint probability densities of the significant wave heights and spectral mean wave periods. Since wave heights and periods are not statistically independent, their joint probability distribution plays a significant role in predicting statistical properties of waves such as the frequency of occurrence of resonant motion which may occur when wave periods are close to the natural motion period of a structural system.

In Figure 4.13 the joint probability distribution of significant wave heights and spectral mean wave periods are presented.

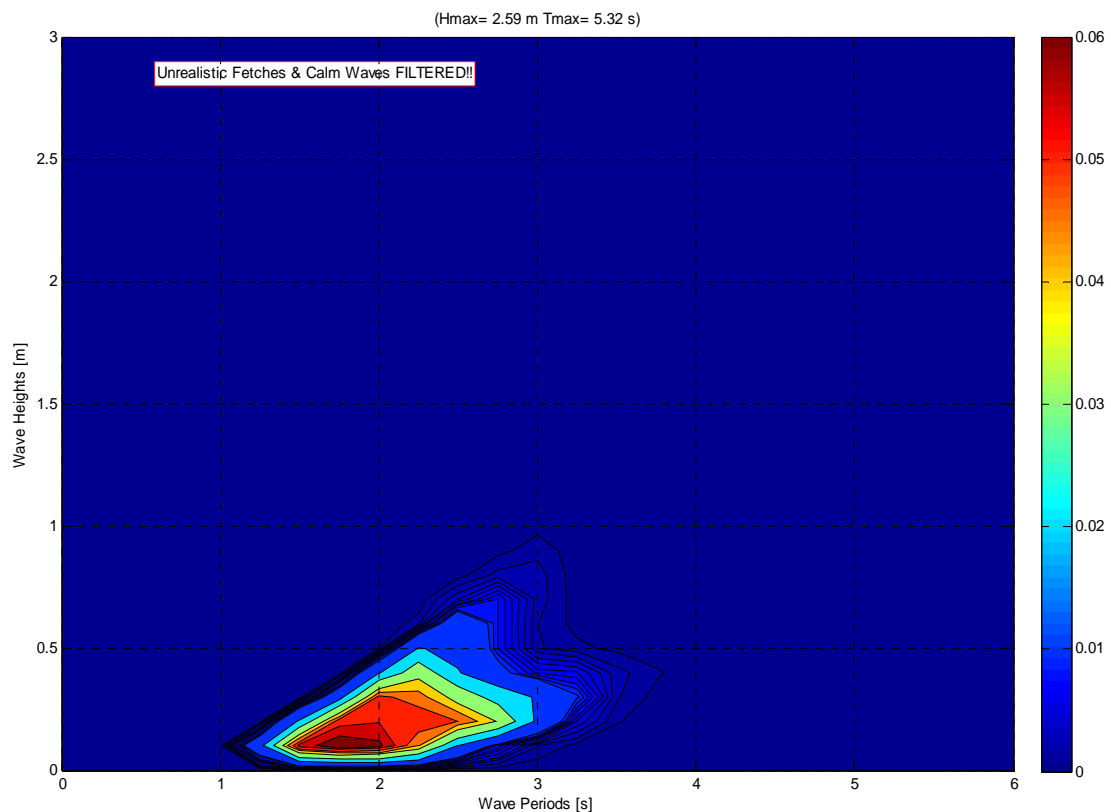


Figure 4.13. Joint probability distribution of significant wave heights and spectral mean periods derived from real-time measurements

4.3. Statistical Presentation of Sea Severity

The most commonly available information on sea severity is the statistical tabulation of significant wave heights obtained through direct measurements over several years. The reliability of the data increases with the number of accumulations. It is highly recommended that data be obtained at least at 3-hour intervals so that a relatively rapid change in the sea conditions will not be missed.

In this study, the short-term wave data (wave burst) was measured with a sampling rate of 4 Hz for 17 minutes duration. Each of these 17-minutes burst data sets are analyzed and a single value of significant wave height is assigned to the 1-hour intervals for a full-

year. The distribution of these long-term record of significant wave heights are compared to well-known probability distributions which appear to best fit the observed data.

It is a general trend that the greater part of significant wave height data is well represented by the log-normal probability distribution. On the other hand, the cumulative distribution function of large significant wave heights can be well represented by the Weibull distribution. A comparison between the histogram of observed significant wave heights and the Log-normal, Weibull and generalized Gamma distributions is given in Figure 4.14.

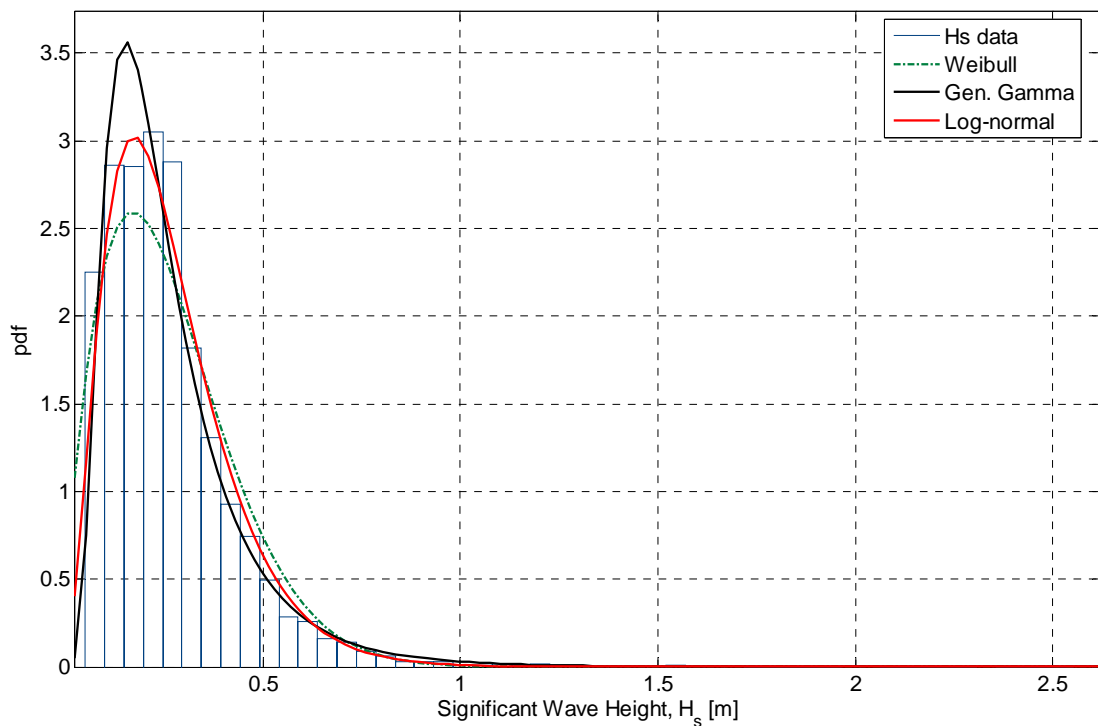


Figure 4.14. Comparison between H_s and well-known probability distributions

As far as is known, log-normal distribution represents significant wave heights well except for large values, and large significant wave height data are well represented by the Weibull distribution. Some empirical model might be proposed by combining these two distributions at a certain value. However, the specification of the transition point is arbitrary in that case.

It is found from the results of analysis that the cumulative distribution function of the standardized generalized Gamma distribution is nearly equal to that of the Log-normal distribution up to 0.90, but the former converges to unity much faster above 0.90. This feature of the generalized Gamma distribution is considered to make use in the statistical analysis of significant wave heights.

A comparison between the cumulative distribution function of significant wave height data and the Log-normal, Weibull and generalized Gamma distributions is given in Figure 4.15. The same results are plotted on a semi-log chart given in Figure 4.16.

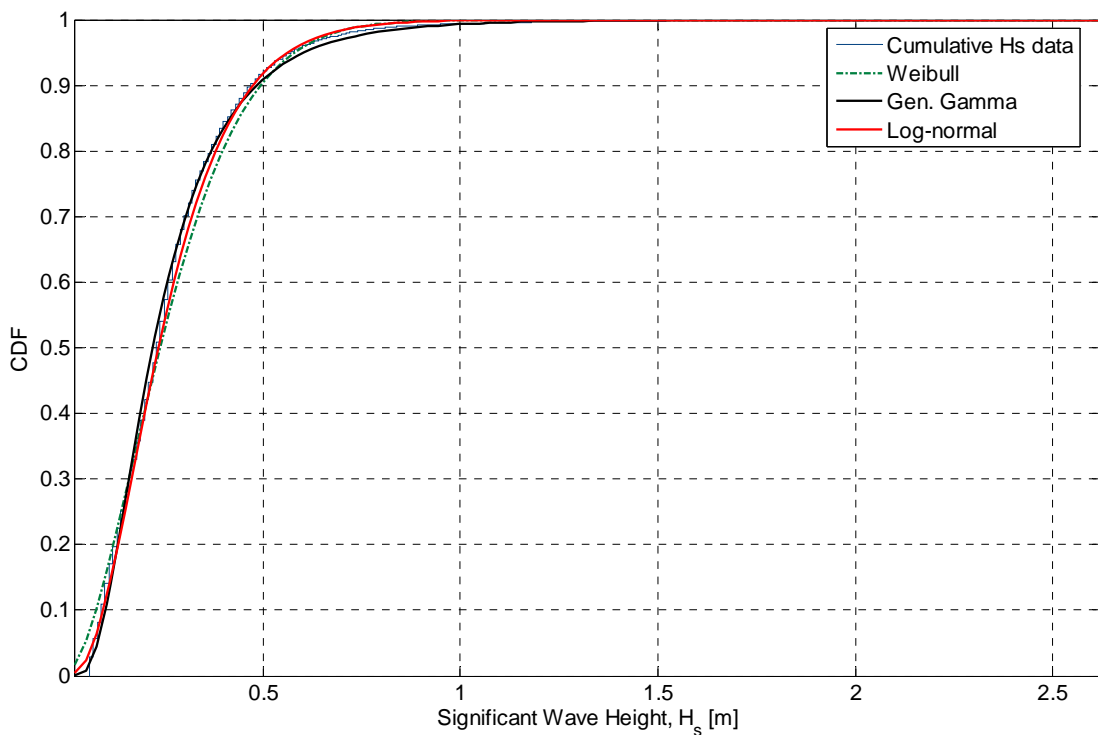


Figure 4.15. Comparison between cumulative H_s and well-known probability distributions

The statistical comparison of observed data and the well-known distributions is carried out using MATLAB Statistical Toolbox-Distribution Fitting Tool. The statistical toolbox gives the opportunity to choose any desired distribution and to compare data easily. However, goodness-of-fit tests are not provided. Therefore, Mathwave-Easyfit 5.1 software is used to derive the goodness-of-fit statistics.

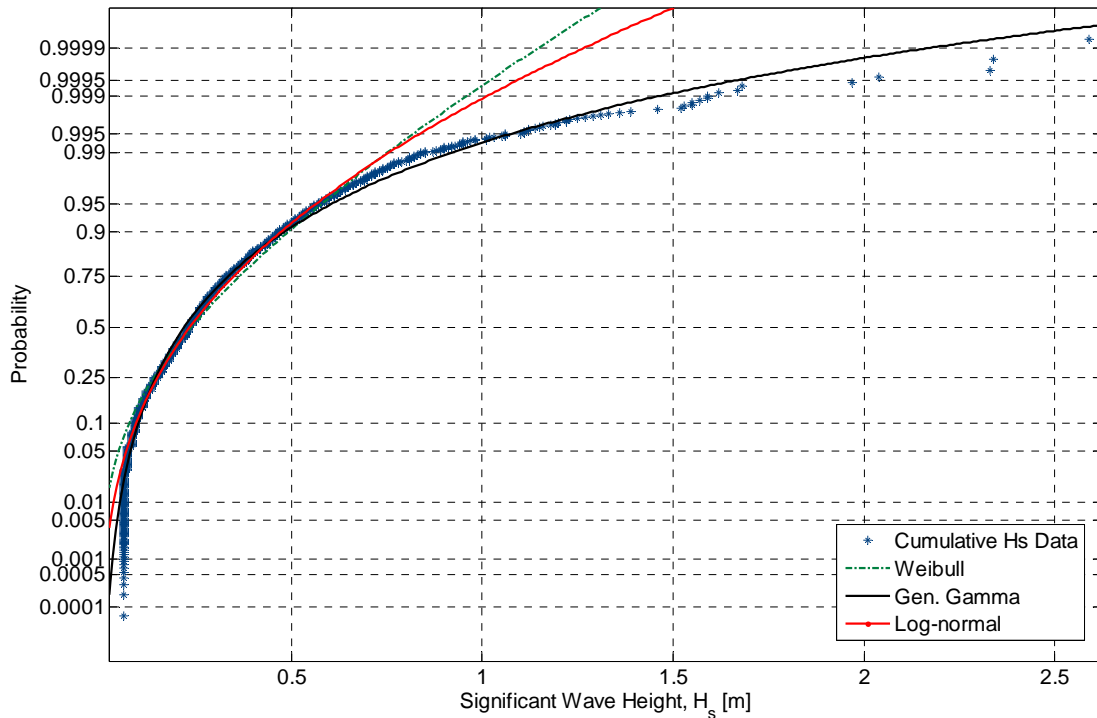


Figure 4.16. Comparison between cumulative H_s and well-known probability distributions shown on a semi-log chart

4.4. Goodness of Fit Test

The analysis results indicate that the generalized Gamma distribution represents the data well in the domains where the Log-normal and Weibull distributions fail to satisfactorily agree with the measured data set.

The semi-log chart given in Figure 4.16 is visually more clear to make a justified conclusion. However, without any statistically based assurance, these figures do not have any statistical significance. Therefore, it is necessary to examine the data sample with so called *goodness-of-fit tests* in statistical inference theory.

Although several goodness of fit tests are available in the literature, only typical tests suitable for analysis of wave data are discussed. One is the χ^2 test, which has been used extensively in various fields of applied statistics, the other is the Kolmogorov-Smirnov's test, which has the advantage of being applicable even for a sample consisting of a small

number of observations. Table 4.1 gives a summary of the sample statistics. Using these parameters, the goodness-of-fit tests including the Chi-square (χ^2) test and the Kolmogorov-Smirnov test are performed.

Table 4.1. Summary of sample statistics

Statistic	Value
Sample Size	8594
Range	2.56
Mean	0.258658
Variance	0.031363
Std. Deviation	0.177097
Coef. of Variation	0.684675
Std. Error	0.00191
Skewness	2.64447
Excess Kurtosis	16.5787

The results of the tests are presented in Table 4.2. Further detail about the test procedure can be found in the Appendices.

Table 4.2. Goodness-of-fit test results

#	Distribution	Chi-Square		Kolmogorov-Smirnov	
		Statistic	Rank	Statistic	Rank
1	Gen. Gamma	267.346	1	0.042321	1
2	Log-Normal	293.047	2	0.047209	2
3	Weibull	607.855	3	0.048075	3
4	3P Weibull	705.176	4	0.061522	4

The goodness-of-fit test results indicate generalized Gamma distribution as the most appropriate probability distribution among others. However, the ranking of the distribution

should not be trusted since the null hypothesis is still rejected. The Chi-Square statistic χ^2 is calculated as 267.346, whereas, the critical value for different significance levels is given in Table 4.3.

Table 4.3. Chi-Square goodness-of-fit test details

Deg. of Freedom	13				
Statistic	267.346				
Rank	1				
α	0.2	0.1	0.05	0.02	0.01
Critical Value	16.9848	19.8119	22.362	25.4715	27.6882
Reject?	Yes	Yes	Yes	Yes	Yes

The critical value χ_* is exceeded for each α value. The null hypothesis implying that the distribution fit is acceptable in that significance level is therefore rejected.

Similarly, the Kolmogorov-Smirnov test details are presented in Table 4.4, which indicates that the generalized Gamma distribution is not in the acceptable significance level for the observed data.

Table 4.4. Kolmogorov-Smirnov goodness-of-fit test details

Sample Size	8594				
Statistic	0.042321				
Rank	1				
α	0.2	0.1	0.05	0.02	0.01
Critical Value	0.011574	0.013193	0.014649	0.016375	0.017572
Reject?	Yes	Yes	Yes	Yes	Yes

5. CONCLUSIONS

In this study, the main objective was to put forth the wave climate of the Aegean Coast of Turkey with a special focus on the Güllük Region. The area in scope is selected as a base for a future coastal development project taking into account the significance of the wind and wave climate.

Any nearshore structural activity is affected by the waves in terms of amplitude, frequency and direction. In this study, the distributions of these parameters are derived by direct measurements via an acoustic Doppler current profiler. On the other hand, these parameters may be estimated by theoretical derivations developed by researchers in the past.

Wind statistics were used to predict waves in addition to the real time wave data. Both long-term (25 years) and local wind data (1 year) were utilized for that purpose. Real time wave measurements showed that the wind statistics are seriously affected from the geographic properties of the measurement station surroundings and swell waves are not easy to distinguish through wind measurements. It is not reliable to make accurate predictions on the wave climate when swell phenomenon is taken into account.

The surrounding Greek islands provide a natural barrier for the region against external waves such that the effective fetches are reduced to approximately 50 km inside the chain of islands except for the gap between Leipsoi and Leros, where the fetch is extended all the way to Island Naxos in that direction. Results of statistical analysis indicated WSW (230° - 250° N) to be the most probable direction which coincides with the 6 km wide gap between these islands. One of the most important findings of this study was that the Güllük Region is seriously affected by the swell waves penetrating through this 6 km wide gap.

Another significant outcome of this thesis is that the Generalized Gamma distribution represents the significant wave heights best; however, it is not satisfactory in terms of

Goodness-of-fit tests. A data set of a longer period might give better results in fitting a well-known distribution.

The results acquired from wave analysis gives invaluable information about the characteristics of a coastal zone. However, the topography and the bathymetry also play a significant role in the feasibility of a construction in that area. The area in scope was surveyed in terms of topography and the nearshore bathymetry up to 30 m depth contour. Final bathymetry map was obtained to define the sea bed characteristics.

Another dimension of this study was to monitor water quality. Environmental studies were carried out simultaneously with the wind and wave measurements during the field activities. Marine life and effect of fisheries on the environment were investigated.

Although the primitive objectives are dealing with the statistical wave analyses, it should be noted that the results of the topographic and bathymetric surveys provide invaluable information about the characteristics of the coastal region. Further efforts might be concentrated on the feasibility of constructional activities. Possible beach nourishment sites are determined and also the development of a marina might be reasonable for further studies.

APPENDIX A: Local Meteorological Statistics

A.1. Time Series of the Yearly Record

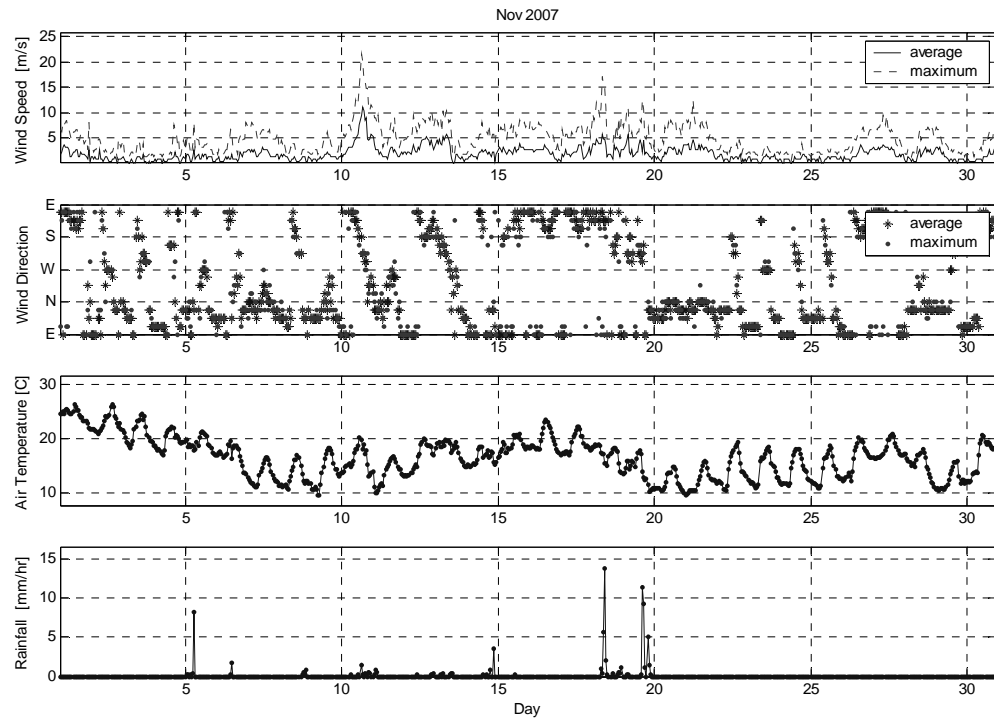


Figure A.1. Time history of local meteorological parameters (November 2007)

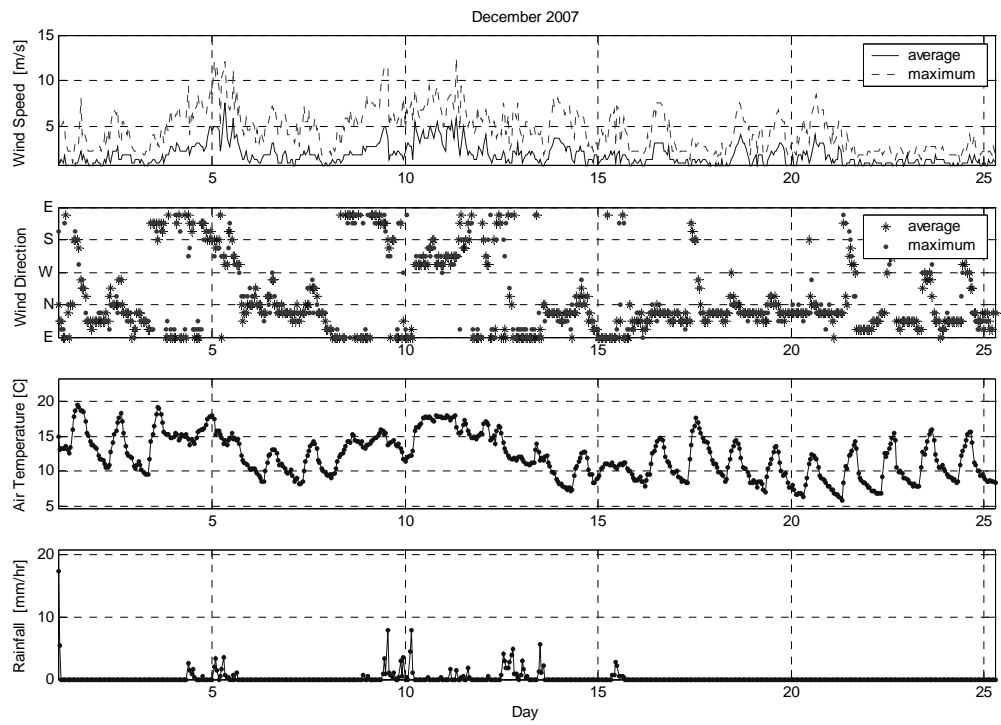


Figure A.2. Time history of local meteorological parameters (December 2007)

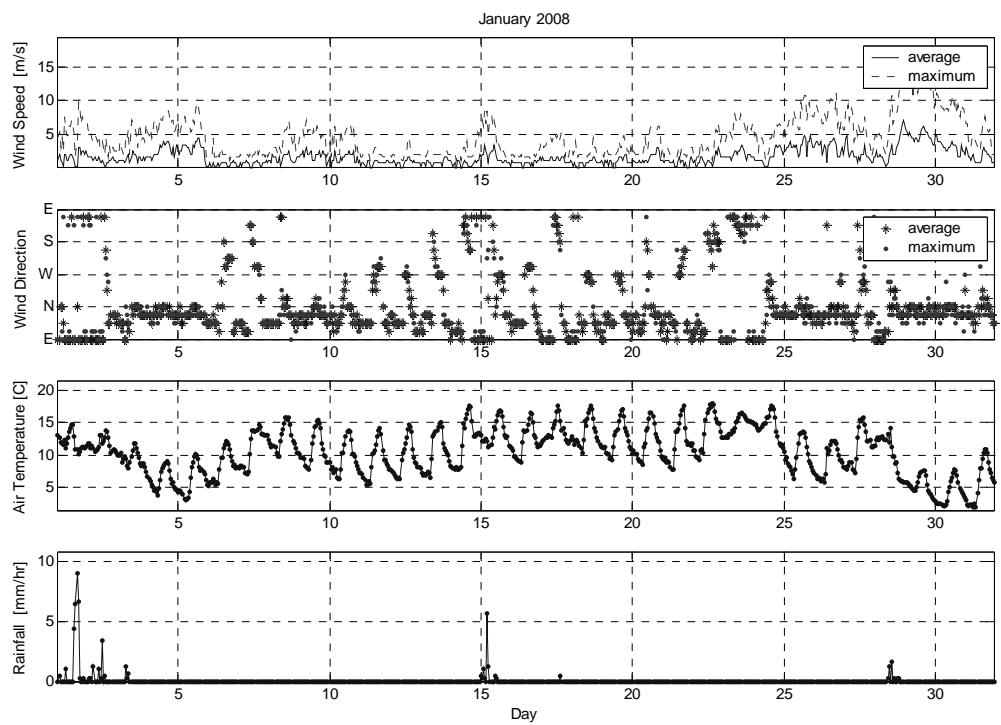


Figure A.3. Time history of local meteorological parameters (January 2008)

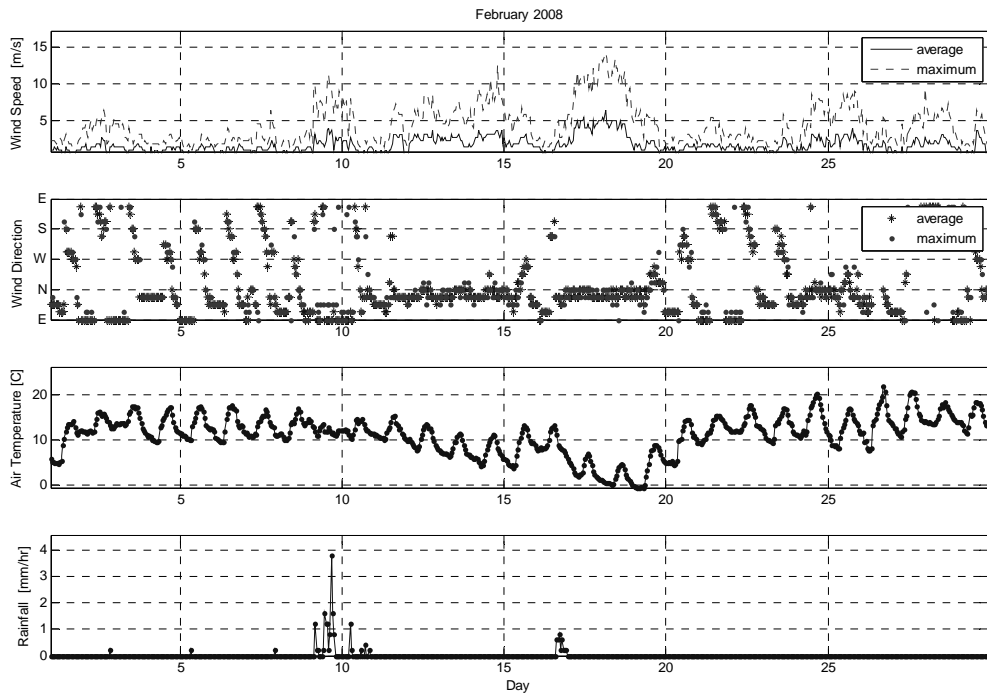


Figure A.4. Time history of local meteorological parameters (February 2008)

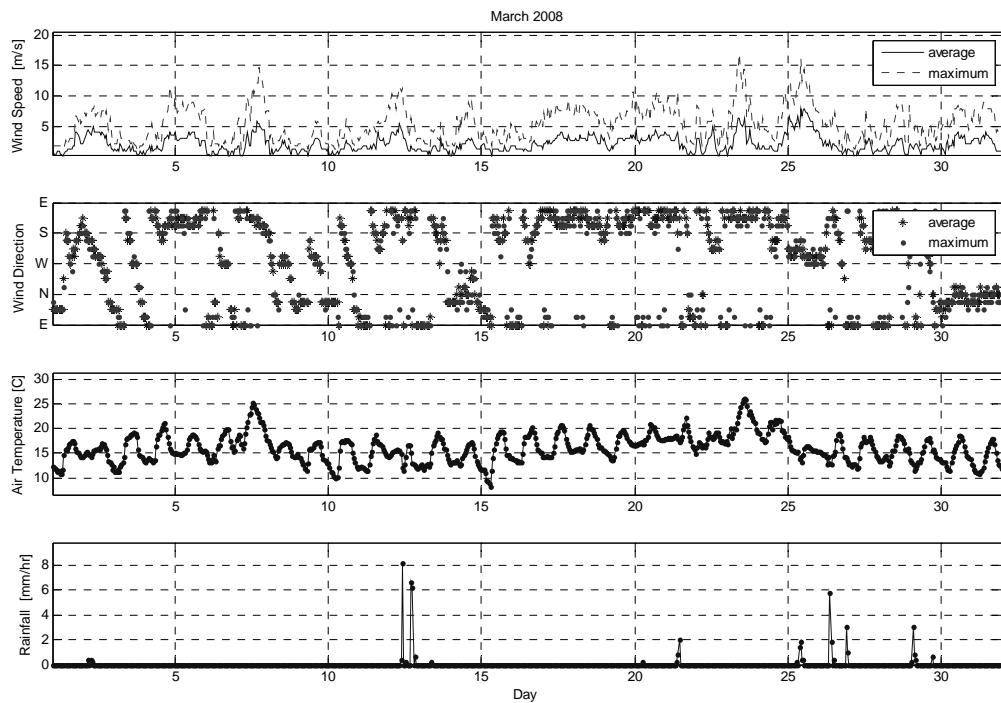


Figure A.5. Time history of local meteorological parameters (March 2008)

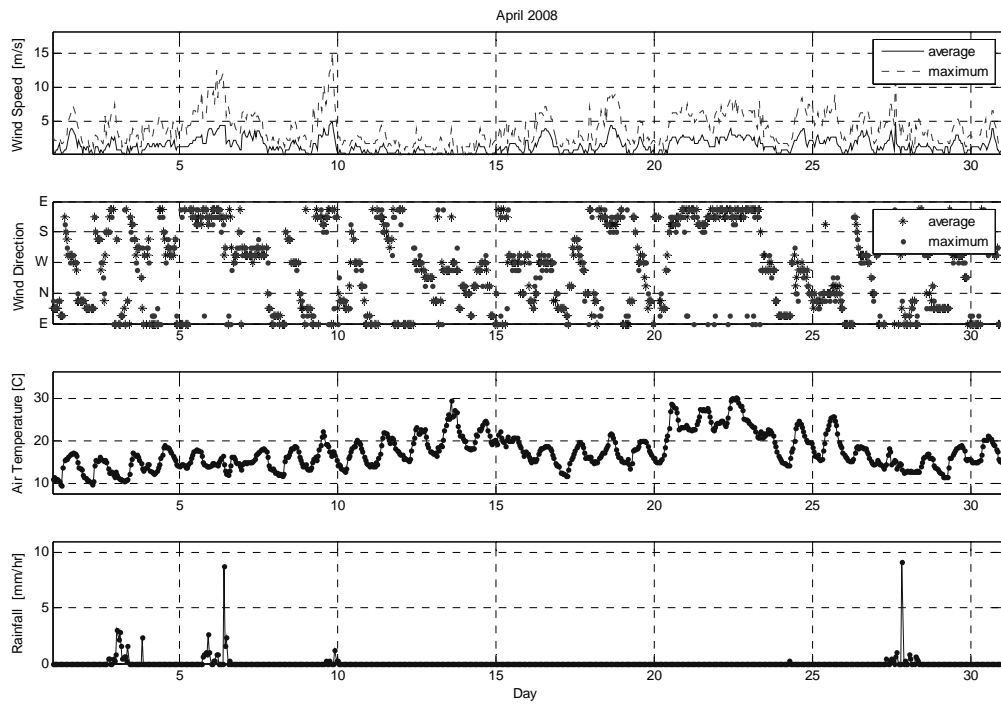


Figure A.6. Time history of local meteorological parameters (April 2008)

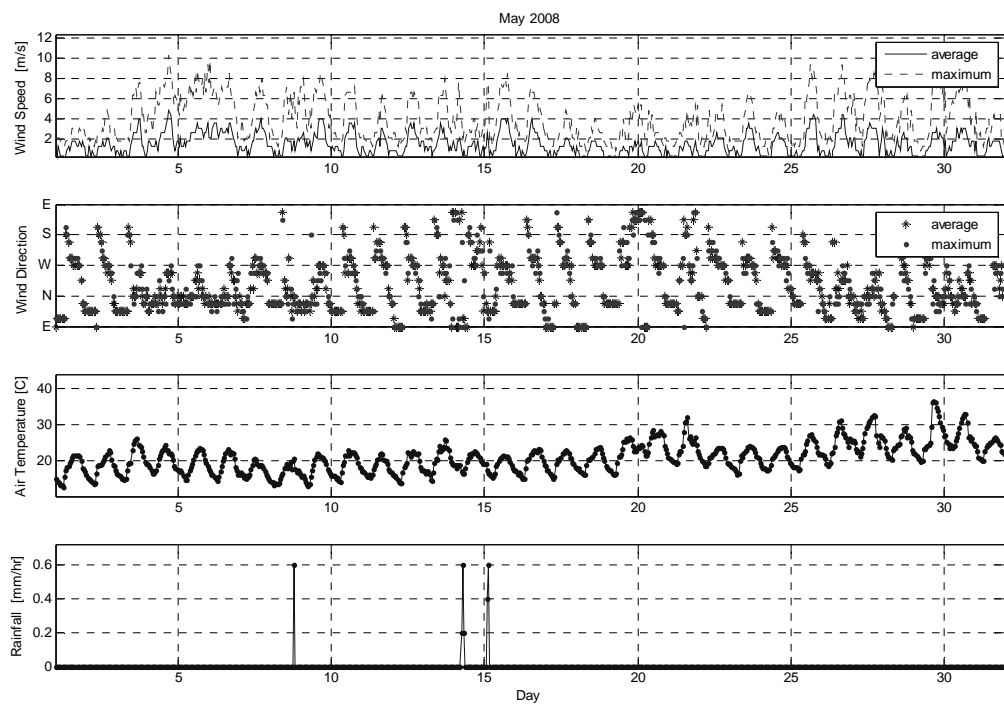


Figure A.7. Time history of local meteorological parameters (May 2008)

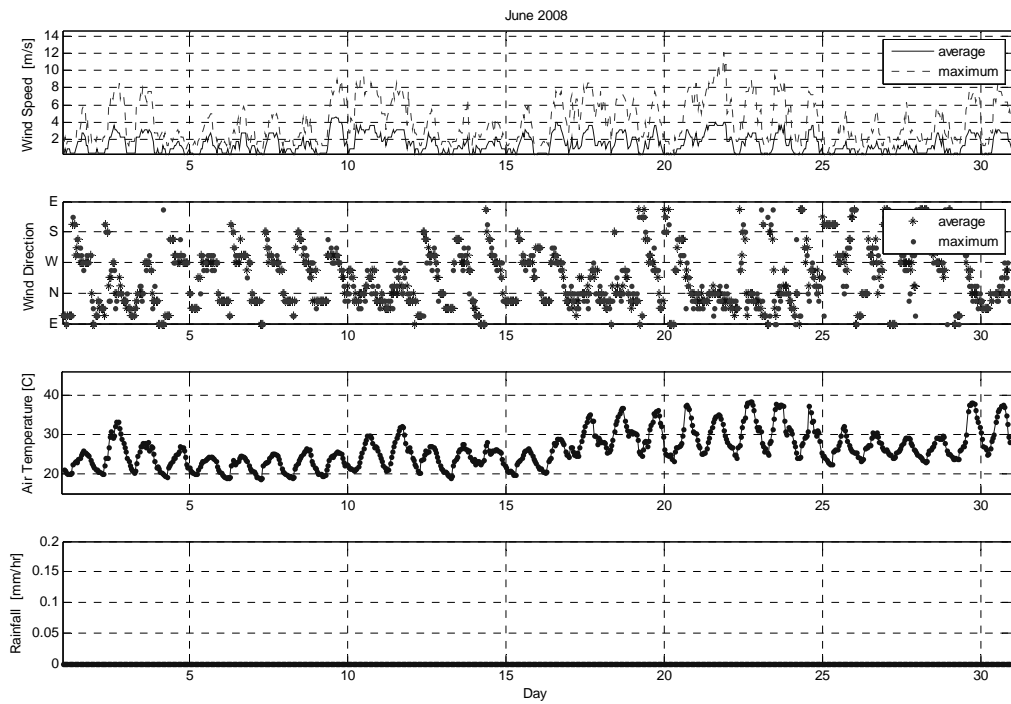


Figure A.8. Time history of local meteorological parameters (June 2008)

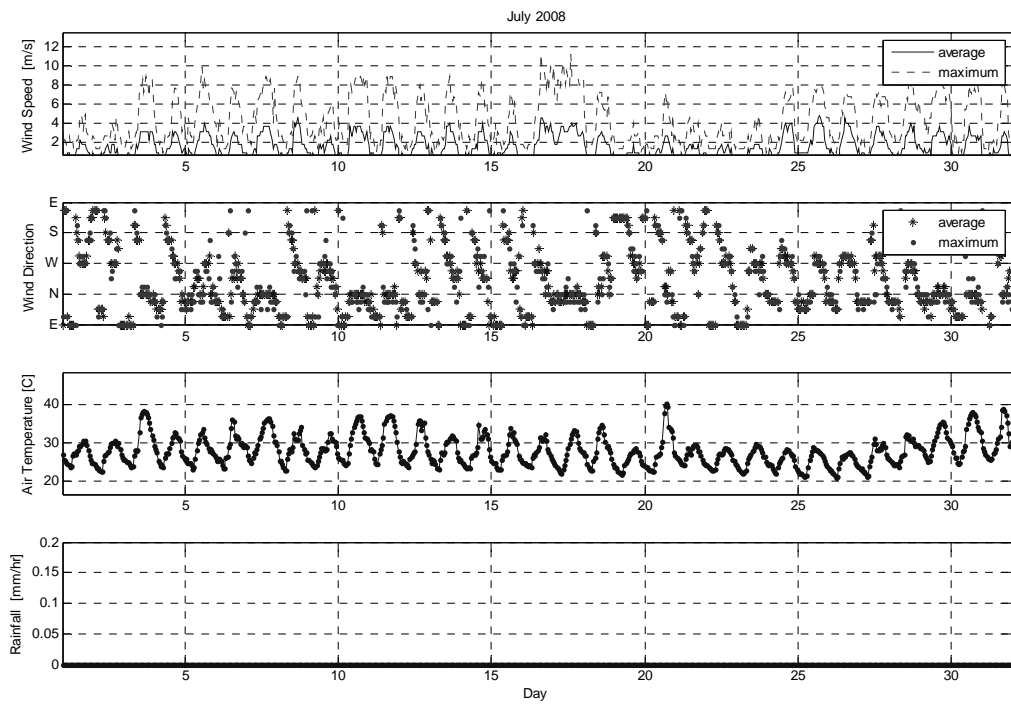


Figure A.9. Time history of local meteorological parameters (July 2008)

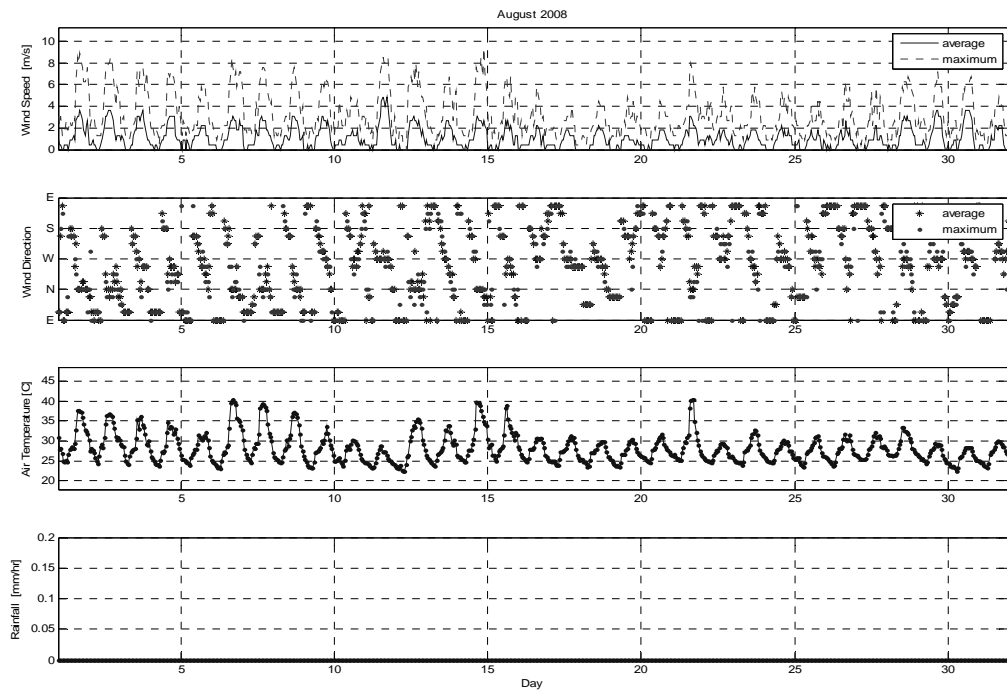


Figure A.10. Time history of local meteorological parameters (August 2008)

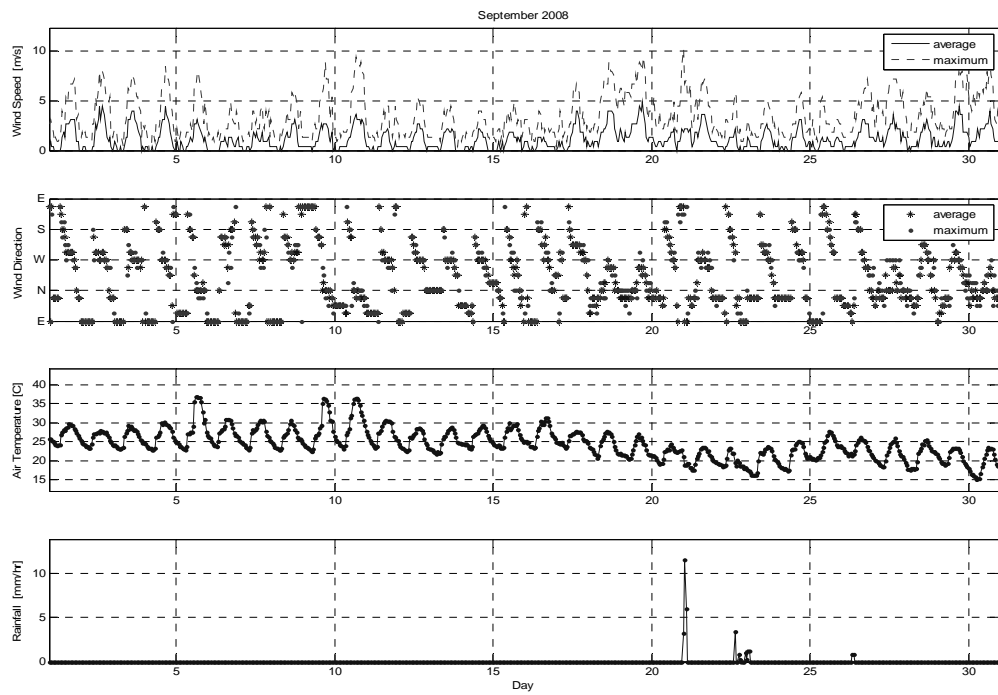


Figure A.11. Time history of local meteorological parameters (September 2008)

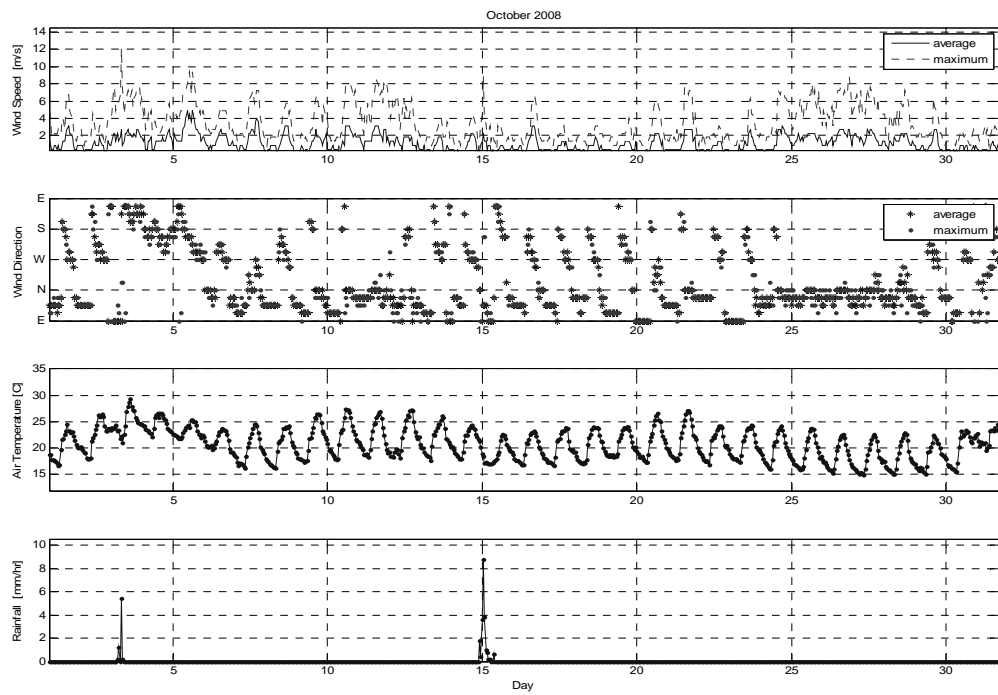


Figure A.12. Time history of local meteorological parameters (October 2008)

A.2. Monthly Histograms and Directional Distributions

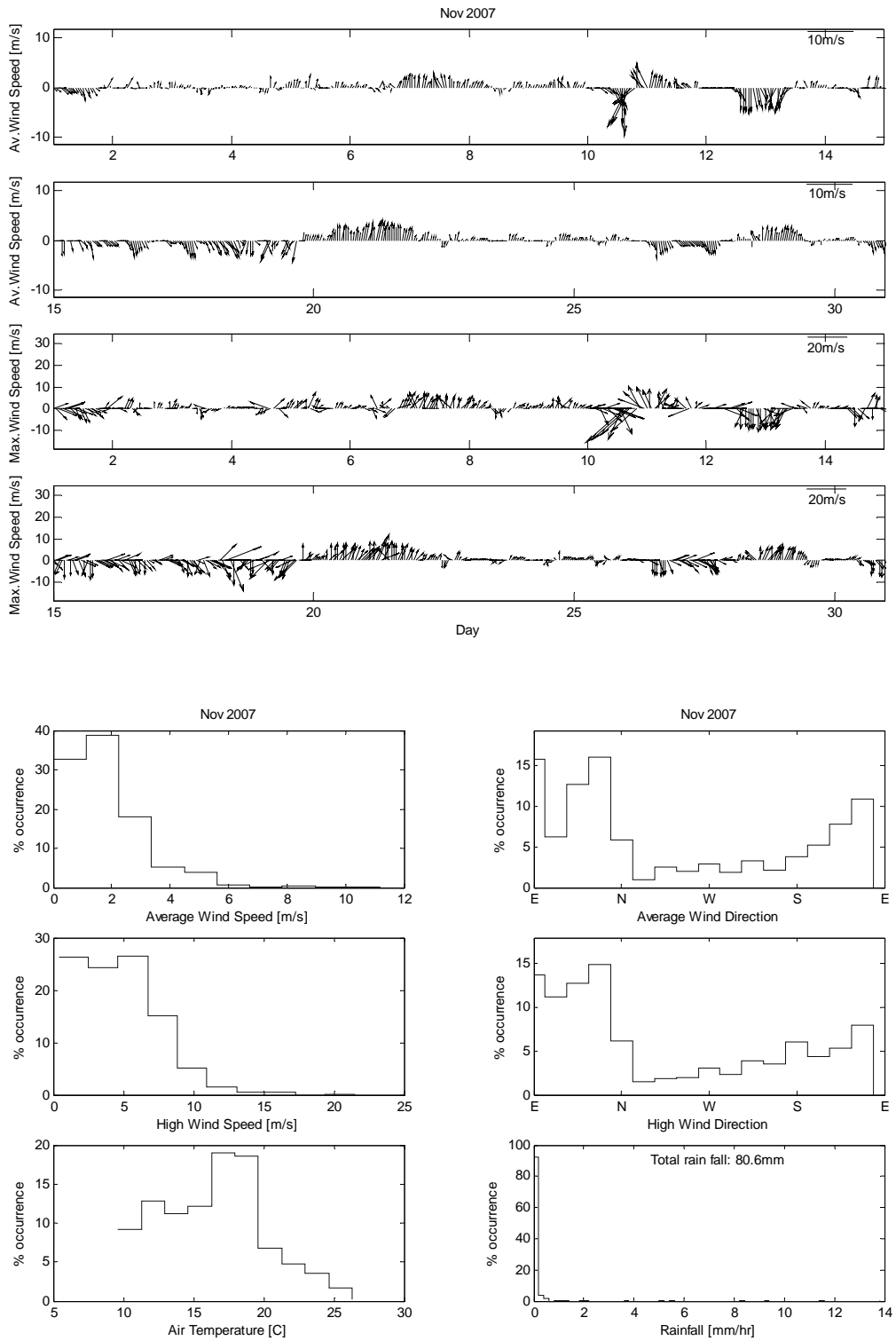


Figure A.13. Directional Wind Speed and Histograms (November 2007)

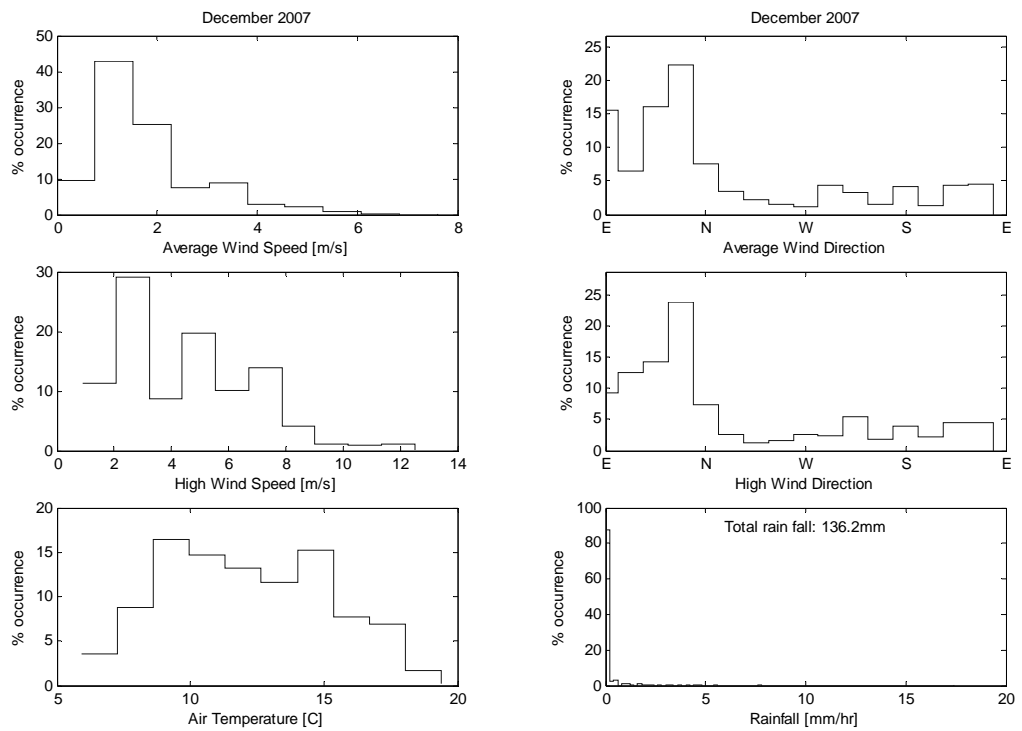
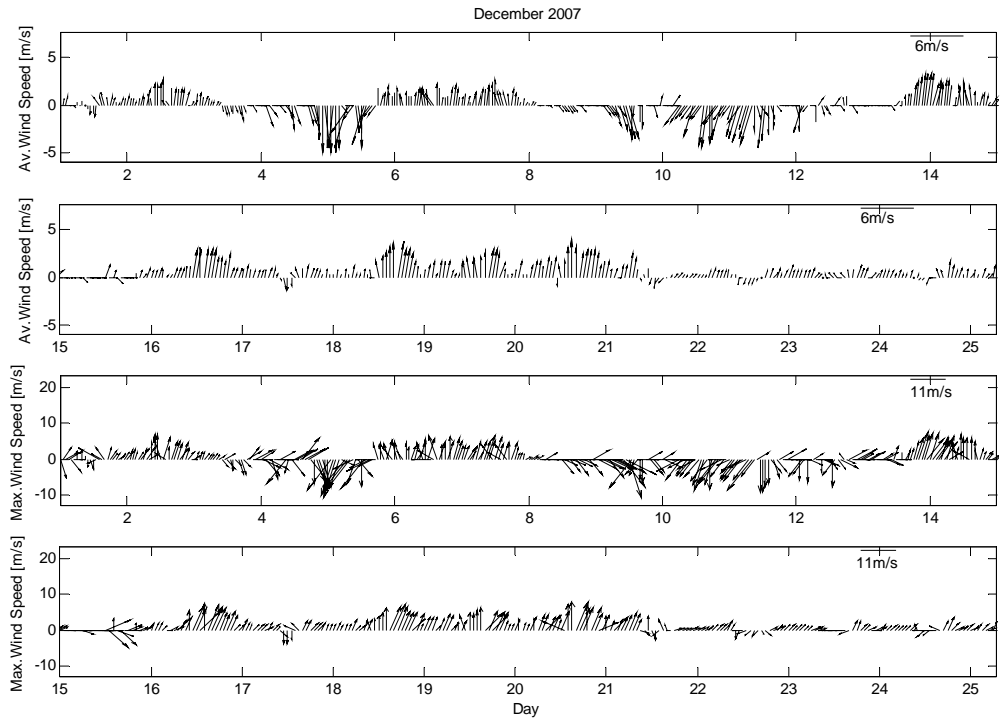


Figure A.14. Directional Wind Speed and Histograms (December 2007)

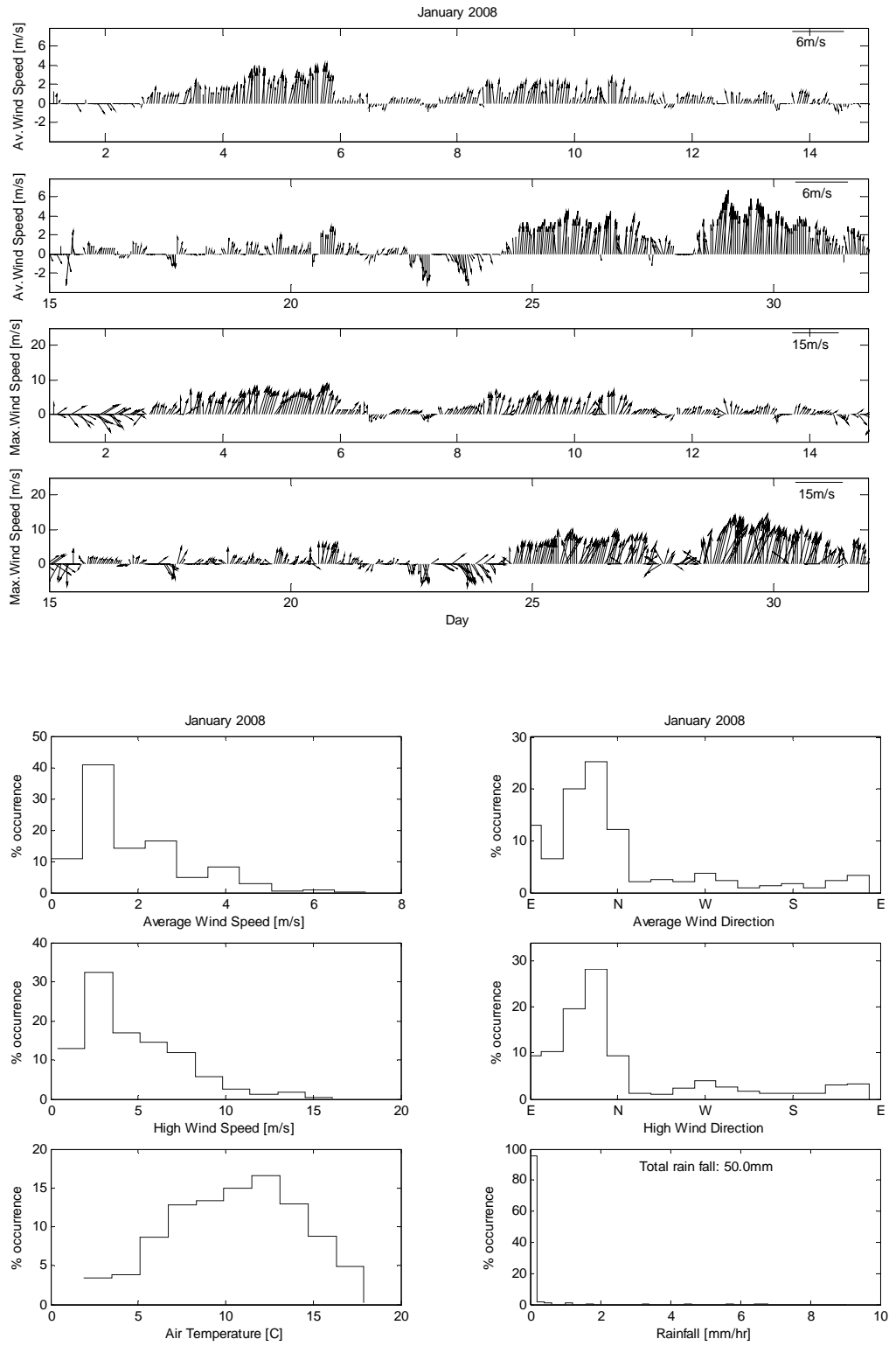


Figure A.15. Directional Wind Speed and Histograms (January 2008)

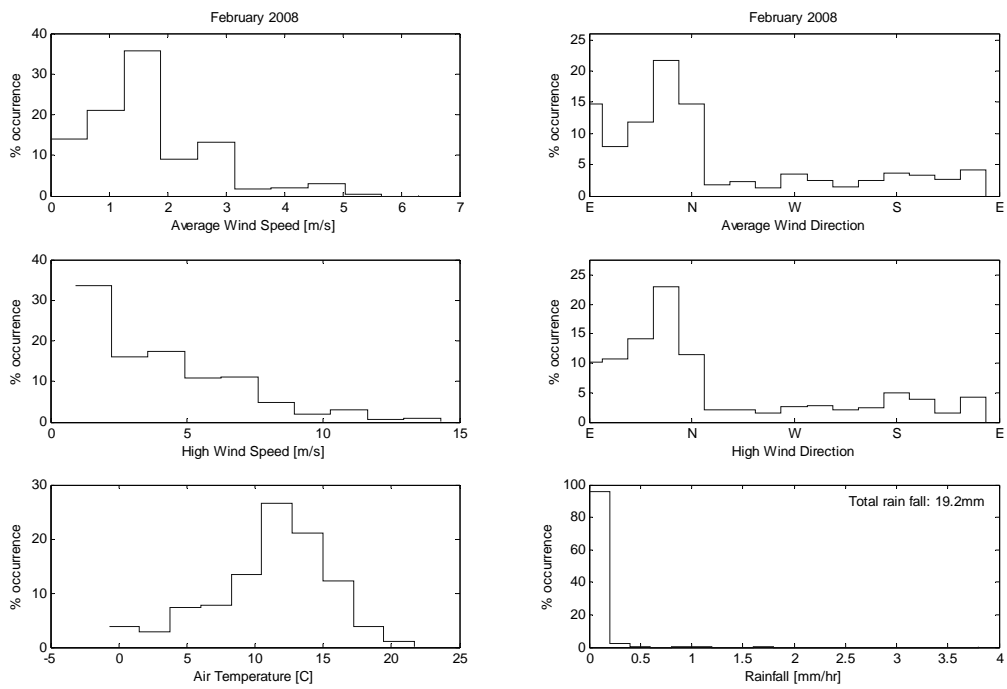
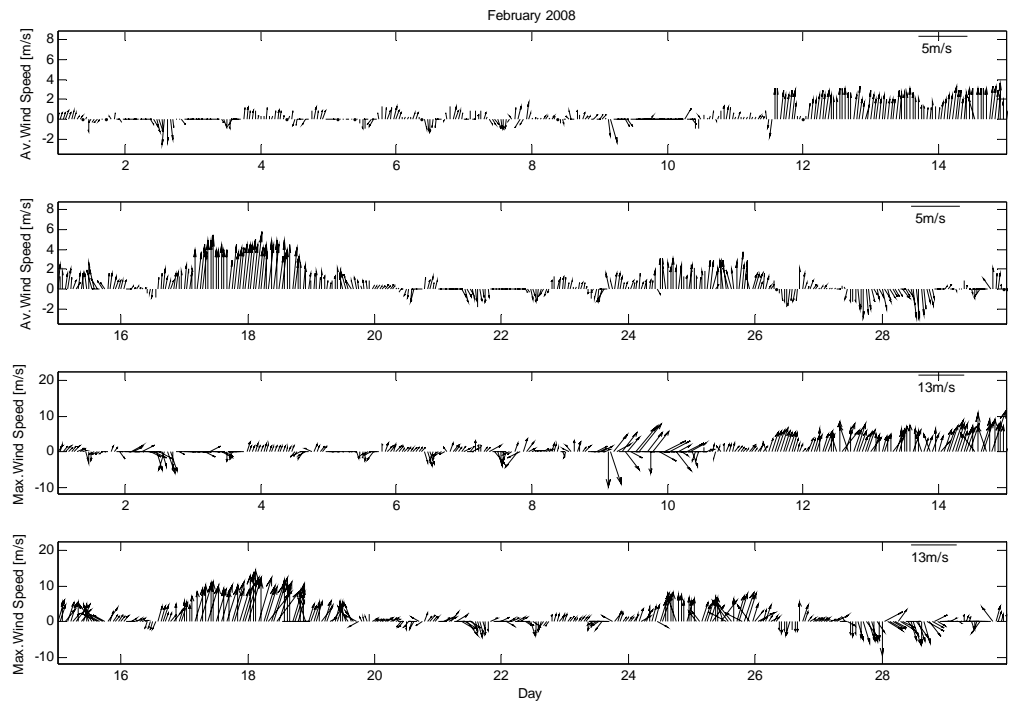


Figure A.16. Directional Wind Speed and Histograms (February 2008)

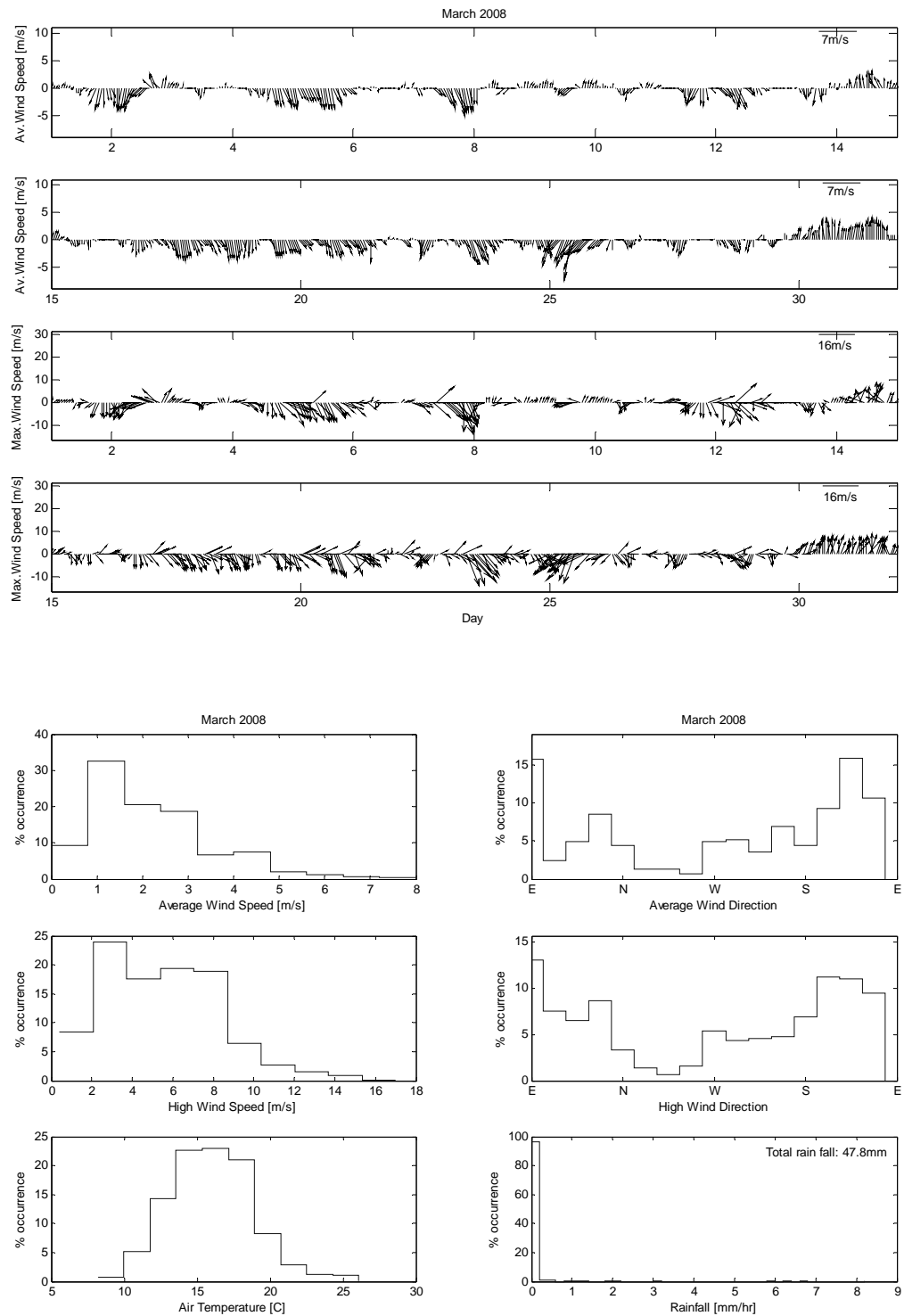


Figure A.17. Directional Wind Speed and Histograms (March 2008)

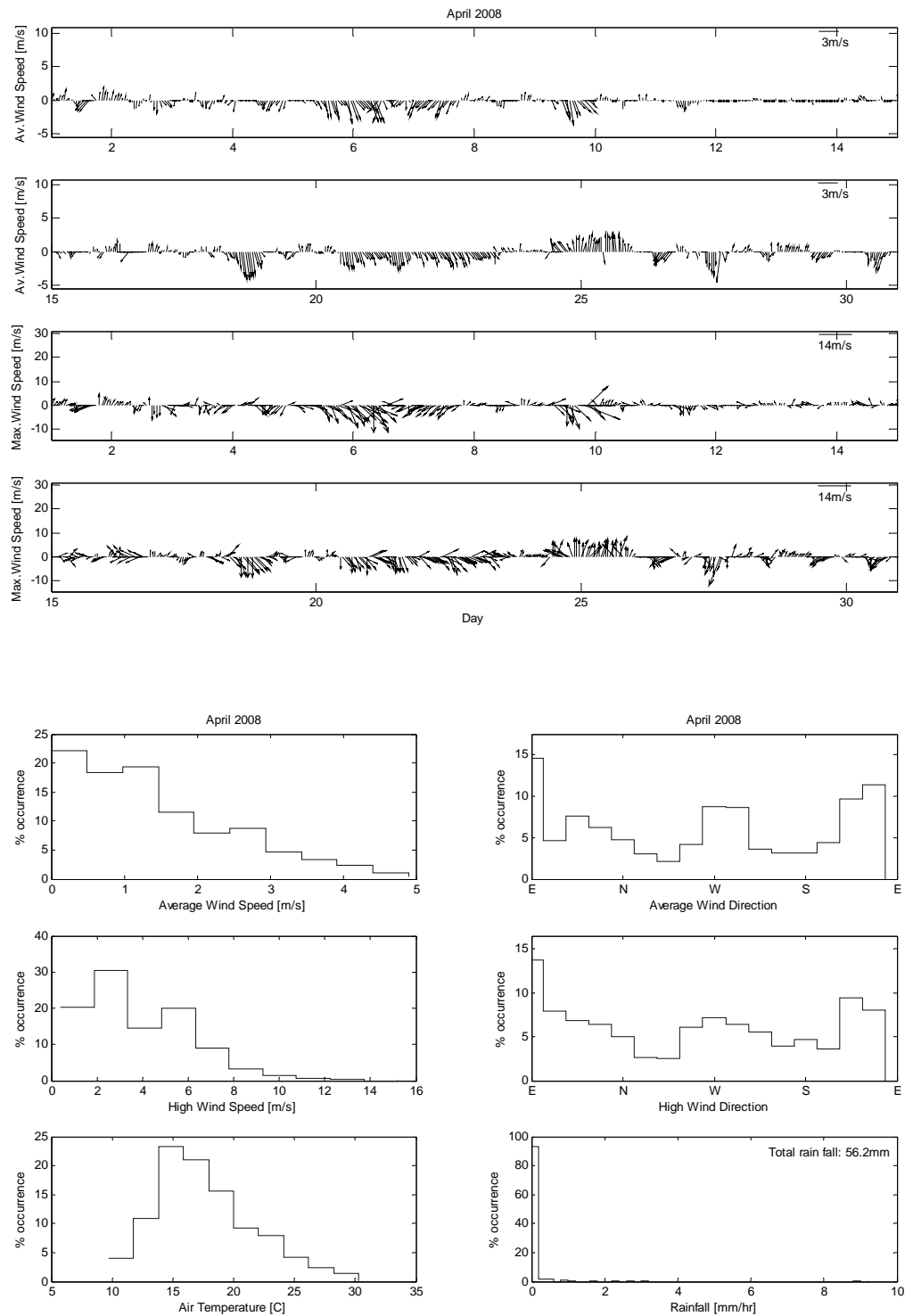


Figure A.18. Directional Wind Speed and Histograms (April 2008)

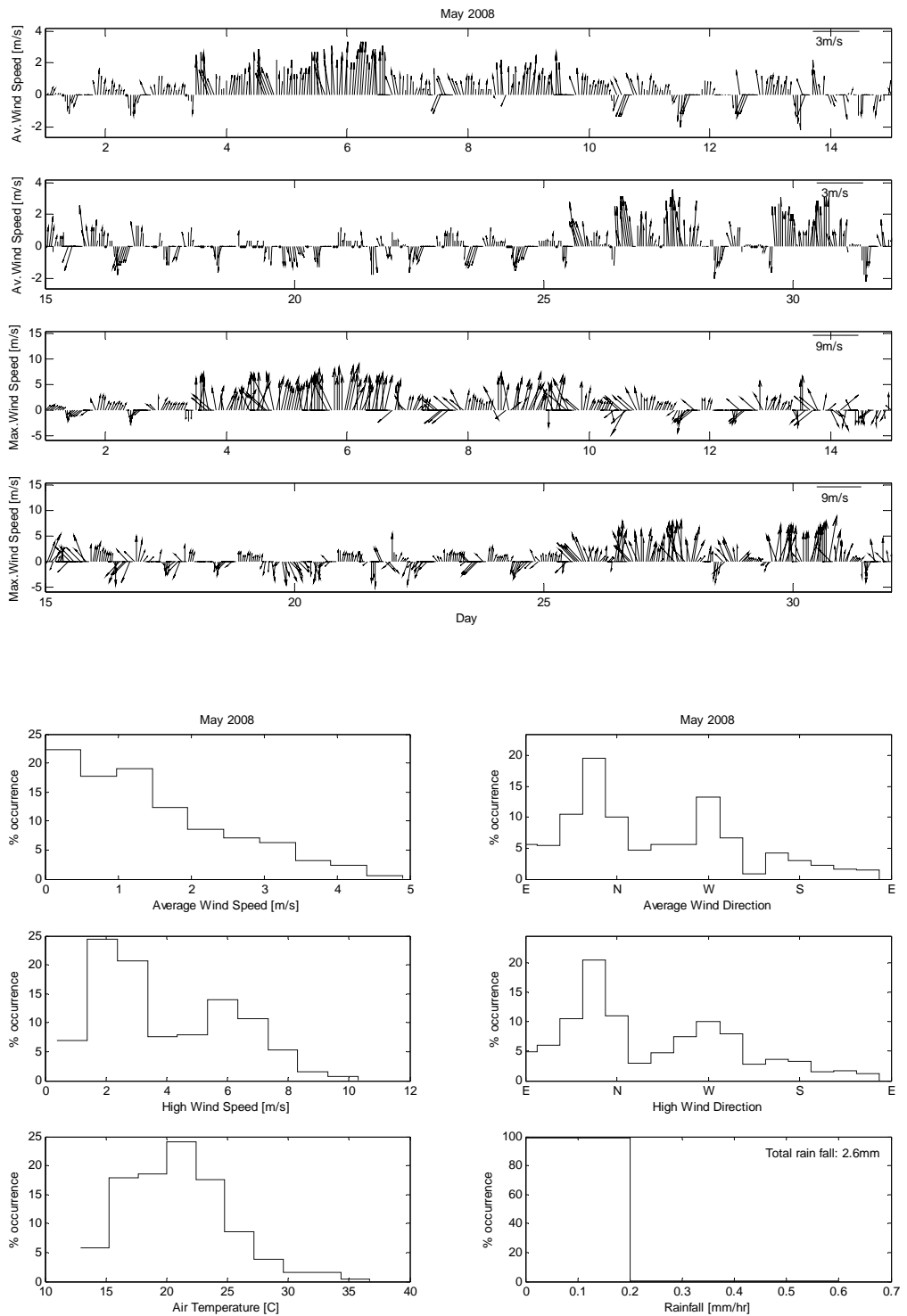


Figure A.19. Directional Wind Speed and Histograms (May 2008)

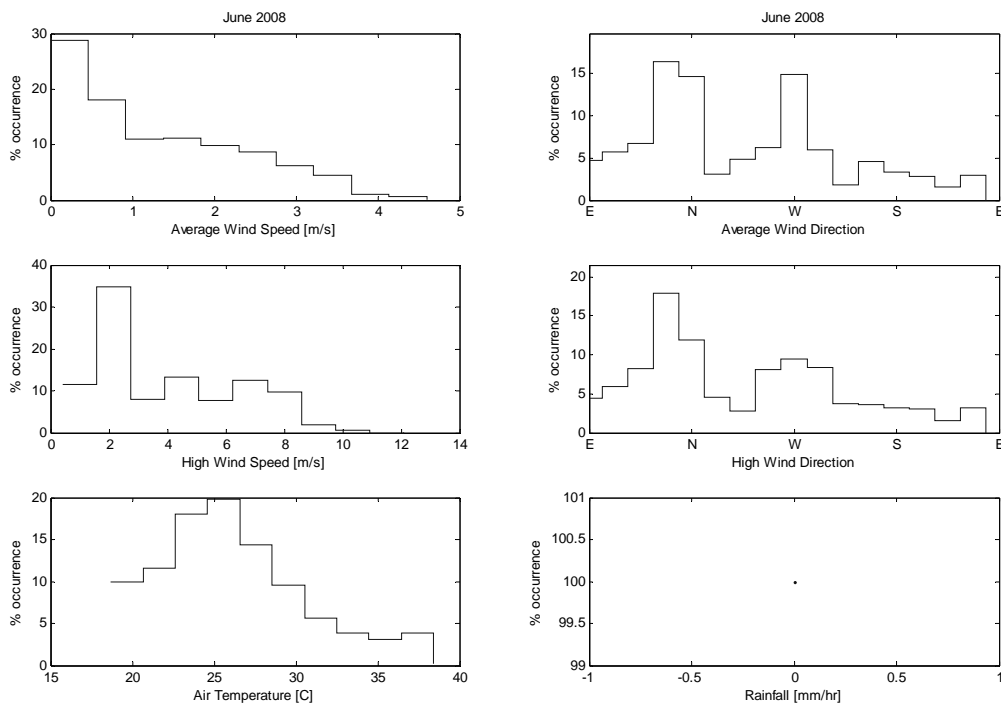
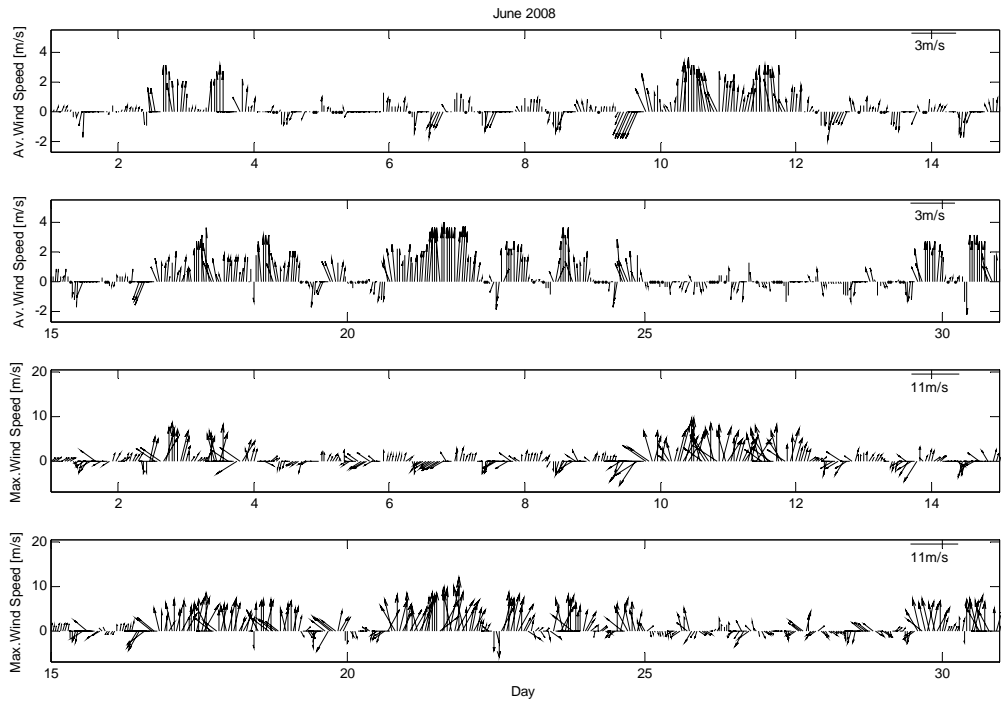


Figure A.20. Directional Wind Speed and Histograms (June 2008)

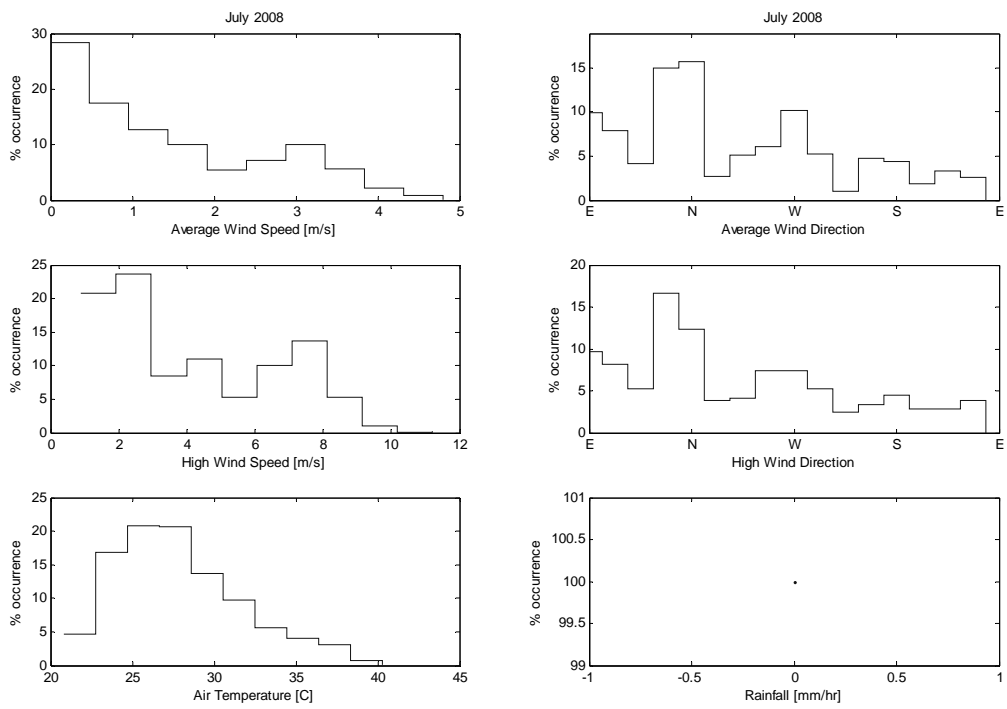
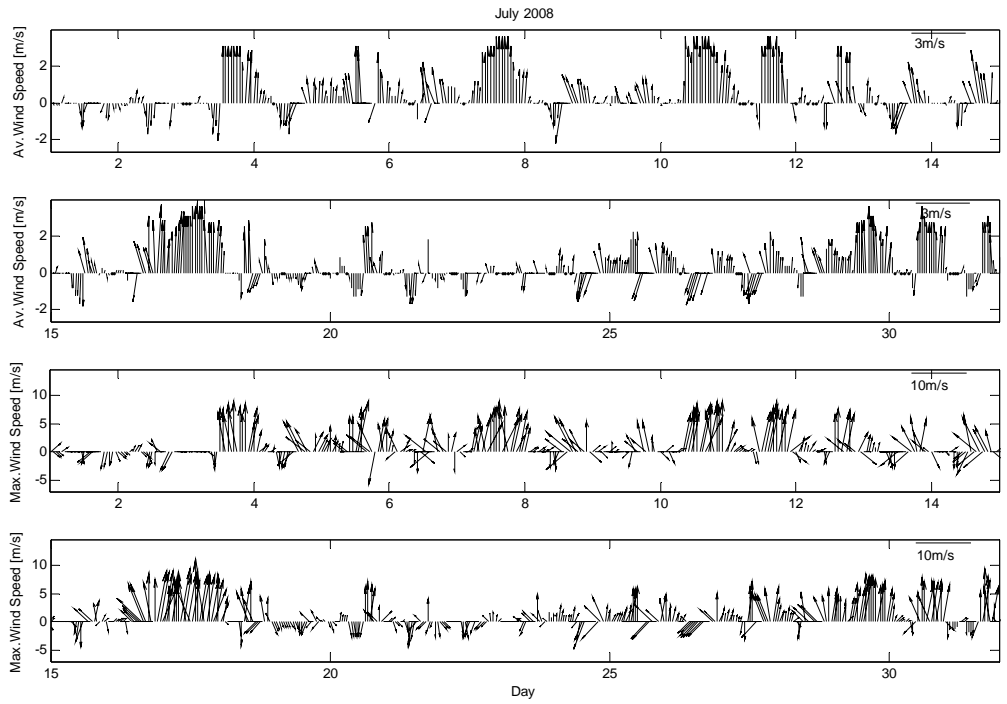


Figure A.21. Directional Wind Speed and Histograms (July 2008)

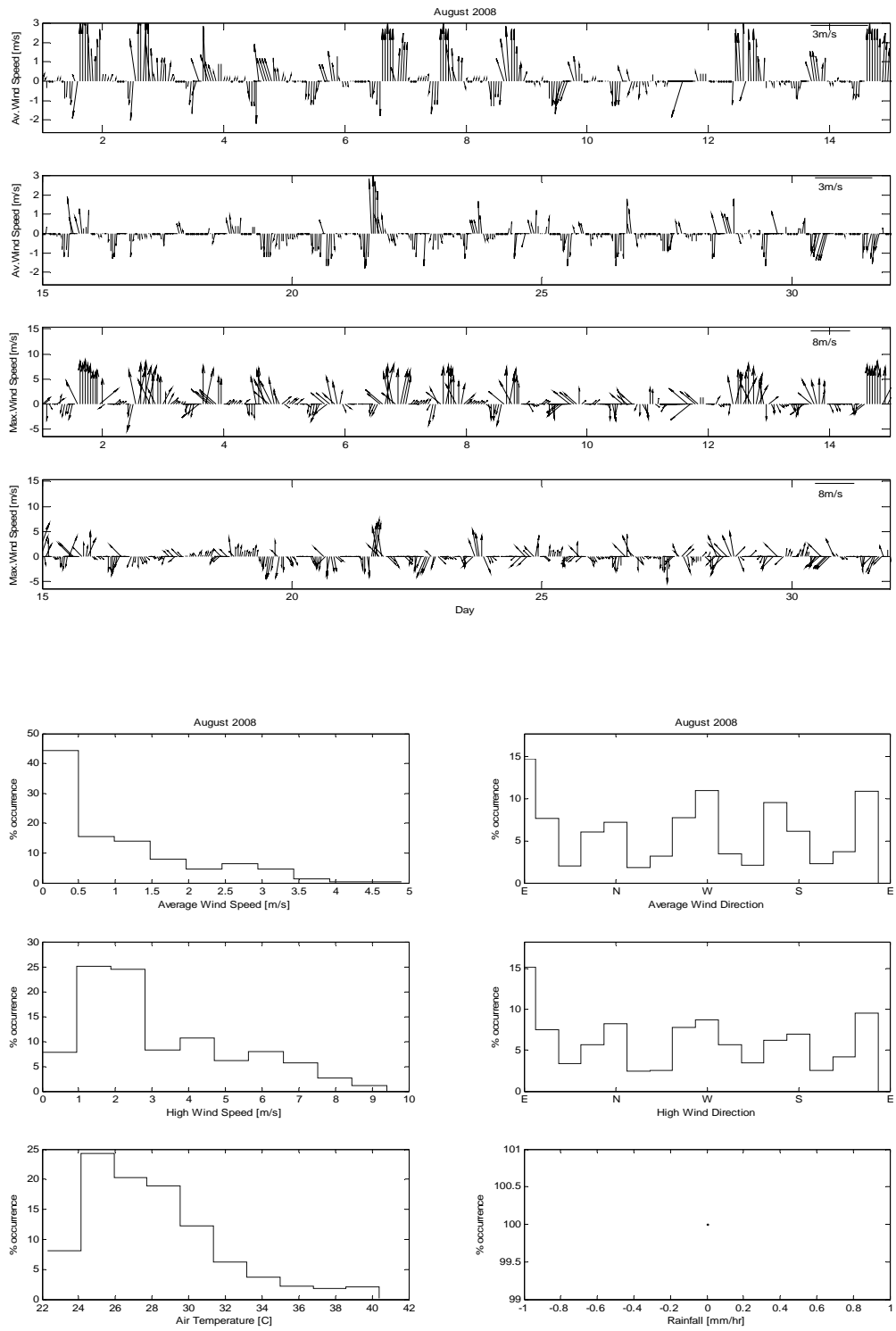


Figure A.22. Directional Wind Speed and Histograms (August 2008)

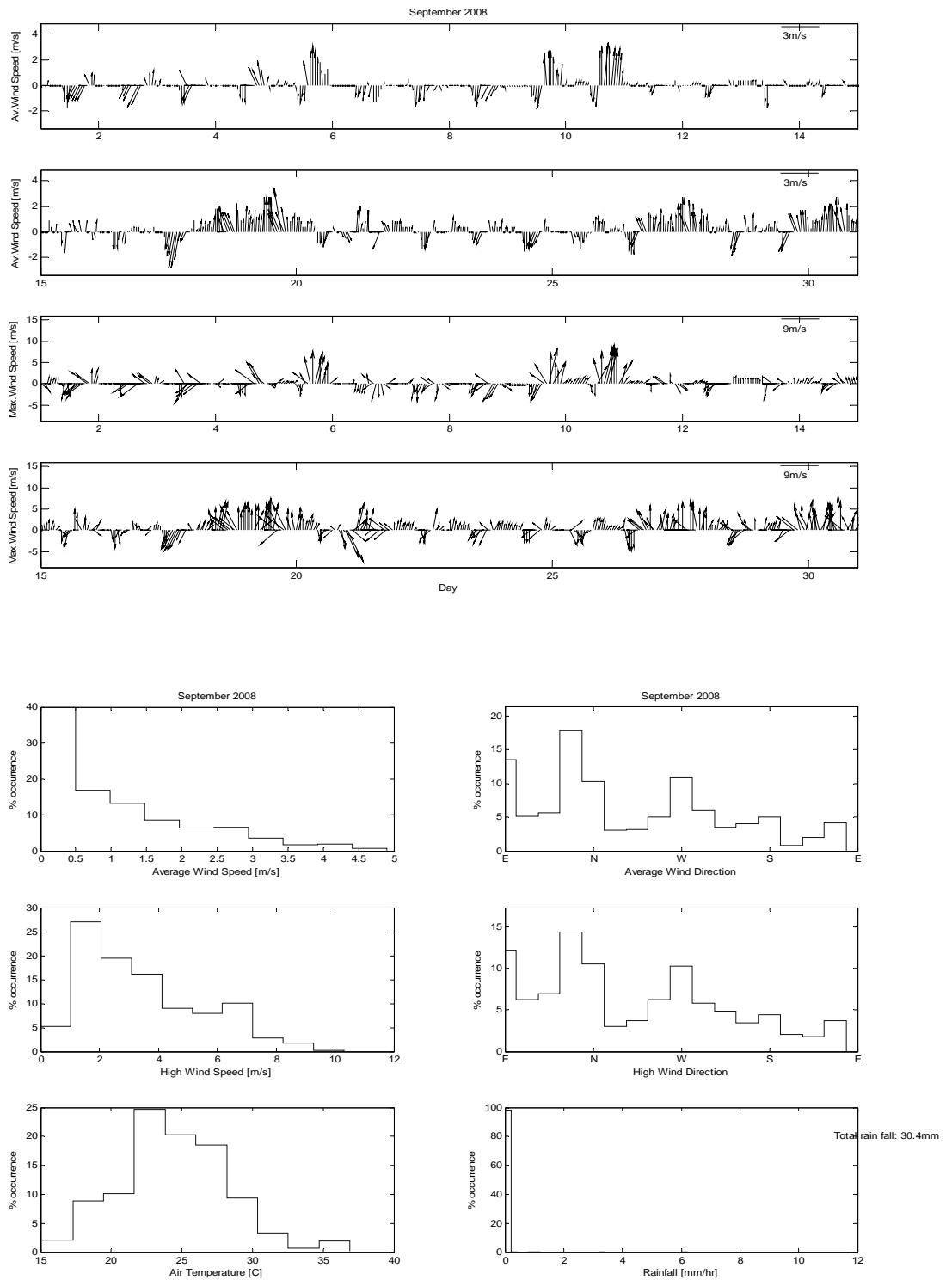


Figure A.23. Directional Wind Speed and Histograms (September 2008)

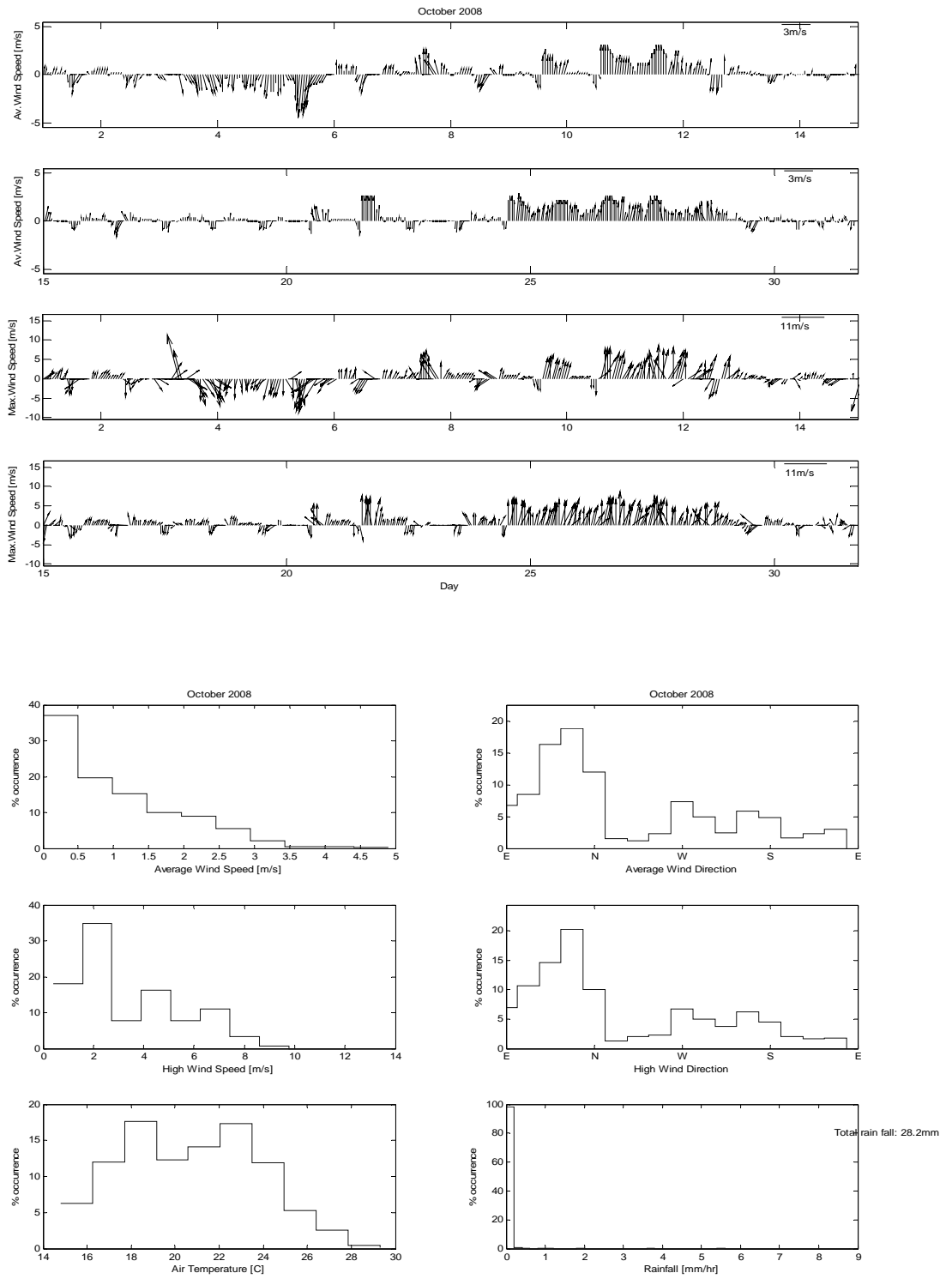


Figure A.24. Directional Wind Speed and Histograms (October 2008)

APPENDIX B: Goodness of Fit Tests

B.1. Chi-Square (χ^2) Test

The key idea of the chi-square test is a comparison of observed and expected values. The comparison is used to calculate the value of the chi-square statistic, which in turn can be compared with the distribution of chi-square to make an inference about a statistical problem.

The definition for chi-square yields:

$$\chi^2 = \sum_{i=1}^n \frac{(o_i - E_i)^2}{E_i} \quad (\text{B.1})$$

where o = observed frequency

E = expected frequency

n = number of possible outcomes of each event.

The observed data are considered to be significant at a level, α , which is usually taken as 0.05; namely, χ^2 test is conducted with 95 percent confidence, or with a 5 percent possible error.

In order to determine the significance level α , the degree of freedom is required. In the case of the chi-square goodness-of-fit test, the number of degrees of freedom (DoF) is equal to the number of terms used in calculating chi-square minus one. Therefore, the degree of freedom for the one-dimensional chi-square statistic is:

$$DoF = n - 1 \quad (\text{B.2})$$

Critical value, χ_* for the chi-square are determined from a statistical table based on the significance level at which the test is being performed (0.05 in this case) and the DoF .

The calculated value of chi-square (χ^2) has to be compared with the critical value, χ_* obtained from the Chi-Square distribution table for the 0.05 level and *DoF* .

If $\chi_* > \chi^2$, then the measured sample is considered to be at the 95 percent level of significance. Otherwise, if the calculated chi-square value is equal to or greater than this critical value, ($\chi^2 \geq \chi_*$) it can be concluded that there is a significant difference between the observed and expected frequencies.

B.2. Kolmogorov-Smirnov Test

This test has the feature that it can be applied to data from a small sample size provided that the parameter of the hypothesized distribution is either assumed or known in advance.

The Kolmogorov-Smirnov test does not consider the difference between the observed frequency of occurrence and the probability of the hypothesized distribution in a classified division; instead, it is concerned with the difference in the cumulative distribution between observed and the hypothesized probability law. The observed sample, therefore, is not classified into groups, but is rearranged in an ordered sequence for this test.

Let x_1, x_2, \dots, x_n be the ordered sample of size n , and let its cumulative distribution be $F_n(x)$ given by

$$F_n(x) = \begin{cases} 0 & x = x_1 \\ r/n & x_r \leq x \leq x_{r+1} \quad r = 1, 2, \dots, (n-1) \\ 1 & x = x_n \end{cases} \quad (\text{B.3})$$

$F_n(x)$ is a step function. In the case where several values are observed to be the same for $x = x_j$, $F_n(x_j)$ jumps significantly. Let $F(x)$ be the cumulative distribution function of

the hypothesized probability distribution. The Kolmogorov-Smirnov test is based on the statistics

$$D_n = \sup |F_n(x) - F(x)| \quad (\text{B.4})$$

where \sup implies the maximum value over the entire range of the sample domain. Kolmogorov shows that if a sample of size n is large (on the order of 35 or greater) the probability of D_n exceeding a certain value ϵ is given approximately by

$$\Pr\{D_n > \epsilon\} = 2 \sum_{r=1}^{\infty} (-1)^{r-1} \exp\{-2r^2 n \epsilon^2\} \quad (\text{B.5})$$

Since this series converges rapidly, we may take the first term only, namely $2 \exp\{-2n \epsilon^2\}$. By letting this value be equal to the level of significance α , we have

$$\epsilon = \sqrt{-\ln(\alpha/2)/2n} = \begin{cases} 1.63/\sqrt{n} & \alpha = 0.01 \\ 1.48/\sqrt{n} & \alpha = 0.025 \\ 1.36/\sqrt{n} & \alpha = 0.05 \end{cases} \quad (\text{B.6})$$

The test is then carried out by which we may reject the hypothesis with level of significance α if the statistics D_n exceeds ϵ .

APPENDIX C: Source Codes

C.1. Wind Statistics

```

clear all
close all

% Wind Statistics
% -----
fname=input('Please enter filename:', 's')
fid=fopen([fname, '.txt']);
[filename] = fopen(fid);
[n,m]=size(filename);
Fname=filename(1:m-4);
i = 0;
while 1
    W = fgetl(fid);
    if ~ischar(W), break, end
    k = findstr(W,9);
    i = i+1;
    if i > 0
        Date(i,1:8)=(W(1:k(1)-1));
        Day(i)=str2num(W(1:2));
        Month(i)=str2num(W(4:5));
        Hour(i)=str2num(W(k(1)+1:k(2)-4));
        TempOut(i)=str2num(W(k(2)+1:k(3)-1));
        Hitemp(i)=str2num(W(k(3)+1:k(4)-1));
        Lowtemp(i)=str2num(W(k(4)+1:k(5)-1));
        WindSpeed(i)=str2num(W(k(7)+1:k(8)-1));
        WindDir(i,1:k(9)-k(8)-1)=W(k(8)+1:k(9)-1);
        HiSpeed(i)=str2num(W(k(10)+1:k(11)-1));
        HiDir(i,1:k(12)-k(11)-1)=W(k(11)+1:k(12)-1);
        Rain(i)=str2num(W(k(16)+1:k(17)-1));
    end
end
fclose(fid);

[n,m]=size(WindSpeed);
for i=1:1:m;
    Adday(i)=Day(i)+Hour(i)/24;
end
for i=1:1:m;
    if (WindDir(i,1)=='E' & WindDir(i,2)==0 & WindDir(i,3)==0);
        AnDir(i)=0;
    elseif (WindDir(i,1)=='E' & WindDir(i,2)=='N' & WindDir(i,3)=='E');
        AnDir(i)=22.5;
    elseif (WindDir(i,1)=='N' & WindDir(i,2)=='E' & WindDir(i,3)==0);
        AnDir(i)=45;
    elseif (WindDir(i,1)=='N' & WindDir(i,2)=='N' & WindDir(i,3)=='E');
        AnDir(i)=67.5;
    elseif (WindDir(i,1)=='N' & WindDir(i,2)==0 & WindDir(i,3)==0);
        AnDir(i)=90 ;
    elseif (WindDir(i,1)=='N' & WindDir(i,2)=='N' & WindDir(i,3)=='W');
        AnDir(i)=112.5;
    end
end

```

```

elseif (WindDir(i,1)=='N' & WindDir(i,2)=='W' & WindDir(i,3)==0);
    AnDir(i)=135;
elseif (WindDir(i,1)=='W' & WindDir(i,2)=='N' & WindDir(i,3)=='W');
    AnDir(i)=157.5;
elseif (WindDir(i,1)=='W' & WindDir(i,2)==0 & WindDir(i,3)==0);
    AnDir(i)=180;
elseif (WindDir(i,1)=='W' & WindDir(i,2)=='S' & WindDir(i,3)=='W');
    AnDir(i)=202.5;
elseif (WindDir(i,1)=='S' & WindDir(i,2)=='W' & WindDir(i,3)==0);
    AnDir(i)=225;
elseif (WindDir(i,1)=='S' & WindDir(i,2)=='S' & WindDir(i,3)=='W');
    AnDir(i)=247.5;
elseif (WindDir(i,1)=='S' & WindDir(i,2)==0 & WindDir(i,3)==0);
    AnDir(i)=270;
elseif (WindDir(i,1)=='S' & WindDir(i,2)=='S' & WindDir(i,3)=='E');
    AnDir(i)=292.5;
elseif (WindDir(i,1)=='S' & WindDir(i,2)=='E' & WindDir(i,3)==0);
    AnDir(i)=315;
elseif (WindDir(i,1)=='E' & WindDir(i,2)=='S' & WindDir(i,3)=='E');
    AnDir(i)=337.5;
end
end

for i=1:1:m;
    if (HiDir(i,1)=='E' & HiDir(i,2)==0 & HiDir(i,3)==0);
        HianDir(i)=0;
    elseif (HiDir(i,1)=='E' & HiDir(i,2)=='N' & HiDir(i,3)=='E');
        HianDir(i)=22.5;
    elseif (HiDir(i,1)=='N' & HiDir(i,2)=='E' & HiDir(i,3)==0);
        HianDir(i)=45;
    elseif (HiDir(i,1)=='N' & HiDir(i,2)=='N' & HiDir(i,3)=='E');
        HianDir(i)=67.5;
    elseif (HiDir(i,1)=='N' & HiDir(i,2)==0 & HiDir(i,3)==0);
        HianDir(i)=90 ;
    elseif (HiDir(i,1)=='N' & HiDir(i,2)=='N' & HiDir(i,3)=='W');
        HianDir(i)=112.5;
    elseif (HiDir(i,1)=='N' & HiDir(i,2)=='W' & HiDir(i,3)==0);
        HianDir(i)=135;
    elseif (HiDir(i,1)=='W' & HiDir(i,2)=='N' & HiDir(i,3)=='W');
        HianDir(i)=157.5;
    elseif (HiDir(i,1)=='W' & HiDir(i,2)==0 & HiDir(i,3)==0);
        HianDir(i)=180;
    elseif (HiDir(i,1)=='W' & HiDir(i,2)=='S' & HiDir(i,3)=='W');
        HianDir(i)=202.5;
    elseif (HiDir(i,1)=='S' & HiDir(i,2)=='W' & HiDir(i,3)==0);
        HianDir(i)=225;
    elseif (HiDir(i,1)=='S' & HiDir(i,2)=='S' & HiDir(i,3)=='W');
        HianDir(i)=247.5;
    elseif (HiDir(i,1)=='S' & HiDir(i,2)==0 & HiDir(i,3)==0);
        HianDir(i)=270;
    elseif (HiDir(i,1)=='S' & HiDir(i,2)=='S' & HiDir(i,3)=='E');
        HianDir(i)=292.5;
    elseif (HiDir(i,1)=='S' & HiDir(i,2)=='E' & HiDir(i,3)==0);
        HianDir(i)=315;
    elseif (HiDir(i,1)=='E' & HiDir(i,2)=='S' & HiDir(i,3)=='E');
        HianDir(i)=337.5;
    end
end

for i=1:1:m;

```

```

        RadDira(i)=AnDir(i)*pi/180;
        RadDirh(i)=HianDir(i)*pi/180;
    end

    for i=1:1:m;
        vxa(i) = WindSpeed(i)*cos(RadDira(i));
        vya(i) = WindSpeed(i)*sin(RadDira(i));
        vxh(i) = HiSpeed(i)*cos(RadDirh(i));
        vyh(i) = HiSpeed(i)*sin(RadDirh(i));
    end

    tmin = min(Adday);
    tmax = max(Adday);
    ymin=0.8*min(HiSpeed);
    ymax=1.2*max(HiSpeed);
    TETamin=0; TETamax=360;
    TEMmin=0.8*min(TempOut);
    TEMmax=1.2*max(TempOut);
    Rmin=0.8*min(Rain);
    Rmax=1.2*max(Rain);
    if Rmax==0;
        Rmax=0.2;
    end

    % Plot wind statistics
    %----- Figure 1
    subplot(4,1,1),plot(Adday,WindSpeed,'-blue',Adday,HiSpeed,':
red'),title(Fname);
    ylabel('Wind Speed [m/s]'),legend('average','maximum'),grid on ;
    axis([tmin tmax ymin ymax]);

    subplot(4,1,2),plot(Adday,AnDir,'*blue',Adday,HianDir,'.red');
    ylabel('Wind Direction '),legend('average','maximum'),grid on;
    set(gca,'YTick',[0:90:360])
    set(gca,'YTickLabel',['E';'N';'W';'S';'E']);
    axis([tmin tmax TETamin TETamax]);

    subplot(4,1,3),plot(Adday,TempOut,'.-blue');
    ylabel('Air Temperature [C]'),grid on;
    axis([tmin tmax TEMmin TEMmax]);

    subplot(4,1,4),plot(Adday,Rain,'.-blue'),xlabel('Day');
    ylabel('Rainfall [mm/hr]'),grid on;
    axis([tmin tmax Rmin Rmax]);

    figure %----- Figure 2
    if (max(Adday)-min(Adday))>15;

        ymin=1.2*min(vya);
        ymax=2.2*max(vxa);
        tmin1=min(Adday);
        tmax1=15;
        tmin2=15;
        tmax2=max(Adday);

        subplot(4,1,1),featherw(Adday,vxa,vya,'black'),title(Fname);
        ylabel('Av.Wind Speed [m/s]')
        axis([tmin1 tmax1 ymin ymax]),hold on;

```

```

    D=(tmax1-tmin1)/(-ymin+ymax)
    X=13.7:3.5*D/(27.5):13.7+fix(max(WindSpeed)-1)*3.5*D/(27.5);
    [l,k]=size(X);
    for j=1:1:k;
        Y(j)=0.95*ymax;
    end
h=plot(X,Y,'-
black'),text(13.5,0.8*ymax,sprintf('%5.0fm/s',fix(max(WindSpeed)-1)));
hold off

subplot(4,1,2),featherw(Adday,vxa,vya,'black');
ylabel('Av.Wind Speed [m/s]')
axis([tmin2 tmax2 ymin ymax]), hold on;
    D=(tmax2-tmin2)/(-ymin+ymax)
    X=(tmax2-1.5):3.5*D/(27.5):(tmax2-1.5)+fix(max(WindSpeed)-
1)*3.5*D/(27.5);
    [l,k]=size(X);
    for j=1:1:k;
        Y(j)=0.95*ymax;
    end
h=plot(X,Y,'-black'),text((tmax2-
1.7),0.8*ymax,sprintf('%5.0fm/s',fix(max(WindSpeed)-1)));
hold off

    ymin=1.2*min(vyh);
    ymax=2.2*max(vxh);
    tmin1=min(Adday);
    tmax1=15;
    tmin2=15;
    tmax2=max(Adday);

subplot(4,1,3),featherw(Adday,vxh,vyh,'black');
ylabel('Max.Wind Speed [m/s]')
axis([tmin1 tmax1 ymin ymax]), hold on;
    D=(tmax1-tmin1)/(-ymin+ymax)
    X=13.7:3.5*D/(27.5):13.7+fix(max(HiSpeed)-1)*3.5*D/(27.5);
    [l,k]=size(X);
    for j=1:1:k;
        Y(j)=0.95*ymax;
    end
h=plot(X,Y,'-
black'),text(13.5,0.8*ymax,sprintf('%5.0fm/s',fix(max(HiSpeed)-1)));
hold off

subplot(4,1,4),featherw(Adday,vxh,vyh,'black');
ylabel('Max.Wind Speed [m/s]'),xlabel('Day')
axis([tmin2 tmax2 ymin ymax]), hold on;
    D=(tmax2-tmin2)/(-ymin+ymax)
    X=(tmax2-1.5):3.5*D/(27.5):(tmax2-1.5)+fix(max(HiSpeed)-
1)*3.5*D/(27.5);
    [l,k]=size(X);
    for j=1:1:k;
        Y(j)=0.95*ymax;
    end
h=plot(X,Y,'-black'),text((tmax2-
1.7),0.8*ymax,sprintf('%5.0fm/s',fix(max(HiSpeed)-1)));
hold off

```

```

else if (max(Adday)-min(Adday))<=15;

    ymin=1.2*min(vya);
    ymax=2*max(vxa);
    tmin1=min(Adday);
    tmax1=max(Adday);

subplot(2,1,1),featherw(Adday,vxa,vya,'black'),title(Fname);
ylabel('Av.Wind Speed [m/s]')
axis([tmin1 tmax1 ymin ymax]), hold on;
    D=(tmax1-tmin1)/(-ymin+ymax)
    X=(max(Adday)-1.8):7.5*D/(27.5):max(Adday)-1.8+fix(max(WindSpeed)-
1)*7.5*D/(27.5);
    [l,k]=size(X);
    for j=1:1:k;
        Y(j)=0.95*ymax;
    end
h=plot(X,Y,'-black'),text(max(Adday)-
1.8,0.8*ymax,sprintf('%5.0fm/s',fix(max(WindSpeed)-1)));
hold off

    ymin=1.2*min(vyh);
    ymax=2*max(vxh);

subplot(2,1,2),featherw(Adday,vxh,vyh,'black');
ylabel('Max.Wind Speed [m/s]'),xlabel('Day')
axis([tmin1 tmax1 ymin ymax]), hold on;
    D=(tmax1-tmin1)/(-ymin+ymax)
    X=max(Adday)-1.8:7.5*D/(27.5):max(Adday)-1.8+fix(max(HiSpeed)-
1)*7.5*D/(27.5);
    [l,k]=size(X);
    for j=1:1:k;
        Y(j)=0.95*ymax;
    end
h=plot(X,Y,'-black'),text(max(Adday)-
1.8,0.8*ymax,sprintf('%5.0fm/s',fix(max(HiSpeed)-1)));
hold off
end

figure %----- Figure 3
%-----
xtitle='Average Wind Speed [m/s]';
x=WindSpeed;
ntotal=length(x);
xmin=min(x); xmax=max(x); xmean=mean(x); xrms=sqrt(mean(x.^2));
dx=(xmax-xmin)/10;
edges=xmin:dx:xmax;
[nbin,bin]=histc(x,edges);
ybar=100*nbin/ntotal;
ipeak=find(ybar==max(ybar));
xpeak=mean(edges(ipeak:ipeak+1));

subplot(3,2,1),stairs(edges,ybar),title(Fname)
xlabel(xtitle),ylabel('% occurrence')
    Speak=xpeak;
    Smin=xmin;
    Smax=xmax;
    Smean=xmean;
    Srms=xrms;

```

```

%-----
xtitle='Average Wind Direction';
x=AnDir;
ntotal=length(x);
xmin=min(x); xmax=max(x); xmean=mean(x); xrms=sqrt(mean(x.^2));
dx=(360-0)/16;
edges=xmin-11.25:dx:xmax+11.25;
[nbin,bin]=histc(x,edges);
ybar=100*nbin/ntotal;
ipeak=find(ybar==max(ybar));
xpeak=(edges(ipeak));

subplot(3,2,2),stairs(edges,ybar),title(Fname);
xlabel(xtitle),ylabel('% occurrence')
lim=1.2*max(ybar), axis([0 360 0 lim]);
set(gca,'XTick',[0:90:360])
set(gca,'XTickLabel',['E';'N';'W';'S';'E']);
Dpeak=xpeak;
%-----
xtitle='High Wind Speed [m/s]';
x=HiSpeed;
ntotal=length(x);
xmin=min(x); xmax=max(x); xmean=mean(x); xrms=sqrt(mean(x.^2));
dx=(xmax-xmin)/10;
edges=xmin:dx:xmax;
[nbin,bin]=histc(x,edges);
ybar=100*nbin/ntotal;
ipeak=find(ybar==max(ybar));
xpeak=mean(edges(ipeak:ipeak+1));

subplot(3,2,3),stairs(edges,ybar)
xlabel(xtitle), ylabel('% occurrence')
HSpeak=xpeak;
HSmin=xmin;
HSmax=xmax;
HSmean=xmean;
HSrms=xrms;
%-----
xtitle='High Wind Direction';
x=HianDir;
ntotal=length(x);
xmin=min(x); xmax=max(x); xmean=mean(x); xrms=sqrt(mean(x.^2));
dx=(360-0)/16;
edges=xmin-11.25:dx:xmax+11.25;
[nbin,bin]=histc(x,edges);
ybar=100*nbin/ntotal;
ipeak=find(ybar==max(ybar));
xpeak=edges(ipeak);

subplot(3,2,4),stairs(edges,ybar)
xlabel(xtitle), ylabel('% occurrence')
lim=1.2*max(ybar), axis([0 360 0 lim]);
set(gca,'XTick',[0:90:360])
set(gca,'XTickLabel',['E';'N';'W';'S';'E']);
HDpeak=xpeak;
%-----
xtitle='Air Temperature [C]';
x=TempOut;
ntotal=length(x);

```

```

xmin=min(x); xmax=max(x); xmean=mean(x); xrms=sqrt(mean(x.^2));
dx=(xmax-xmin)/10;
edges=xmin:dx:xmax;
[nbin,bin]=histc(x,edges);
ybar=100*nbin/ntotal;
ipeak=find(ybar==max(ybar));
xpeak=mean(edges(ipeak:ipeak+1));

subplot(3,2,5),stairs(edges,ybar)
xlabel(xtitle), ylabel('% occurrence')
    meanHitemp=mean(Hitemp);
    meanLowtemp=mean(Lowtemp);
    Tpeak=xpeak;
    Tmin=xmin;
    Tmax=xmax;
    Tmean=xmean;
    Trms=xrms;
%-----
xtitle='Rainfall [mm/hr]';
totalrain=sum(Rain);
x=Rain;
ntotal=length(x);
xmin=min(x); xmax=max(x); xmean=mean(x); xrms=sqrt(mean(x.^2));
dx=0.2;
edges=xmin:dx:xmax;
[nbin,bin]=histc(x,edges);
ybar=100*nbin/ntotal;
ipeak=find(ybar==max(ybar));
    if size(edges)==1;
        xpeak=mean(edges(ipeak));
    else
        xpeak=mean(edges(ipeak:ipeak+1));
    end

subplot(3,2,6),stairs(edges,ybar)
xlabel(xtitle), ylabel('% occurrence')
text(max(Rain)-0.4,80,sprintf('Total rain fall: %3.1fmm',totalrain))
%-----

% Detect the number Of Rainy Day
[q,irainyday]=find(Rain~=0);nrainyday=1;
for i=1:1:size(irainyday')-1;
    if
        (Month(irainyday(i+1))==Month(irainyday(i))&Day(irainyday(i+1))~=Day(irai
nyday(i)));
            nrainyday=nrainyday+1
        elseif
        (Month(irainyday(i+1))~=Month(irainyday(i))&Day(irainyday(i+1))~=Day(irai
nyday(i)));
            nrainyday=nrainyday+1
        end
end
[q,c]=size(irainyday');
if (q==0);
    nrainyday=0
end
%-----

Rpeak=xpeak;

```

```

Rmin=xmin;
Rmax=xmax;
Rmean=xmean;
Rrms=xrms;

if (-11.25<= Dpeak & Dpeak < (11.25));
    Ddrpeak='E';
elseif (11.25<=Dpeak& Dpeak<33.75);
    Ddrpeak='ENE';
elseif (33.75<=Dpeak& Dpeak<56.25);
    Ddrpeak='NE';
elseif (56.25<=Dpeak & Dpeak<78.75);
    Ddrpeak='NNE';
elseif (78.75<=Dpeak& Dpeak<101.25);
    Ddrpeak='N';
elseif (101.25<=Dpeak& Dpeak<123.75);
    Ddrpeak='NNW';
elseif (123.75<=Dpeak& Dpeak<146.25);
    Ddrpeak='NW';
elseif (146.25<=Dpeak& Dpeak<168.75);
    Ddrpeak='WNW';
elseif (168.75<=Dpeak& Dpeak<191.25);
    Ddrpeak='W';
elseif (191.25<=Dpeak& Dpeak<213.75);
    Ddrpeak='WSW';
elseif (213.75<=Dpeak& Dpeak<236.25);
    Ddrpeak='SW';
elseif (236.25<=Dpeak& Dpeak<258.75);
    Ddrpeak='SSW';
elseif (258.75<=Dpeak& Dpeak<281.25);
    Ddrpeak='S';
elseif (281.25<=Dpeak& Dpeak<303.75);
    Ddrpeak='SSE';
elseif (303.75<=Dpeak& Dpeak<326.25);
    Ddrpeak='SE';
elseif (326.25<=Dpeak& Dpeak<348.75);
    Ddrpeak='ESE';
elseif (348.75<=Dpeak& Dpeak<=371.25);
    Ddrpeak='E';
end

if (-11.25<= HDpeak & HDpeak < (11.25));
    HDrpeak='E';
elseif (11.25<=HDpeak& HDpeak<33.75);
    HDrpeak='ENE';
elseif (33.75<=HDpeak& HDpeak<56.25);
    HDrpeak='NE';
elseif (56.25<=HDpeak & HDpeak<78.75);
    HDrpeak='NNE';
elseif (78.75<=HDpeak& HDpeak<101.25);
    HDrpeak='N';
elseif (101.25<=HDpeak& HDpeak<123.75);
    HDrpeak='NNW';
elseif (123.75<=HDpeak& HDpeak<146.25);
    HDrpeak='NW';
elseif (146.25<=HDpeak& HDpeak<168.75);
    HDrpeak='WNW';
elseif (168.75<=HDpeak& HDpeak<191.25);
    HDrpeak='W';
elseif (191.25<=HDpeak& HDpeak<213.75);

```

```

    HDrpeak='WSW';
elseif (213.75<=HDpeak& HDpeak<236.25);
    HDrpeak='SW';
elseif (236.25<=HDpeak& HDpeak<258.75);
    HDrpeak='SSW';
elseif (258.75<=HDpeak& HDpeak<281.25);
    HDrpeak='S';
elseif (281.25<=HDpeak& HDpeak<303.75);
    HDrpeak='SSE';
elseif (303.75<=HDpeak& HDpeak<326.25);
    HDrpeak='SE';
elseif (326.25<=HDpeak& HDpeak<348.75);
    HDrpeak='ESE';
elseif (348.75<=HDpeak& HDpeak<=371.25);
    HDrpeak='E';
end

[a,b] = max(WindSpeed);
[c,d]=max(HiSpeed);

% Write final statistics to an Excel sheet
fid = fopen('Monthly Statistics.xls','a');
fprintf(fid,'%s',Fname,' ')
fprintf(fid,'%s','Hourly Average Speed(m/s) ')
AS = [Smin;Smax;Smean;Speak;Srms];
fprintf(fid,' Min: %5.2f Max: %5.2f Mean:%5.2f Peak:%5.2f
Rms:%5.2f',AS);
fprintf(fid,' Predominant Dir %s',Ddrpeak)
fprintf(fid,' Dir. Of Max.Av.Speed %s\n',WindDir(b,1:3))
fprintf(fid,'%s',' Hourly Maximum Speed(m/s) ')
HS = [HSmin;HSmax;HSmean;HSpeak;HSrms];
fprintf(fid,'Min: %5.2f Max: %5.2f Mean:%5.2f Peak:%5.2f
Rms:%5.2f',HS);
fprintf(fid,' Predominant Dir %s',HDrpeak)
fprintf(fid,' Dir. Of Max Hi Speed %s\n',HiDir(d,1:3))
fprintf(fid,'%s',' Rain(mm/hr) ')
R=[Rmin;Rmax;Rmean;Rpeak;Rrms;totalrain;nrainyday]
fprintf(fid,'Min: %5.2f Max: %5.2f Mean:%5.2f Peak:%5.2f Rms:%5.2f
Total:%5.2f Rainy Day:%5.0f\n',R);
fprintf(fid,'%s',' Temperature(C) ')
T=[Tmin;Tmax;Tmean;Tpeak;Trms;meanHitemp;meanLowtemp]
fprintf(fid,'Min: %5.2f Max: %5.2f Mean:%5.2f Peak:%5.2f Rms:%5.2f
Mean High Temp:%5.2f Mean Low Temp:%5.2f\n\n',T);
fclose(fid)
%----- 22.03.2007

```

C.2. Wave Statistics Contour Plots

```

close all
clear all
% Wave Statistics Contour Plotter
% Revised on 20.03.2009
% ----- Input file -----
choose=menu('Do you want to filter fetches & calm waves ?' , 'YES','NO');
if(choose==1);

A=xlsread('TIMEset AKBUK.xls'); % Input files loaded seperately
B=xlsread('TIMEset BODRUM.xls'); %
C=xlsread('TIMEset AWAC.xls'); %

    fa=A(:,4); % excluding unrealistic fetches
    fetch_akbuk=find(fa==0); % from AKBUK data set
    A(fetch_akbuk,:)=[]; % and
    calm_akbuk=find(A(:,5)<=0.05); % filtering out calm waves
A(calm_akbuk,:)=[]; % from AKBUK data set

    fb=B(:,4); % excluding unrealistic fetches
    fetch_bodrum=find(fb==0); % from BODRUM data set
    B(fetch_bodrum,:)=[]; % and
    calm_bodrum=find(B(:,5)<=0.05); % filtering out calm waves
B(calm_bodrum,:)=[]; % from BODRUM data set

    fc=C(:,1); % filtering out calm waves
    calm_awac=find(fc<=0.05); % from AWAC data set
C(calm_awac,:)=[]; %

TB=B(:,6); TA=A(:,6); TAW=C(:,5);
HB=B(:,5); HA=A(:,5); HAW=C(:,1);
HA(isnan(HA)) = []; % NaNs removed
HB(isnan(HB)) = []; % NaNs removed
HAW(isnan(HAW))= []; % NaNs removed
TA(isnan(TA)) = []; % NaNs removed
TB(isnan(TB)) = []; % NaNs removed
TAW(isnan(TAW))= []; % NaNs removed

FILTER='Unrealistic Fetches & Calm Waves FILTERED!!!'

clear A B C calm_awac calm_akbuk calm_bodrum fetch_bodrum fetch_akbuk
display('Data is filtered according to fetches and calm data is
excluded!')
else
[NUM,TXT,RAW]=xlsread('TIMEset.xls');

TB=NUM(:,12); TA=NUM(:,6); TAW=NUM(:,17);
HB=NUM(:,11); HA=NUM(:,5); HAW=NUM(:,13);
FILTER='Unrealistic Fetches & Calm Waves INCLUDED!!!'

clear RAW NUM TXT
display('Calm Data is not filtered !')
end
display('Data set loaded successfully!')

```

```

% ----- select plot options -----
option=menu('Select Plot Options:', 'JPDF of H&T from BODRUM', 'JPDF of H&T
from AKBUK', 'JPDF of H&T from AWAC');
if (option==1);
    Tm=TB;
    Hm=HB;
    TTL='BODRUM'
elseif (option==2);
    Tm=TA;
    Hm=HA;
    TTL='AKBUK'
elseif (option==3);
    Tm=TAW;
    Hm=HAW;
    TTL='AWAC'
end
% -----
D(:,1)=Tm;
D(:,2)=Hm;

Tmax=max(Tm);
UT=1+fix(Tmax);      dT=0.25;
Hmax=max(Hm);
UH=1+fix(Hmax);     dH=0.1;

TX=UT*0.1; TY=UH*0.95;

Xn=1+fix(UT/dT);
Yn=1+fix(UH/dH);
% ----- plot results using hist2d.m -----
display('Please Wait! Plotting selected figures ...')

Hout=hist2d(D,Xn,Yn,[0 UT],[0 UH]);

title( {[sprintf('Joint Probability Distribution of H&T from
%s',TTL)];[sprintf('(Hmax= %3.2f m Tmax= %3.2f s)',Hmax,Tmax)]});
xlabel('Wave Periods [s]'), ylabel('Wave Heights [m]');
text(TX,TY,FILTER,'BackgroundColor',[1 1 1],'EdgeColor',[1 0 0]),
colorbar, grid on;

%----- 20.03.2009 -----

```

C.3. Wave Statistics Polar Plots

```

close all
clear all
% Wave Statistics Polar Plotter
% Revised on 20.03.2009
% Revised on 22.03.2009
% ----- Input file -----
choose=menu('Do you want to filter fetches & calm waves ?' , 'YES, filter
!!', 'NO, keep it calm!!');
if(choose==1);
A=xlsread('TIMEset AKBUK.xls'); % Input files loaded seperately
B=xlsread('TIMEset BODRUM.xls'); %
C=xlsread('TIMEset AWAC.xls'); %

    fa=A(:,4); % excluding unrealistic fetches
    fetch_akbuk=find(fa==0); % from AKBUK data set
    A(fetch_akbuk,:)=[]; % and
    calm_akbuk=find(A(:,5)<=0.02); % filtering out calm waves
A(calm_akbuk,:)=[]; % from AKBUK data set

    fb=B(:,4); % excluding unrealistic fetches
    fetch_bodrum=find(fb==0); % from BODRUM data set
    B(fetch_bodrum,:)=[]; % and
    calm_bodrum=find(B(:,5)<=0.02); % filtering out calm waves
B(calm_bodrum,:)=[]; % from BODRUM data set

    fc=C(:,1); % filtering out calm waves
    calm_awac=find(fc<=0.05); % from AWAC data set
C(calm_awac,:)=[]; %

DB=B(:,2); DA=A(:,2); DAW=C(:,8);
TB=B(:,6); TA=A(:,6); TAW=C(:,5);
HB=B(:,5); HA=A(:,5); HAW=C(:,1);

HA(isnan(HA)) = []; % NaNs removed
HB(isnan(HB)) = []; % NaNs removed
HAW(isnan(HAW))= []; % NaNs removed
TA(isnan(TA)) = []; % NaNs removed
TB(isnan(TB)) = []; % NaNs removed
TAW(isnan(TAW))= []; % NaNs removed
DA(isnan(DA)) = []; % NaNs removed
DB(isnan(DB)) = []; % NaNs removed
DAW(isnan(DAW))= []; % NaNs removed

FILTER='(Unrealistic Fetches & Calm Waves FILTERED!!)'

clear A B C calm_awac calm_akbuk calm_bodrum fetch_bodrum fetch_akbuk
display('Data is filtered according to fetches and calm data is
excluded!')
else
[NUM,TXT,RAW]=xlsread('TIMEset.xls');

DB=NUM(:,8); DA=NUM(:,2); DAW=NUM(:,20);
TB=NUM(:,12); TA=NUM(:,6); TAW=NUM(:,17);
HB=NUM(:,11); HA=NUM(:,5); HAW=NUM(:,13);
FILTER='(Unrealistic Fetches & Calm Waves INCLUDED!!)'

```

```

clear RAW NUM TXT
display('Calm Data is not filtered !')
end
% -----

opt=menu('Please Select:', 'BODRUM Wave Heights', 'BODRUM Periods', 'AKBUK
Wave Heights', 'AKBUK Periods', 'AWAC Wave Heights', 'AWAC Periods');
if (opt==1);
    P=HB;
    P_max=max(P) ;
    P_min=min(P) ;
    DIR=DB;
    HB_max=P_max
    SS='H_B_o_d';
    ST='Wave Heights derived from BODRUM data';
    Sd='m';
elseif (opt==2);
    P=TB;
    P_max=max(P) ;
    P_min=min(P) ;
    DIR=DB;
    TB_max=P_max
    SS='T_B_o_d';
    ST='Periods derived from BODRUM data';
    Sd='s';
elseif (opt==3);
    P=HA;
    P_max=max(P) ;
    P_min=min(P) ;
    DIR=DA;
    HA_max=P_max
    SS='H_A_k_b';
    ST='Wave Heights derived from AKBUK data';
    Sd='m';
elseif (opt==4);
    P=TA;
    P_max=max(P) ;
    P_min=min(P) ;
    DIR=DA;
    TA_max=P_max
    SS='T_A_k_b';
    ST='Periods derived from AKBUK data';
    Sd='s';
elseif (opt==5);
    P=HAW;
    P_max=max(P) ;
    P_min=min(P) ;
    DIR=DAW;
    HAW_max=P_max
    SS='H_m_0';
    ST='Wave Heights from AWAC data';
    Sd='m';
elseif (opt==6);
    P=TAW;
    P_max=max(P) ;
    P_min=min(P) ;
    DIR=DAW;
    TAW_max=P_max
    SS='T_m_0_2';
    ST='Periods from AWAC data';

```

```

        Sd='s';
end
% -----

if round(P_max)==fix(P_max) % Polar coordinate R is described. U&L
    U=round(P_max)+1 ; % show the upper&lower boundaries of R,
else % respectively.
    U=round(P_max); %
end %
L=fix(P_min) ; %
delta=U-L %
dr=delta/12 % There are 12steps in each17 direction
dr=(fix(100*dr))/100 % from L to U ---> dr: step size

DIR=90-DIR ; % Polar coordinate THETA is described.
for i=1:length(DIR); % originally 0=N 45=NE 90=E 135=SE
    if DIR(i)<0 % 225=SW 270=W 315=NW ...
        DIR(i)=360+DIR(i) ; % These are converted to MATLAB polar
    end % coordinates with E=0
end % N=90 S=270 ...
% -----

M=round(delta/dr)+1 ; % size(Z)=MxN
N=17 ; % M: variable according to dr and U,L

Z=zeros(M,N); %
for m=1:M ; %
for n=1:N ; %
    for i=1:length(DIR); %
        if ((n-1)*22.5-11.25<=DIR(i) & DIR(i)<22.5*(n)-11.25 & (m-1)*dr<=P(i)
& P(i)<m*dr )
            Z(m,n)=Z(m,n)+1 ; %
        end %
    end %
end %
end %
Zk=zeros(M,1) ; % 0& 360 degrees correspond to the same
Zk=Z(:,1)+Z(:,N) ; % direction(E).Their values are equated
Z(:,1)=Zk ; % to prevent discontinuity in polar
Z(:,N)=Zk ; % plots.
%
Z=flipud(Z); % Z matrix should be inverted to plot
% realistic results in polar diagram.

SUM=sum(sum(Z)); % Z is converted to probability from
Z=(Z/SUM)*100 ; % discrete numbers
display('Z matrix created succesfully!')
% -----
% ----- find predominant direction -----
s1=sum(Z(:,1)); s2=sum(Z(:,2));
s3=sum(Z(:,3)); s4=sum(Z(:,4));
s5=sum(Z(:,5)); s6=sum(Z(:,6));
s7=sum(Z(:,7)); s8=sum(Z(:,8));
s9=sum(Z(:,9)); s10=sum(Z(:,10));
s11=sum(Z(:,11)); s12=sum(Z(:,12));
s13=sum(Z(:,13)); s14=sum(Z(:,14));
s15=sum(Z(:,15)); s16=sum(Z(:,16));
s17=sum(Z(:,17));
S=[s1 s2 s3 s4 s5 s6 s7 s8 s9 s10 s11 s12 s13 s14 s15 s16 s17]
xpeak=find(S==max(S))

```

```

if      (xpeak==1);  preDIR='E' ;
elseif (xpeak==2);  preDIR='ENE' ;
elseif (xpeak==3);  preDIR='NE' ;
elseif (xpeak==4);  preDIR='NNE' ;
elseif (xpeak==5);  preDIR='N' ;
elseif (xpeak==6);  preDIR='NNW' ;
elseif (xpeak==7);  preDIR='NW' ;
elseif (xpeak==8);  preDIR='WNW' ;
elseif (xpeak==9);  preDIR='W' ;
elseif (xpeak==10); preDIR='WSW' ;
elseif (xpeak==11); preDIR='SW' ;
elseif (xpeak==12); preDIR='SSW' ;
elseif (xpeak==13); preDIR='S' ;
elseif (xpeak==14); preDIR='SSE' ;
elseif (xpeak==15); preDIR='SE' ;
elseif (xpeak==16); preDIR='ESE' ;
elseif (xpeak==17); preDIR='E' ;
end
% -----
% ----- plot results using polar3d.m -----
display('Please Wait! Plotting selected figures ...')

polar3d(Z,0,2*pi,L,U,1,'contour');

title( [sprintf('%s      %s',ST, FILTER)];[sprintf('%smax= %3.3f
%s',SS,max(P),Sd)]],hold on;

text(-U/3,-U*1.2,[sprintf(' Predominant Direction: %s
',preDIR)],'EdgeColor',[1 0 0],'LineWidth',2)

text(U*1.1*cosd(0)-U/25,U*1.1*sind(0),'E')
text(U*1.1*cosd(22.5)-U/25,U*1.1*sind(22.5),'ENE')
text(U*1.1*cosd(45)-U/25,U*1.1*sind(45),'NE')
text(U*1.1*cosd(67.5)-U/25,U*1.1*sind(67.5),'NNE')
text(U*1.1*cosd(90),U*1.1*sind(90),'N')
text(U*1.1*cosd(112.5)-U/25,U*1.1*sind(112.5),'NNW')
text(U*1.1*cosd(135)-U/25,U*1.1*sind(135),'NW')
text(U*1.1*cosd(157.5)-U/15,U*1.1*sind(157.5),'WNW')
text(U*1.1*cosd(180)-U/25,U*1.1*sind(180),'W')
text(U*1.1*cosd(202.5)-U/15,U*1.1*sind(202.5),'WSW')
text(U*1.1*cosd(225)-U/25,U*1.1*sind(225),'SW')
text(U*1.1*cosd(247.5)-U/25,U*1.1*sind(247.5),'SSW')
text(U*1.1*cosd(270),U*1.1*sind(270),'S')
text(U*1.1*cosd(292.5)-U/25,U*1.1*sind(292.5),'SSE')
text(U*1.1*cosd(315)-U/25,U*1.1*sind(315),'SE')
text(U*1.1*cosd(337.5)-U/25,U*1.1*sind(337.5),'ESE')

display('          Plot completed ! ')
%----- 18.02.2009
%----- 20.03.2009
%----- 22.03.2009

```

C.4. Wave Statistics Correlation Codes

```

close all
clear all
% Wave Statistics Corelator
% Revised on 14.04.2009
% ----- Input file -----
[NUM,TXT,RAW]=xlsread('TIMEset.xls');
RAW_backup=RAW;
L=length(RAW);
tarikh= RAW(3:L,1);
    DB=NUM(:,8);
    TB=NUM(:,12);
    HB=NUM(:,11);

    DA=NUM(:,2);
    TA=NUM(:,6);
    HA=NUM(:,5);

    DAW=NUM(:,20);
    TAW=NUM(:,17);
    HAW=NUM(:,13);
L=length(tarikh)
clear RAW NUM TXT
display('Data set loaded successfully!')
% -----
% ----- Filter missing data -----
HBnNAN=HB;      HBnNAN(isnan(HBnNAN)) = [];
HAnNAN=HA;      HAnNAN(isnan(HAnNAN)) = [];
HAWnNAN=HAW;    HAWnNAN(isnan(HAWnNAN)) = [];
TBnNAN=TB;      TBnNAN(isnan(TBnNAN)) = [];
TAnNAN=TA;      TAnNAN(isnan(TAnNAN)) = [];
TAWnNAN=TAW;    TAWnNAN(isnan(TAWnNAN)) = [];
% -----
option=menu('Select plot option:', 'Time Histories', 'Histograms');
display('Please Wait! Plotting selected figures ...')

if (option==1); % ----- Time History

N=1:L;
v=find(HB==max(HB))
x=find(HA==max(HA))
z=find(HAW==max(HAW))
p=find(TB==max(TB))
q=find(TA==max(TA))
r=find(TAW==max(TAW))
% -----
figure % Figure #1 - Wave Heights
% -----
subplot(3,1,1), plot(N,HB, ': black',v,HB(v), '* magenta'); legend('BODRUM
set', 'max')
title('Time History of Predicted and Measured Wave Heights for Nov.07 -
Nov.08')
xlim([0 8785]); ylim([0 3]); ylabel('Predicted Heights [m]');
text(3500,2.7,[sprintf('max wave height predicted: %3.2f
m',max(HB))], 'BackgroundColor',[0 1 1])
set(gca, 'XTick',[0:732:8784]);

```

```

set(gca,'XTickLabel',{'Nov.07','Dec.07','Jan.08','Feb.08','Mar.08','Apr.0
8','May.08','Jun.08','Jul.08','Aug.08','Sep.08','Oct.08','Nov.08'});
grid on;

subplot(3,1,2), plot(N,HA,': blue',x,HA(x),'* magenta'); legend('AKBUK
set','max')
xlim([0 8785]); ylim([0 3]); ylabel('Predicted Heights [m]');
text(3500,2.7,[sprintf('max wave height predicted: %3.2f
m',max(HA))],'BackgroundColor',[0 1 1])
set(gca,'XTick',[0:732:8784]);
set(gca,'XTickLabel',{'Nov.07','Dec.07','Jan.08','Feb.08','Mar.08','Apr.0
8','May.08','Jun.08','Jul.08','Aug.08','Sep.08','Oct.08','Nov.08'});
grid on;

subplot(3,1,3), plot(N,HAW,'- red',z,HAW(z),'* magenta'); legend('AWAC
set','max')
xlim([0 8785]); ylim([0 3]); ylabel('Measured Heights [m]');
text(3500,2.7,[sprintf('max wave height measured: %3.2f
m',max(HAW))],'BackgroundColor',[0 1 1])
set(gca,'XTick',[0:732:8784]);
set(gca,'XTickLabel',{'Nov.07','Dec.07','Jan.08','Feb.08','Mar.08','Apr.0
8','May.08','Jun.08','Jul.08','Aug.08','Sep.08','Oct.08','Nov.08'});
grid on;
% -----
figure                                %   Figure #2 - Wave Periods
% -----
subplot(3,1,1), plot(N,TB,': black',p,TB(p),'* magenta'); legend('BODRUM
set','max')
title('Time History of Predicted and Measured Wave Periods for Nov.07 -
Nov.08')
xlim([0 8785]); ylim([0 6]); ylabel('Predicted Periods [s]');
text(3800,5.2,[sprintf('max wave period predicted: %3.2f
s',max(TB))],'BackgroundColor',[1 1 0])
set(gca,'XTick',[0:732:8784]);
set(gca,'XTickLabel',{'Nov.07','Dec.07','Jan.08','Feb.08','Mar.08','Apr.0
8','May.08','Jun.08','Jul.08','Aug.08','Sep.08','Oct.08','Nov.08'});
grid on;

subplot(3,1,2), plot(N,TA,': blue',q,TA(q),'* magenta'); legend('AKBUK
set','max')
xlim([0 8785]); ylim([0 6]); ylabel('Predicted Periods [s]');
text(3800,5.2,[sprintf('max wave period predicted: %3.2f
s',max(TA))],'BackgroundColor',[1 1 0])
set(gca,'XTick',[0:732:8784]);
set(gca,'XTickLabel',{'Nov.07','Dec.07','Jan.08','Feb.08','Mar.08','Apr.0
8','May.08','Jun.08','Jul.08','Aug.08','Sep.08','Oct.08','Nov.08'});
grid on;

subplot(3,1,3), plot(N,TAW,'- red',r,TAW(r),'* magenta'); legend('AWAC
set','max')
xlim([0 8785]); ylim([0 6]); ylabel('Measured Periods [s]');
text(3800,5.2,[sprintf('max wave period measured: %3.2f
s',max(TAW))],'BackgroundColor',[1 1 0])
set(gca,'XTick',[0:732:8784]);
set(gca,'XTickLabel',{'Nov.07','Dec.07','Jan.08','Feb.08','Mar.08','Apr.0
8','May.08','Jun.08','Jul.08','Aug.08','Sep.08','Oct.08','Nov.08'});
grid on;
% -----

```

```

figure                                %   Figure #3 - Wave Directions
% -----
subplot(3,1,1), plot(N,DB,'. black'); legend('BODRUM set')
title('Time History of Wind & Wave Directions for Nov.07 - Nov.08')
xlim([0 8785]); ylim([0 360]); ylabel('Wind Directions');
set(gca,'YTick',[0:45:360]);
set(gca,'YTickLabel',{'N','NE','E','SE','S','SW','W','NW','N'});
set(gca,'XTick',[0:732:8784]);
set(gca,'XTickLabel',{'Nov.07','Dec.07','Jan.08','Feb.08','Mar.08','Apr.0
8','May.08','Jun.08','Jul.08','Aug.08','Sep.08','Oct.08','Nov.08'});
grid on;

subplot(3,1,2), plot(N,DA,'. blue'); legend('AKBUK set')
xlim([0 8785]); ylim([0 360]); ylabel('Wind Directions');
set(gca,'YTick',[0:45:360]);
set(gca,'YTickLabel',{'N','NE','E','SE','S','SW','W','NW','N'});
set(gca,'XTick',[0:732:8784]);
set(gca,'XTickLabel',{'Nov.07','Dec.07','Jan.08','Feb.08','Mar.08','Apr.0
8','May.08','Jun.08','Jul.08','Aug.08','Sep.08','Oct.08','Nov.08'});
grid on;

subplot(3,1,3), plot(N,DAW,'- red'); legend('AWAC set')
xlim([0 8785]); ylim([0 360]); ylabel('Wave Directions');
set(gca,'YTick',[0:45:360]);
set(gca,'YTickLabel',{'N','NE','E','SE','S','SW','W','NW','N'});
set(gca,'XTick',[0:732:8784]);
set(gca,'XTickLabel',{'Nov.07','Dec.07','Jan.08','Feb.08','Mar.08','Apr.0
8','May.08','Jun.08','Jul.08','Aug.08','Sep.08','Oct.08','Nov.08'});
grid on;
% -----
elseif (option==2); % ----- Histograms
% -----
figure                                %   Figure #4 - Wave Heights
% -----
dH=0.1                                % step size for histogram bins
hi=0:dH:2.5;                          % bins
hj=hi+dH/2;                          % center of the bins

[nB,s]=hist(HB,hi);                   % Distribution of BODRUM record...
pHB=nB/sum(nB)/dH;                   % as probability distribution

[nA,s]=hist(HA,hi);                   % Distribution of AKBUK record...
pHA=nA/sum(nA)/dH;                   % as probability distribution

[nAW,s]=hist(HAW,hi);                 % Distribution of the wave record...
pHAW=nAW/sum(nAW)/dH;                % as probability distribution

plot(hi,pHB,'-o black',hi,pHA,'-+ blue',hi,pHAW,'- red'),hold on;

ipeak=find(pHB==max(pHB));
Hpeak=hi(ipeak);
text(0.6,7.1,sprintf('BODRUM: mean= %3.2fm    max=%3.2fm
peak=%3.2fm',mean(HBnNAN),max(HB),Hpeak))
ipeak=find(pHA==max(pHA));
Hpeak=hi(ipeak);
text(0.6,6.8,sprintf('AKBUK: mean= %3.2fm    max=%3.2fm
peak=%3.2fm',mean(HAnNAN),max(HA),Hpeak))
ipeak=find(pHAW==max(pHAW));
Hpeak=hi(ipeak);

```

```

text(0.6,6.5,sprintf('AWAC: mean= %3.2fm    max=%3.2fm
peak=%3.2fm',mean(HAWnNAN),max(HAW),Hpeak))

text(0.6,7.5,[sprintf('dH:  %3.2f m  ',dH)],'BackgroundColor',[0 1 1])

title('Probability Distribution of Predicted and Measured Wave Heights
(Nov 07 - Nov 08)'),grid on;
legend('BODRUM winds','AKBUK winds','AWAC waves');
xlabel('H_m [m]'),ylabel('pdf ( H_m )'),hold off;
% -----
figure                                %   Figure #5 - Wave Periods
% -----
dT=0.5                                % step size for histogram bins
ti=0:dT:5;                             % bins
tj=ti+dT/2;                            % center of the bins

[nB,s]=hist(TB,ti);                    % Distribution of BODRUM record...
pTB=nB/sum(nB)/dT;                    % as probability distribution

[nA,s]=hist(TA,ti);                    % Distribution of AKBUK record...
pTA=nA/sum(nA)/dT;                    % as probability distribution

[nAW,s]=hist(TAW,ti);                  % Distribution of the wave record...
pTAW=nAW/sum(nAW)/dT;                 % as probability distribution

plot(ti,pTB,'-o black',ti,pTA,'-+ blue',ti,pTAW,'- red'),hold on;

ipeak=find(pTB==max(pTB));
Tpeak=ti(ipeak);
text(1.6,1.28,sprintf('BODRUM: mean= %3.2fs    max=%3.2fs
peak=%3.2fs',mean(TBnNAN),max(TB),Tpeak))
ipeak=find(pTA==max(pTA));
Tpeak=ti(ipeak);
text(1.6,1.22,sprintf('AKBUK: mean= %3.2fs    max=%3.2fs
peak=%3.2fs',mean(TAnNAN),max(TA),Tpeak))
ipeak=find(pTAW==max(pTAW));
Tpeak=ti(ipeak(1));
text(1.6,1.16,sprintf('AWAC: mean= %3.2fs    max=%3.2fs
peak=%3.2fs',mean(TAWnNAN),max(TAW),Tpeak))

text(1.6,1.35,[sprintf('dT:  %3.2f s  ',dT)],'BackgroundColor',[1 1 0])
title('Probability Distribution of Predicted and Measured Wave Periods
(Nov 07 - Nov 08)'),grid on;
legend('BODRUM winds','AKBUK winds','AWAC waves');
xlabel('T [s]'),ylabel('pdf ( T )'),hold off;
% -----
figure                                %   Figure #6 - Directions
% -----
dD=22.5                                % step size for histogram bins
di=0:dD:360;                            % bins

[nB,s]=hist(DB,di);                    % Distribution of BODRUM record...
pDB=nB/sum(nB)/dD;                    % as probability distribution

[nA,s]=hist(DA,di);                    % Distribution of AKBUK record...
pDA=nA/sum(nA)/dD;                    % as probability distribution

[nAW,s]=hist(DAW,di);                  % Distribution of AWAC record...

```

```

pDAW=nAW/sum(nAW)/dD;           % as probability distribution

plot(di,pDB,'-o black',di,pDA,'-+ blue',di,pDAW,'-red'),hold on;

ipeak=find(pDB==max(pDB));
Dpeak=mean(di(ipeak));
    if (Dpeak==0);           Ddrpeak='N';
    elseif (Dpeak==22.5);   Ddrpeak='NNE';
    elseif (Dpeak==45);     Ddrpeak='NE';
    elseif (Dpeak==67.5);   Ddrpeak='ENE';
    elseif (Dpeak==90);     Ddrpeak='E';
    elseif (Dpeak==112.5);  Ddrpeak='ESE';
    elseif (Dpeak==135);    Ddrpeak='SE';
    elseif (Dpeak==157.5);  Ddrpeak='SSE';
    elseif (Dpeak==180);    Ddrpeak='S';
    elseif (Dpeak==202.5);  Ddrpeak='SSW';
    elseif (Dpeak==225);    Ddrpeak='SW';
    elseif (Dpeak==247.5);  Ddrpeak='WSW';
    elseif (Dpeak==270);    Ddrpeak='W';
    elseif (Dpeak==292.5);  Ddrpeak='WNW';
    elseif (Dpeak==315);    Ddrpeak='NW';
    elseif (Dpeak==337.5);  Ddrpeak='NNW';
    elseif (Dpeak==360);    Ddrpeak='N';
    end
text(100,0.028,sprintf('BODRUM Predominant Direction:  %s',Ddrpeak))

ipeak=find(pDA==max(pDA));
Dpeak=di(ipeak);
    if (Dpeak==0);           Ddrpeak='N';
    elseif (Dpeak==22.5);   Ddrpeak='NNE';
    elseif (Dpeak==45);     Ddrpeak='NE';
    elseif (Dpeak==67.5);   Ddrpeak='ENE';
    elseif (Dpeak==90);     Ddrpeak='E';
    elseif (Dpeak==112.5);  Ddrpeak='ESE';
    elseif (Dpeak==135);    Ddrpeak='SE';
    elseif (Dpeak==157.5);  Ddrpeak='SSE';
    elseif (Dpeak==180);    Ddrpeak='S';
    elseif (Dpeak==202.5);  Ddrpeak='SSW';
    elseif (Dpeak==225);    Ddrpeak='SW';
    elseif (Dpeak==247.5);  Ddrpeak='WSW';
    elseif (Dpeak==270);    Ddrpeak='W';
    elseif (Dpeak==292.5);  Ddrpeak='WNW';
    elseif (Dpeak==315);    Ddrpeak='NW';
    elseif (Dpeak==337.5);  Ddrpeak='NNW';
    elseif (Dpeak==360);    Ddrpeak='N';
    end
text(100,0.026,sprintf('AKBUK Predominant Direction:  %s',Ddrpeak))

ipeak=find(pDAW==max(pDAW));
Dpeak=mean(di(ipeak));
    if (Dpeak==0);           Ddrpeak='N';
    elseif (Dpeak==22.5);   Ddrpeak='NNE';
    elseif (Dpeak==45);     Ddrpeak='NE';
    elseif (Dpeak==67.5);   Ddrpeak='ENE';
    elseif (Dpeak==90);     Ddrpeak='E';
    elseif (Dpeak==112.5);  Ddrpeak='ESE';
    elseif (Dpeak==135);    Ddrpeak='SE';
    elseif (Dpeak==157.5);  Ddrpeak='SSE';
    elseif (Dpeak==180);    Ddrpeak='S';

```

```

elseif (Dpeak==202.5); Ddrpeak='SSW';
elseif (Dpeak==225); Ddrpeak='SW';
elseif (Dpeak==247.5); Ddrpeak='WSW';
elseif (Dpeak==270); Ddrpeak='W';
elseif (Dpeak==292.5); Ddrpeak='WNW';
elseif (Dpeak==315); Ddrpeak='NW';
elseif (Dpeak==337.5); Ddrpeak='NNW';
elseif (Dpeak==360); Ddrpeak='N';
end
text(100,0.024,sprintf('AWAC mean(T_m_0_2) Predominant Direction:
%s',Ddrpeak))

set(gca,'XLim',[0 360]);
set(gca,'XTick',[0:22.5:360]);
set(gca,'XTickLabel',{'N','NNE','NE','ENE','E','ESE','SE','SSE','S','SSW',
,'SW','WSW','W','WNW','NW','NNW','N'});
title('Probability Distribution of Predicted and Measured Wind&Wave
Directions (Nov 07 - Nov 08)'),grid on;
legend('BODRUM winds','AKBUK winds','AWAC mean waves');
xlabel('Directions (coming from)'),ylabel('pdf ( Directions )'),hold off;
end

display(' Plot completed ! ')
%----- 26.02.2009
%----- 14.04.2009

```

REFERENCES

- Battjes, J.A., 1972. "Long term wave height distributions at seven stations around the British Isles", *Deutsche Hydrographische Zeitschrift*, Vol. 25, pp. 179–189.
- Burrows, R. and B. A. Salih, 1986. "Statistical modelling of long-term wave climates", *Proc. Coastal Engineering Conference*, Taipei, pp. 42–56.
- Cartwright, D. E. and M. S. Longuet-Higgins, 1956, "The Statistical Distribution of the Maxima of a Random Function", *Proc. Roy. Soc. London, Ser. A*, 237, pp. 212-32.
- Dean, R. G. and R. A. Dalrymple, 1984, *Water Wave Mechanics for Engineers and Scientists*, Prentice-Hall Inc., New Jersey.
- Goda, Y., 1985, *Random Seas and Design of Maritime Structures*, University of Tokyo Press, Tokyo.
- Ferreira, J.A. and C. Guedes Soares, 1999. "Modelling the long-term distribution of significant wave height with the beta and gamma models", *Ocean Engineering* Vol. 26(8), pp. 713–725.
- Golshani, A., S. Taebi and V. Chegini, 2007, "Wave Hindcast and Extreme Value Analysis for the Southern Part of the Caspian Sea", *Coastal Engineering Journal*, Vol. 49, No. 4, pp. 443-459.
- Guedes Soares, C. and A. C. Henriques, 1996. "On the Statistical uncertainty in long-term distributions of significant wave height", *Journal of Offshore Mechanics and Arctic Engineering* Vol. 11, pp. 284–291.
- Hasselmann, K. *et al.*, 1973, "Measurements of Wind-wave Growth and Swell Decay During the Joint North Sea Wave Project (JONSWAP)", *Deutsche Hydrographische Institute.*, Hamburg.

- Haver, S., 1985, "Wave climate of northern Norway", *Applied Ocean Research*, Vol. 7, pp. 85–92.
- Jaspers, N.H., 1956, "Statistical distribution patterns of ocean waves and of wave induced stresses and motions with engineering applications", *Transactions Society Naval Architects and Marine Engineers*, Vol. 64, pp. 375–432.
- Longuet-Higgins, M. S., 1952, "On the Statistical Distribution of the Heights of Sea Waves", *Marine Research*, Vol. 11, No. 3, pp. 245-66.
- Mathiesen, J. and E. Bitner-Gregersen, 1990, "Joint distribution for significant wave height and zero-crossing period ", *Applied Ocean Research*, No.12, pp.93-103.
- Ochi, M. K., 1979, "A series of JONSWAP wave spectra for offshore structure design", *Proc. Behavior of Offshore Structures Conference*, London, pp. 75–86.
- Ochi, M. K., 1990, *Applied Probability and Stochastic Processes*, John Wiley & Sons, New York.
- Ochi, M.K., 1992. "New approach for estimating the severest sea state from statistical data", *Proceedings Coastal Engineering Conference*, ASCE, Venice, 512–525.
- Ochi, M .K., 1998, *Ocean Waves - The Stochastic Approach*, University Press, Cambridge.
- Otay, N. E. and G. Topçu, 2008, *Bozbüük Environmental Monitoring Program Final Report*, Boğaziçi University, İstanbul.
- Otay, N. E. and G. Topçu, 2006, *Bozbüük Coastal Development Plan Field Study Report*, Boğaziçi University, İstanbul.
- Shore Protection Manual, 1984, *U.S. Army Coastal Engineering Research Center*, Washington, D. C., USA

- Tayfun, M. A., 1981, "Distribution of Crest-to trough Wave Heights", *Journal of Waterway, Port, Coastal and Ocean Engineering*, Vol. 107, pp. 149-158.
- Tayfun, M. A., 1990, "Distribution of large wave heights.", *Journal of Waterway, Port, Coast. and Ocean Engineering.*, ASCE, 116(6), pp. 686-707.
- Tayfun, M. A., 1993, "Joint distribution of large wave heights and associated periods", *Journal of Waterway, Port, Coastal, and Ocean Engineering*, 119 (3), pp. 261–273.
- Work, A. P., 2008, "Nearshore Directional Wave Measurements by Surface-following Buoy and Acoustic Doppler Current Profiler", *Ocean Engineering*, 35, pp. 727-737.